(29)

A TRIDENT SCHOLAR
PROJECT REPORT

NO. 89

"A COMPUTERIZED HOT-WIRE INVESTIGATION OF
THE STABILITY OF SEPARATED SHEAR LAYERS
WITH APPLICATION TO SHIP SILENCING"

A COMPUTERIZED HOT-WIRE INVESTIGATION

OF THE STABILITY OF SEPARATED SHEAR LAYERS

WITH APPLICATION TO SHIP SILENCING

A Trident Scholar Project Report

by

Midshipman David M. Schubert, Jr., 1/c

U. S. Naval Academy

Annapolis, Maryland

DDC

RECEIVED
OCT 20 1977
D

S. A. Elder

Professor S. A. Elder, Physics Dept
Adviser

Accepted for Trident Scholar Committee

Chairman

Date **23 May 1977**

ABSTRACT

A study was made of the stability of a two-dimensional air jet. The initially laminar flow was excited using sound from a loudspeaker. Due to instability of the free boundary layers, the initial disturbance caused by sound pressure was found to be amplified exponentially.

The laminar flow was found to turn turbulent at a downstream distance of approximately five jet widths, in agreement with earlier studies by Sato. At this distance, the amplification rate of the disturbance became less than exponential.

Use was made of a new computer-assisted hot wire technique. The position of the jet profile was recorded at different times referenced to the phase of the sound wave. Random jet fluctuations were removed by computer averaging, leaving only the periodic component of the disturbance. Measurements of wavelength, phase velocity and amplification factor of the disturbances made using this technique are compared to available theoretical values.

Comparison of the results to space and time dependent instability models show that the disturbances of the jet amplify in space rather than in time, in agreement with the prediction of Michalke. Some slight non-linear effects were noted even though the magnitude of the excitation was only 0.33% of the jet's speed. This agrees with recent studies by Moore who predicts non-linear effects at excitation levels as small as 0.02%.

The results of this study are applicable to studies of flow-induced cavity resonance, which is a major cause of sonar self-noise and of vibrations in ships and aircraft.

ACKNOWLEDGEMENTS

I would like to thank Dr. Samuel Elder, my Trident
Advisor, for his direction and help in theoretical
consideration and in data analysis. My thanks also to
Mr. Charles Robertson, who constructed the jet, and to
Mr. Norman Stead, who found or built much of the equipment
used in the experiment.

TABLE OF CONTENTS

ILLUSTRATIONS

I. BACKGROUND

The topic under investigation is boundary layer instability. A boundary layer is a thin region in a fluid flow where the velocity decreases rapidly. The phenomenon called flow noise is due to the instability of these boundary layers. In general, there are two types of boundary layers. One type is bounded by a wall, as for example the flow of water through a pipe. The velocity of the fluid flow decreases with proximity to the wall of the pipe. At the wall, velocity is zero. The other type of boundary layer is called a free boundary layer or shear layer, and it occurs in such things as jets, wakes, and open cavities.[1] There are no solid boundaries in the flow field. It is the stability of these free boundary layers which I am studying.

A characteristic common to free boundary layers is the existence of an inflexion point. It was shown by Rayleigh almost 100 years ago that velocity profiles in an inviscid fluid which have inflexion points are unstable relative to certain oscillatory disturbances.[2] It was shown later that the addition of viscosity has only a damping influence on the oscillations.[3]

Sato studied the stability and transition of a two dimensional jet.[4] He used a laminar jet of air which issued from a narrow slit. A small disturbance was introduced to the flow using a loudspeaker, and data was taken with a hot wire anemometer. It was found that at certain frequencies

the sound wave caused fluctuations of the jet's velocity at the same frequency. Furthermore, it was found that the magnitude of these fluctuations increased with distance downstream from the slit.

The thin jet studied by Sato is bounded by two shear layers. It was found that there are two modes of oscillation excited by the driving sound pressure wave. In one of the modes, the fluctuations are symmetrical with respect to the center line. In the other case, the oscillations are at a lower frequency and are anti-symmetric.

Sato's work dealt only with rms values for the oscillating velocity components. He had no means of preserving phase relationships. Recently, Dr. Elder of the U. S. Naval Academy has developed a computer assisted hot wire (CASH) technique for measuring oscillating velocity profiles.[5] Using computer averaging, the CASH technique can record how the velocity fluctuates with the phase of the driving sound pressure wave.

I have attempted to duplicate the conditions of Sato's experiment, using the computer-assisted technique to observe phase-related phenomena which Sato could not see. The results of the experiment are compared also to solutions of Rayleigh's model of temporally growing velocity fluctuations[6], and to Michalke's solution for spatially amplified disturbances in a free boundary layer.[7]

The study of jet boundary layers has direct application to studies of flow-induced cavity resonance. This is a high-intensity vibration that can occur in open wheel wells, bomb bay doors, and main sea water injection scoops.[8,9] It has also been recognized as an important source of shipboard vibration and self-noise.[10] This is caused by the instability of the airstream which moves across the open cavity. The boundary layer is a two dimensional free boundary layer similar to the one in my jet. The resonance can reach magnitudes great enough to cause dizziness and nausea of an aircraft's crew, or even failure of parts of the airplane.

II. DESCRIPTION OF APPARATUS

a. 2-Dimensional Jet. The jet used in the experiment issues from a rectangular slit. The X direction measures horizontal distance from the slit and the Y direction is up and down from the center of the jet. See Figure 1 for the general layout of the apparatus. Air is blown into a settling chamber (40 cm wide x 40 cm deep) where it passes through a series of six fine (64 mesh) screens. The air flow is accelerated as the width of the chamber tapers smoothly to a six mm wide channel which is 110 cm long. This long channel gives the smoothed air time to develop a parabolic flow. The transverse width of the channel remains a constant 40cm. Measurements indicate no velocity component in the Z direction except at the extreme outer edges of the slit. This justifies the assumption of the jet's two dimensionality.
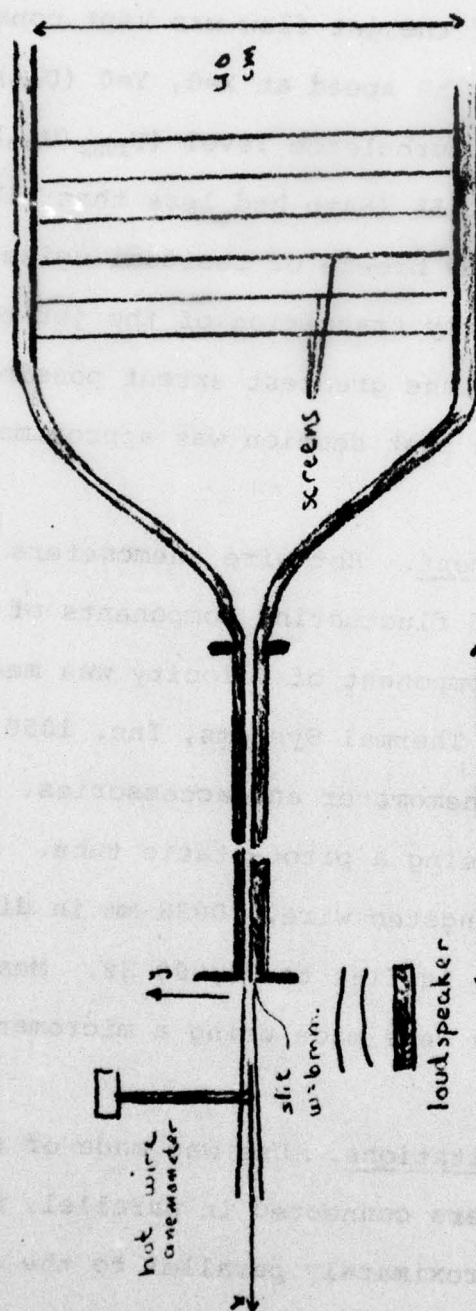
Figure 1

Diagram of Apparatus

The mean velocity of the jet flow was kept constant during the experiment. The speed at X=0, Y=0 (U_{OO}) was ten meters/second. The turbulence level (U_{rms}/U_{OO}) at the slit was approximately .15% (Sato had less than .1% turbulence).

It was found that any breeze or residual noise in the room tended to cause early transition of the jet to turbulence. These were minimized to the greatest extent possible. Background noise at the test section was approximately 72 dB. (re. .0002 microbar)

b. Hot Wire Equipment. Hot wire anemometers were used to measure the mean and fluctuating components of the velocity profile. Only the X component of velocity was measured. Equipment used was the Thermal Systems, Inc. 1050 series constant temperature anemometer and accessories. The hot wire probe was calibrated using a pitot-static tube. The hot wire sensors are made of tungsten wire, .0038 mm in diameter. The frequency response is flat to 85,000 Hz. Measurements in the X and Y directions were made using a micromanipulator to a precision of 0.1 mm.

c. Artifical Excitations. Use was made of two 4 x 8 inch polyplanar speakers connected in parallel, which produced a flat wave front approximately parallel to the direction of the jet's flow. An automatic level regulator was used to make the acoustic frequency response flat. The intensity of the sound at the test section was 93 dB including background noise. The intensity of the sound was uniform throughout the test section, and there were no noticeable resonance effects

(standing waves, etc.). The direction of sound propagation was made perpendicular to the flow direction.

d. The CASH Technique. The computer used is a PDP-8/I minicomputer. The program used is written in function-modified 8K FOCAL.[11] This program was developed for Midshipman Stanley Mack, a former Trident Scholar who studied flow induced cavity resonance using a turbulent air flow obtained from a small wind tunnel.[12] The computer records two signals simultaneously; the reference (sound pressure wave) signal, and the signal from the hot wire. The computer is set up to take 20 samples per cycle of the reference signal, and average the data over 100 cycles. Averaging removes turbulent (non-periodic) variation from the hot wire signal. Many points can be taken and phase referenced to show how the entire velocity profile appears at different phases of the driving wave. Using this method, the velocity profile can be "frozen in time" (phase), and it can be seen directly how the profile looks as it undergoes its fluctuations. A sample run of the program is shown in Figure 2. The first column is the average value of the oscillator signal taken 20 times per cycle. The record column is the oscillator signal's standard deviation. The third column is the average values of the hot wire signal which correspond to the different phases given in column 1. The fourth column is the standard deviation of the hot wire signal over 100 cycles.

V_{osc}	σ_{21c}	U_{inst}	σ_v
6.1155	0.0000	1.3626	0.0697
6.2455	0.0000	1.3526	0.0697
5.6565	0.0000	1.5025	0.0697
5.6474	0.0000	1.7530	0.0697
5.3456	0.0000	1.6232	0.0697
5.0100	0.0000	1.6235	0.0593
4.6513	0.0000	1.5339	0.0593
4.3525	0.0000	1.4144	0.0495
4.1534	0.0000	1.2749	0.0495
4.0140	0.0000	1.0757	0.0399
3.9541	0.0000	0.5365	0.0299
4.0535	0.0000	0.7476	0.0199
4.2132	0.0000	0.7072	0.0199
4.4522	0.0000	0.7561	0.0199
4.7613	0.0000	0.9761	0.0299
5.0697	0.0000	1.2251	0.0495
5.4153	0.0000	1.4442	0.0495
5.7072	0.0000	1.6136	0.0495
5.9363	0.0000	1.7530	0.0593
6.0757	0.0000	1.3426	0.0697

0.3450

Figure 2

Sample Computer Printout for one Data Point

III. Experimental Results

a. <u>The Mean Velocity Profile - Natural Transition of</u>
<u>the Set</u>. The mean velocity profile of the jet in the laminar
region depends on the velocity distribution at the slit.
When the width of the slit is small compared to the length
of the channel, the velocity profile at the slit is parabolic.[13]
This is because the boundary layer at the wall of the channel
is thick enough to cover the entire cross section of the jet.

The mean velocity profile of the jet is shown in Figure 3.
The change in the velocity distribution with distance down-
stream is gradual as long as the flow remains laminar. Near
the center of the jet, (y=0) the velocity changes quite
slowly with both x and y, while at the inflexion points, where
the velocity change with y is maximum, the velocity is almost
independent of x. The change is somewhat greater in the outer
parts of the jet, where the boundary conditions change
suddenly due to the removal of the walls at the slit. There
is a sudden widening of the jet between x=40 and 50 mm. The
peak velocity drops sharply and the shear layers widen
considerably. This corresponds to the transition from
laminar to turbulent flow.

b. <u>Spontaneous fluctuations of the jet</u>. Sato saw two
modes of fluctuation in his jet. They are at different
frequencies and have different phase characteristics. The
mode at the lower frequency has longitudinal velocity
fluctuations which are antisymmetric with respect to the
center line of the jet. This mode has a very small or
negligible component at the central plane of the jet, but
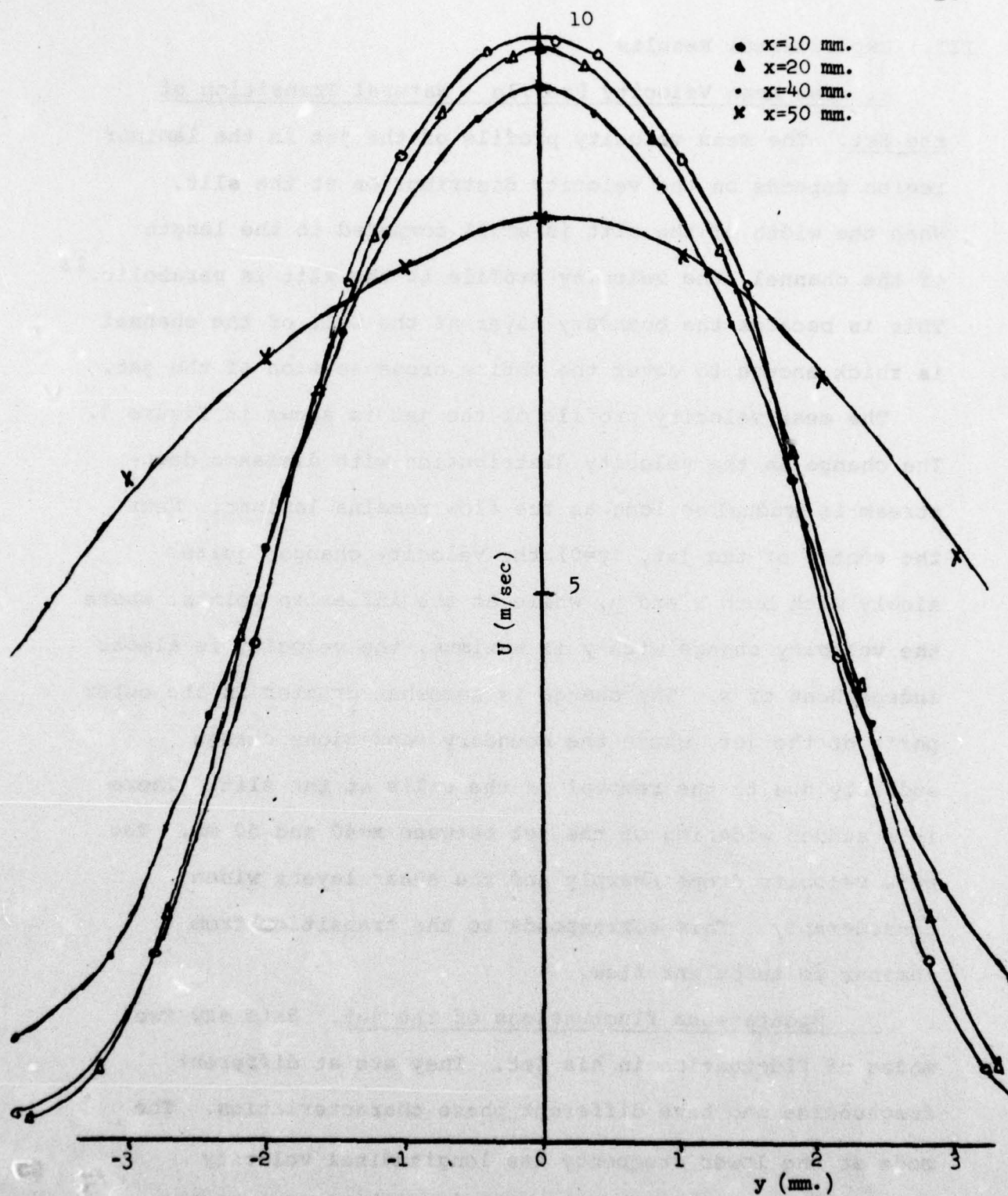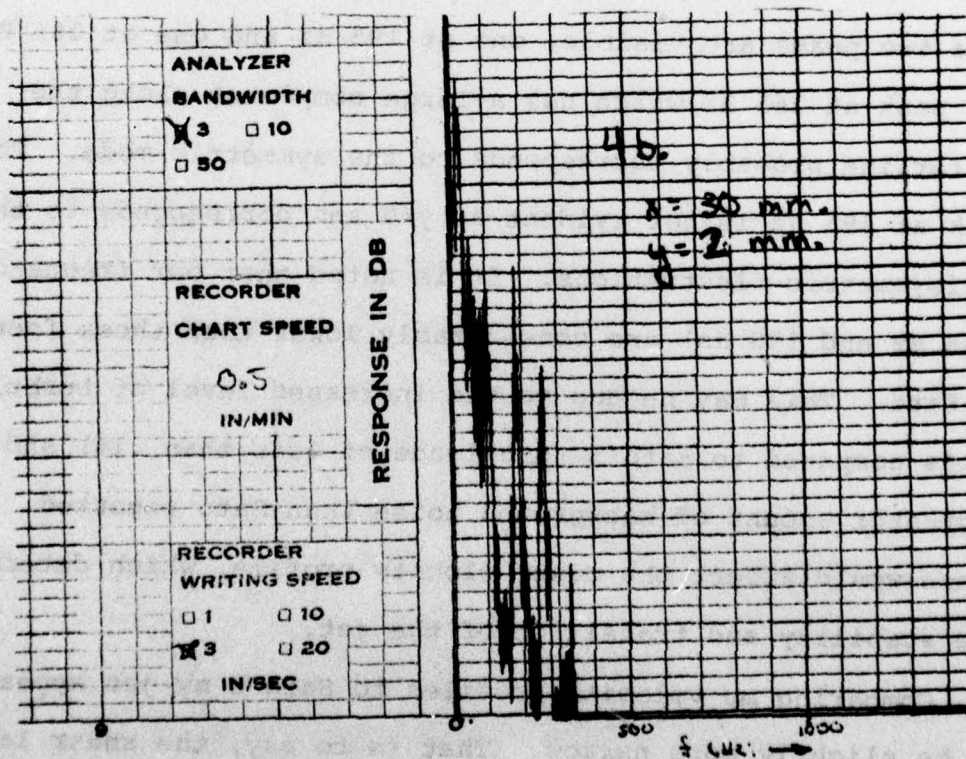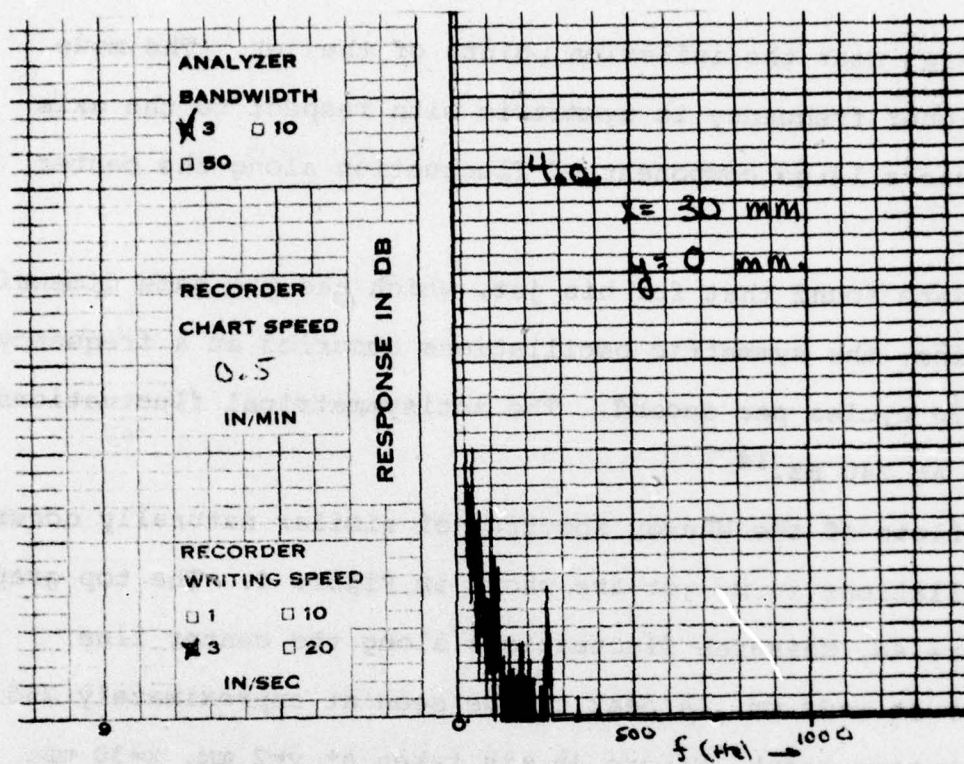
Mean Velocity Profile

Figure 3

Figure 4.

is large near the inflexion points of the jet. The mode
at higher frequency is symmetric with respect to the axis
and has a large component of fluctuation along the center
line.

Sato found that for his jet, which had the same dimensions
as mine, the symmetric oscillations occurred at a frequency
of 420 cycles per second. The antisymmetrical fluctuations
were at 240 Hz.[14]

Plots of the energy spectrum of similar naturally occurring
oscillations in my jet are shown in Figure 4. The top graph,
Figure 4a, measures fluctuations along the center line
(y=0) at x=30 mm. A peak can be seen at approximately 265 Hz.
The bottom graph, Figure 4b, is taken at y=2 mm, x=30 mm.
Here two peaks are visible, one at 195 Hz and one at 265 Hz.
The peak at 265 Hz which has a large component along the
centerline probably corresponds to the symmetric mode. The
peak at 195 Hz is not evident at y=0 and corresponds to the
antisymmetric fluctuations. It is noted that our frequencies
(265 Hz and 195 Hz) are considerably lower than those found
by Sato. This may be due to the increased level of turbulence,
(.15% compared to Sato's turbulence of less than .1%) and to
a greater amount of background noise than Sato reported.
These would affect the mean velocity profile, which determines
the stability and transition of the jet.

Comparing my velocity profiles to Sato's my jet appears
to be slightly more narrow. That is to say, the shear layers

are closer together than those shown by Sato. This would mean that my jet has more interaction between shear layers than Sato's.

Sato states that when the velocity distribution is nearly parabolic, the antisymmetric fluctuation prevails. He states that if either the width of the jet or the flow's speed is increased, the mean velocity distribution changes and the antisymmetrical mode of fluctuation vanishes.[15]

Comparing the relative sizes of the high and low frequency peaks in Figure 4b, we see that the lower (antisymmetric) mode has considerably more energy than does the symmetric mode. This is in contrast to Sato who shows the symmetric oscillations to be considerably more energetic than the ones at lower frequency.

Although the wind speed and wind channel dimensions are the same as Sato's, my jet favors the antisymmetric mode, whereas Sato's jet has a greater symmetric component. As will be shown later, the strengthening of the antisymmetric fluctuations in my jet seems to be due to the differences in the velocity profile that were mentioned above.

c. Driven Fluctuations of the Jet. The sound pressure produced by the loudspeakers was kept at a constant level during the experiment by a GR Model 1569 automatic level regulator. The sound particle velocity in the vicinity of the jet was estimated from pressure gradient measurement to be about 3.3 cm/sec. Thus, this excitation level, relative

to the jet's speed was about 3.3 cm/sec/1000 cm/sec ≈ .33%.
Effects of excitation at frequencies from 60 to 1000 Hz were
observed visually on the oscilloscope. Amplification of
the velocity fluctuations at the same frequency as the
driving wave was noted for all frequencies up to 470 Hz.
Above 470 Hz there was no amplified velocity component at
the driving frequency. There was a noticeable maximum in
fluctuations when the jet was driven at 195-200 Hz. This
corresponds to the frequency of the strong antisymmetric
peak shown in the natural frequency plot. For some reason
there was not a maximum noted when the driving wave was in
the vicinity of the natural symmetric mode frequency (265 Hz).
It is noted also that at all frequencies examined, the velocity
fluctuations shifted 180° in phase at the center of the jet.
The fluctuations were smallest at the center line and
greatest at approximately two mm on either side of the center
line (in the region of the inflexion points). These are
the characteristics of the antisymmetric type of fluctuations.
Symmetric oscillations were not observed to be excited by the
sound wave at any frequency.

The effects of excitation on the jet have been studied in
depth using 200 Hz as the driving frequency. This was chosen
as the driving frequency for which the maximum rate of velocity
fluctuation was attained. Figure 5 shows the effects of
excitation on the jet's mean velocity profile. At x=20 mm,
the mean velocity is almost unchanged by the presence of the
sound, except for a small increase in velocity at the outer

Mean Velocity Profiles

• unexcited
△ excited

U (m/sec)

x=20 mm.

• unexcited
▲ excited

x=40 mm.

y (mm)
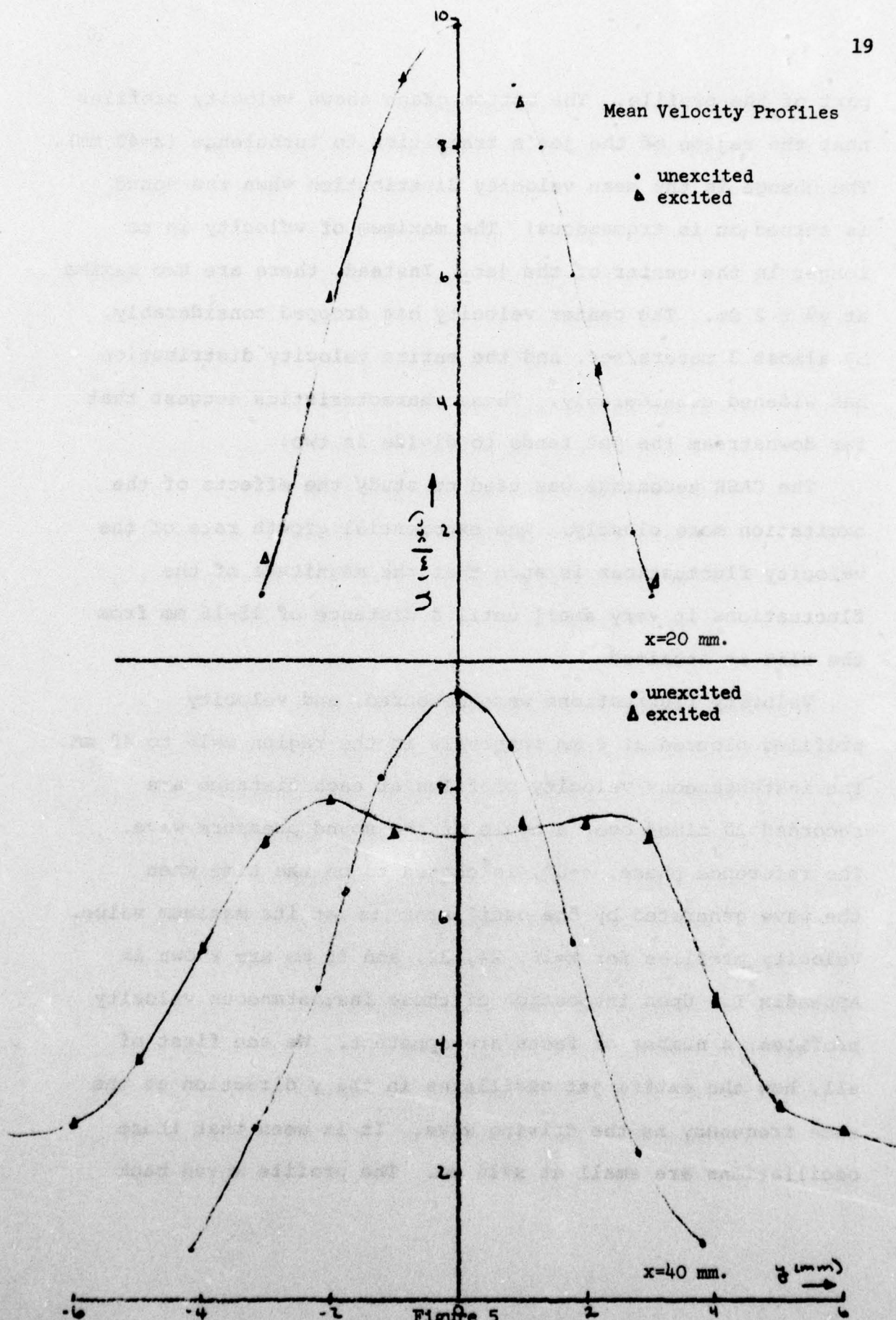
Figure 5

part of the profile. The bottom graph shows velocity profiles near the region of the jet's transition to turbulence (x=40 mm). The change in the mean velocity distribution when the sound is turned on is tremendous! The maximum of velocity is no longer in the center of the jet. Instead, there are two maxima at y= ± 2 mm. The center velocity has dropped considerably, by almost 3 meters/sec. and the entire velocity distribution has widened considerably. These characteristics suggest that far downstream the jet tends to divide in two.

The CASH technique was used to study the effects of the excitation more closely. The exponential growth rate of the velocity fluctuations is such that the magnitude of the fluctuations is very small until a distance of 15-16 mm from the slit is attained.

Velocity fluctuations were measured, and velocity profiles plotted at 4 mm intervals in the region x=16 to 40 mm. The instantaneous velocity profiles at each distance are recorded 20 times over a cycle of the sound pressure wave. The reference phase, $\phi = 0°$, is chosen to be the time when the wave generated by the oscillator is at its maximum value. Velocity profiles for x=16, 24, 32, and 40 mm are shown in Appendix I. Upon inspection of these instantaneous velocity profiles, a number of facts are apparent. We see first of all, how the entire jet oscillates in the y direction at the same frequency as the driving wave. It is seen that these oscillations are small at x=16 mm. The profile moves back

and forth, but the shape of the velocity distribution does
not change significantly. At x=24 mm, the jet is slightly
wider, and the magnitude of the fluctuations has increased.
However, the shape of the velocity profile still does not
change significantly as it oscillates. Further downstream, at
x=32 mm, the outer region of the jet has widened still further.
The fluctuations are very noticeable, and they distort the
velocity profile. The peak of the profile is wider when the
jet is near the equilibrium (center) position. The velocity
peak becomes narrower as the jet moves toward the outer limits
of its fluctuation. When the fluctuation is at its maximum,
(see ϕ=126°, 306°) the velocity profile develops a flat
region on the side opposite to the velocity maximum.

At x=40 mm, we see immediately that the jet is splitting
into 2 components. One of the peaks is larger than the other.
The two peaks move 180° out of phase with each other. As the
two peaks move toward the maximum fluctuation (ϕ=18°, 36°),
both peaks are prominent and well defined. After the maximum
displacement from the center is reached, and the two peaks
begin to move toward the center, the smaller peak shrinks and
the velocity profile on that side becomes very irregular
(ϕ=72, 90, 252, 270). As the larger peak nears the center,
the maximum velocity gets bigger until it is nearly back to
the slit value of 10 m/sec. The smaller peak has also moved
to the center and reinforces the larger peak (ϕ=108°, 306°).
At this point, the central part of the velocity profile

resembles the profile at distances closer to the slit. The
outer parts of the boundary layers are much wider than they are
closer to the slit. As the maximum passes the center ($y=0$),
the smaller peak reappears and the magnitude of the major
peak decreases ($\phi=162°$, $342°$).

Further insight to the behavior of the jet is obtained
by studying only the fluctuating components of the velocity.
These are given by u, defined as $u = U_{instantaneous} - U_{mean}$.
Plots of u fluctuations at $x=24$, 32, and 40 mm are shown in
Appendix II. The fluctuations at $x=24$ cm are almost purely
antisymmetrical. The fluctuation of the jet at the center is
very small. As we move away from the center of the jet, the
velocity fluctuations increase to a maximum at about two mm
away from the centerline. This is in the vicinity of the
inflexion points, where the slope of the velocity profile is
greatest. There is a phase reversal at or near the centerline
of the jet, i.e. the u fluctuations change sign. There are
phase reversals again at $y= \pm 3.6$ mm, near the outer edge of
the jet.

The intensity of the u fluctuations varies also with the
phase (ϕ) of the driving wave. At $x=24$ mm, the magnitude of
u is greatest at $\phi=0°$ and $\phi=180°$. These angles correspond to
the maximum displacement of the jet to the left and right of
the centerline, respectively. At $\phi=90°$ and $180°$, u is at
its minimum. This corresponds to the times when the jet is
at its equilibrium position.

At x=32, the values of u are larger. The maxima and minima of u do not occur at the same values of ϕ as they did at x=24 mm. Maxima occur at $\phi=126°$ and 306°. Minima are at $\phi=216°$ and 36°. The fluctuations, although antisymmetric in nature, are no longer purely antisymmetric. There is an appreciable velocity component at the origin, (y=0) which is most noticeable at $\phi=216°$ and 36°, the minima of the antisymmetrical fluctuations. The phase shift near the edges of the jet is still present near y=4 mm.

The u fluctuations at x=40 mm are quite turbulent. There are considerable components of both symmetric and antisymmetric velocity fluctuations. The symmetric oscillations correspond to the 2 peaks of the velocity profile, and the antisymmetric oscillations are due to the fact that one peak is larger than the other. Although there are phase reversals of the u fluctuations, as shown by the graphs, they vary with the phase of the driving wave. There is no specific y distance where a phase reversal occurs at all values of ϕ.

Using the instantaneous velocity profiles, we can see how specific points of the velocity profile move in the y direction. It is possible to plot the position of the peak velocity, for example, as a function of x and y at different values of ϕ. Figure 6 is a plot of the position of the velocity peak between x=16 mm and x=40 mm at $\phi=0°$. The general shape of the locus of points is an amplified sinusoid. The dotted line represents the maximum

Position of Velocity Maximum at $\phi = 0°$
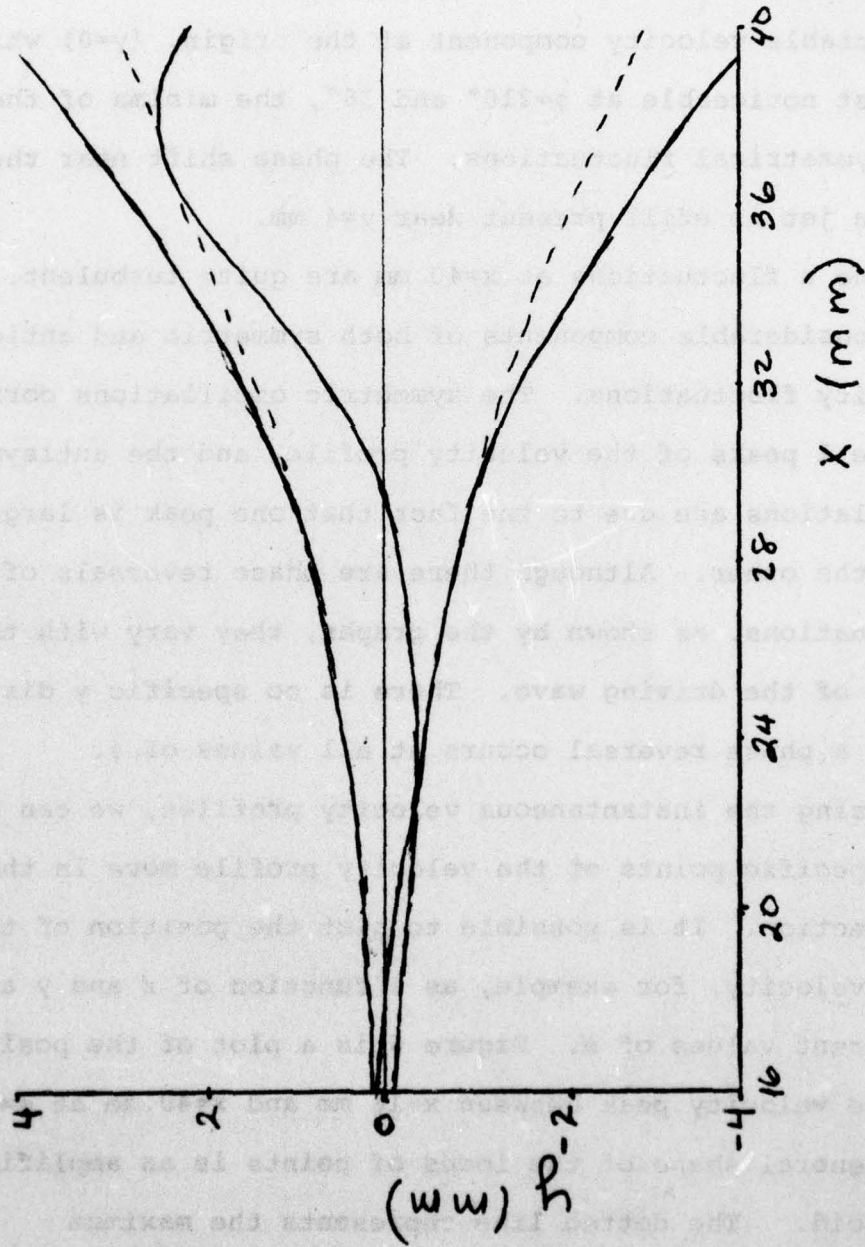
Figure 6

amount of displacement in the y direction which occurs during a cycle of the sound wave. The solid line is an exponential function, which the jet's fluctuations should follow according to linearized theory. We can see that for x less than 30 mm, the growth is exponential. At distances between 30 and 40 mm downstream, the disturbance is still amplifying, but the growth rate is less than exponential.

Figure 7 shows the position of the two inflexion points and the velocity peak at $\phi = 0°$, $90°$, $180°$, and $360°$.

The peak and the two inflexion points all fluctuate in phase. The amount of displacement from equilibrium is approximately the same at the inflexion points as it is at the peak. The observation that the inflexion points do not seem to spread out in relation to the jet's center as the distance downstream increases is of great interest. The apparent widening of the jet measured from average values is due to the fact that the jet's fluctuations to either side of the center line are increasing with distance downstream. We see from the instantaneous profiles that the width of the central part of the velocity profile (the region between the inflexion points) remains fairly constant.

The position of the velocity peak is much easier to measure than that of the inflexion points. At distances of 36 and 40 mm downstream, when the flow is becoming noticeably turbulent and the jet is splitting, the locations of the
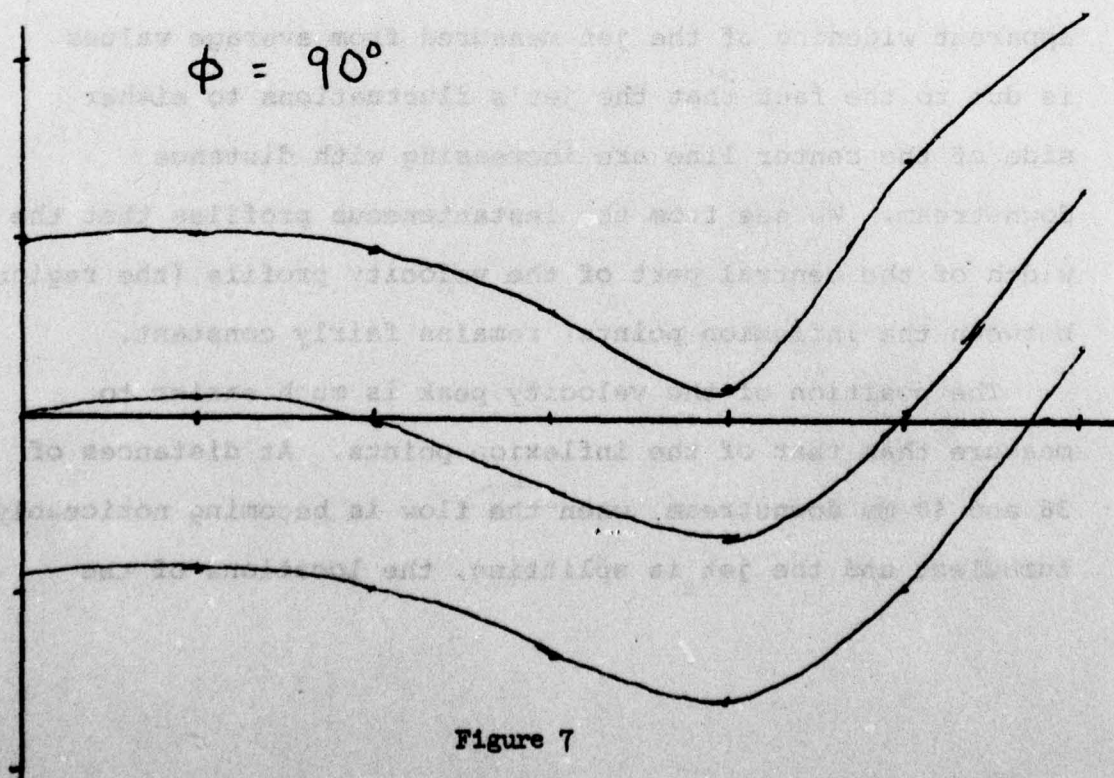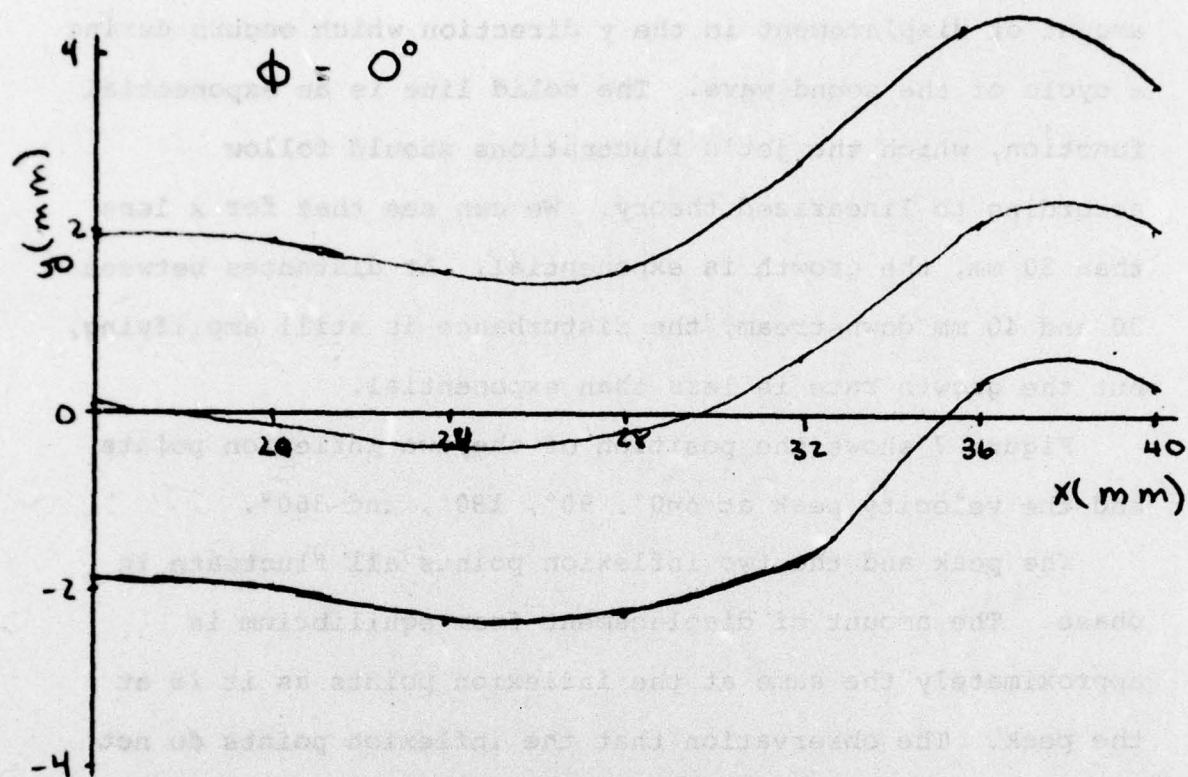
Figure 7
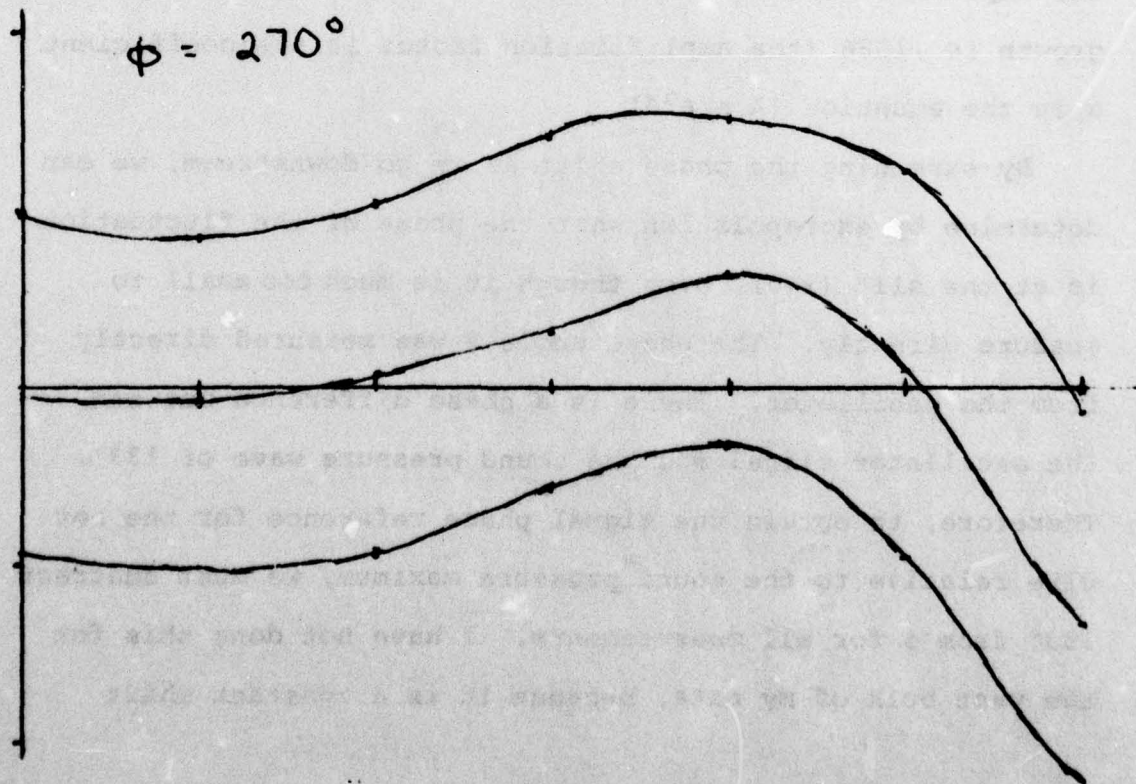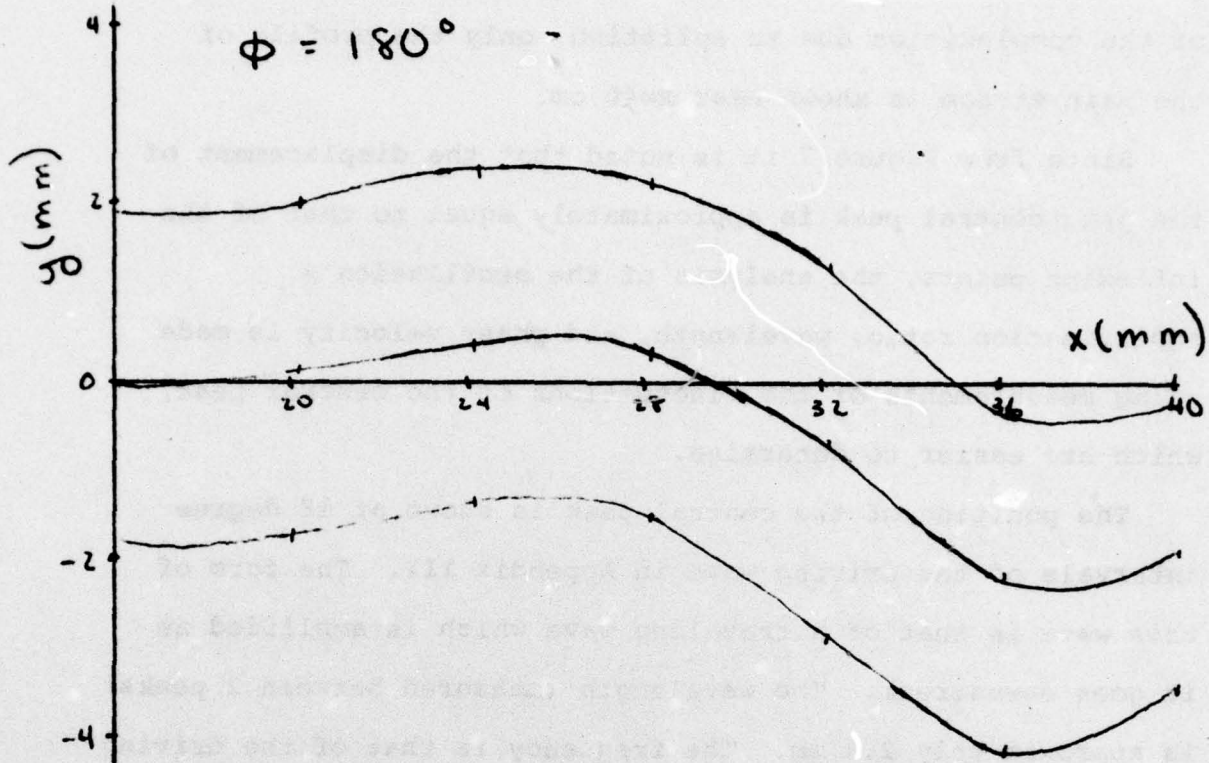
inflexion points are especially hard to determine. Because of the complexities due to splitting, only the profile of the main stream is shown near x=40 cm.

Since from Figure 7 it is noted that the displacement of the jet's central peak is approximately equal to that of the inflexion points, the analysis of the oscillation's amplification ratio, wavelength, and phase velocity is made using measurements of the fluctuations of the central peak, which are easier to determine.

The position of the central peak is shown at 18 degree intervals of the driving wave in Appendix III. The form of this wave is that of a traveling wave which is amplified as it goes downstream. The wavelength (measured between 2 peaks) is approximately 2.4 mm. The frequency is that of the driving wave, 200 Hz. The phase velocity of the wave is 480 cm/sec. The amplification factor measured for the region of exponential growth is .1586 (the amplification factor is the coefficient α in the equation ($A = e^{\alpha x}$).

By examining the phase shift as we go downstream, we can determine by extrapolation what the phase of the fluctuation is at the slit (x=0), even though it is much too small to measure directly. The phase angle ϕ was measured directly from the oscillator. There is a phase difference between the oscillator signal and the sound pressure wave of 133°. Therefore, to obtain the signal phase reference for the hot wire relative to the sound pressure maximum, we must subtract 133° from ϕ for all measurements. I have not done this for the vast bulk of my data, because it is a constant shift

Time of Max Fluctuation vs. Distance Downstream

Convection speed = 483 cm/sec (slope^{-1})

at origin, jet leads sound pressure by 42°

x (mm)

time (millisecs)
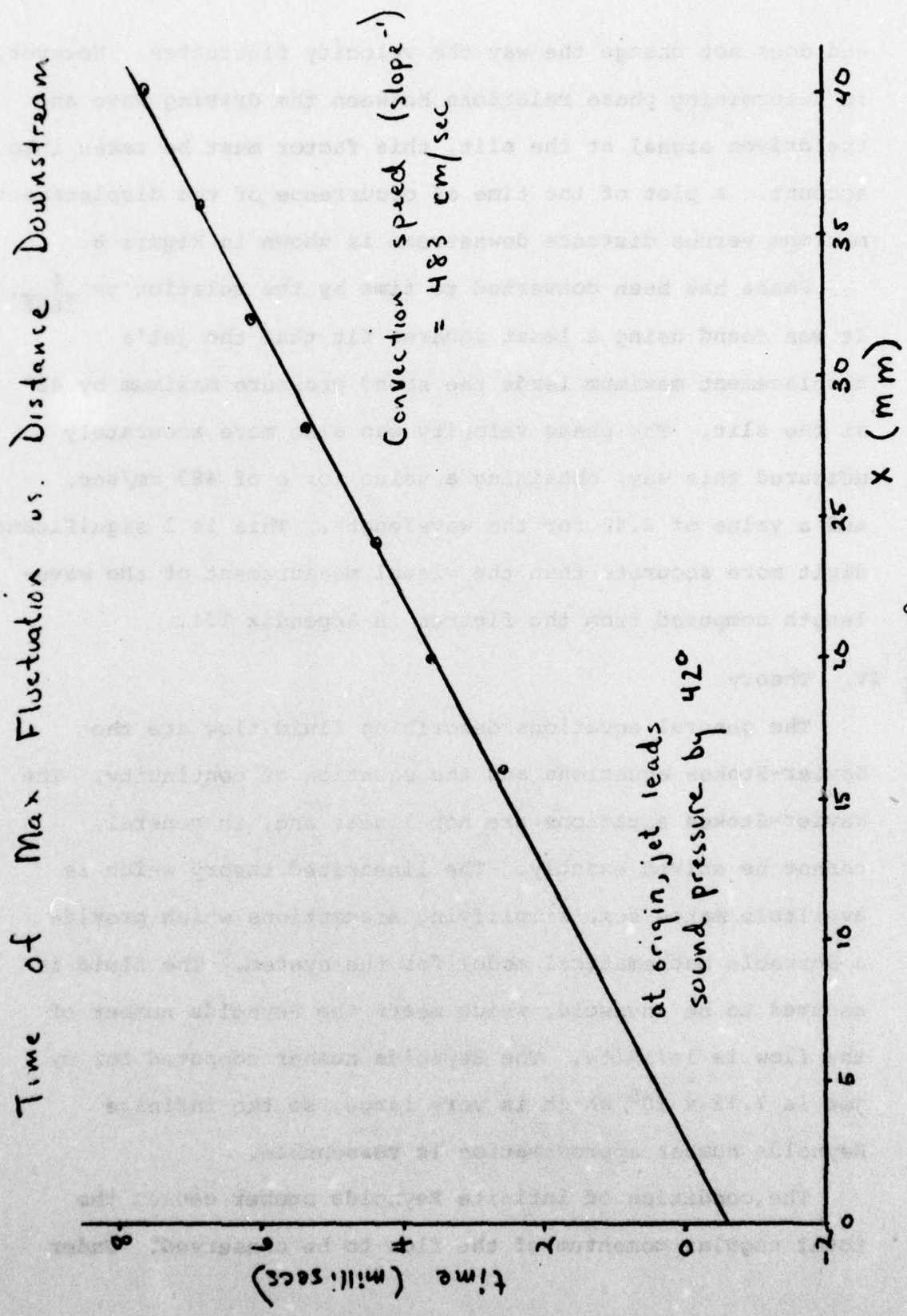
Figure 8

and does not change the way the velocity fluctuates. However, in determining phase relations between the driving wave and the driven signal at the slit, this factor must be taken into account. A plot of the time of occurrence of the displacement maximum versus distance downstream is shown in Figure 8.

Phase has been converted to time by the relation $t = \frac{\phi}{360f}$. It was found using a least squares fit that the jet's displacement maximum leads the sound pressure maximum by 42° at the slit. The phase velocity was also more accurately measured this way, obtaining a value for c of 483 cm/sec, and a value of 2.42 for the wavelength. This is 1 significant digit more accurate than the visual measurement of the wavelength computed from the figures in Appendix III.

IV. Theory

The general equations describing fluid flow are the Navier-Stokes equations and the equation of continuity. The Navier-Stokes equations are non-linear and, in general, cannot be solved exactly. The linearized theory which is available makes some simplifying assumptions which provide a workable mathematical model for the system. The fluid is assumed to be inviscid, which means the Reynolds number of the flow is infinite. The Reynolds number computed for my jet is 7.18×10^5, which is very large, so the infinite Reynolds number approximation is reasonable.

The condition of infinite Reynolds number causes the total angular momentum of the flow to be conserved. Under

this condition the Navier-Stokes equations may be replaced by the Helmholtz vorticity equation. $\frac{dZ}{dt} = 0$

Z is the vorticity, which is composed of a mean value Z_0 and a fluctuating component z. For the two dimensional jet studied here, $z = \frac{\partial v}{\partial x} - \frac{\partial u}{\partial y}$, where u is the fluctuating component of the velocity in the x direction and v is the fluctuating velocity component in the y direction. The equation of continuity for an incompressible fluid gives $\frac{du}{dx} + \frac{dv}{dy} = 0$.

Taking $Z_0 = - \frac{dU}{dy}$ and combining these equations, we obtain the Rayleigh equation;[16] $(U - \frac{\omega}{k}) [\frac{d^2 v}{dy^2} - k^2 v] - \frac{d^2 U}{dy^2} v = 0$ where U = the x component of the mean velocity (cm/sec), ω = angular frequency (rad/sec) and k = wave number (cm^{-1}). The values of ω and k are the constants of the equation, and are determined by the boundary conditions of the velocity distribution.

In Rayleigh's "The Theory of Sound" chapter 21, he assumed the value of k to be real and made ω complex in the form $\omega = \omega_r + i\omega_i$ This implied that unstable growth takes place in time, and is therefore referred to as a temporal model. The imaginary part of ω is the amplification factor for the disturbance. In a time t, the disturbance grows by a factor of $\exp(\omega_i t)$.

Rayleigh made a further simplification by assuming a velocity profile made up of straight lines. In such a profile,

the vorticity is constant in the straight line regions and changes only where there is a corner. Rayleigh studies the v fluctuations which he assumes to be of the form $v=A_i e^{\pm k(y-y_i)}$ He then matches boundary conditions at the corners (y_i) of the flow distribution to come up with solutions for specific velocity distributions.

Figure 9 shows a straight line approximation to the velocity profile of my jet, measured at x=10 mm. There are four discontinuities, at points A, B, C, and D. There are five different layers of constant vorticity.

The width of region II = b, which is also the width of region IV. The width of region III is designated by b'. The velocity in region III is U_o, and the vorticity in region II and IV is U_o/b. The v disturbances are written in terms of $\gamma=\exp(-kb)$ and $\gamma'=\exp(-kb')$. Rayleigh gives us the following equation for the fluctuation[17] of the jet:
$$(\frac{2b\omega}{U_o})^2 + (\pm\gamma'\mp\gamma'\gamma^2+2kb) \frac{2b\omega}{U_o} \pm \gamma'-1+2kb+\gamma^2(1\mp\gamma'\mp2kb\gamma') = 0$$
The upper signs correspond to what Rayleigh calls symmetrical disturbances, and the lower signs to antisymmetrical disturbances. This equation is a quadratic in terms of ω, and for a given value of k can be solved using the quadratic formula. By varying k, we can find the value where the imaginary part of ω is greatest. This corresponds to the value of ω for which the instability is greatest.

Rayleigh did not carry out any numerical calculations for this case. However, using this technique, we calculate that
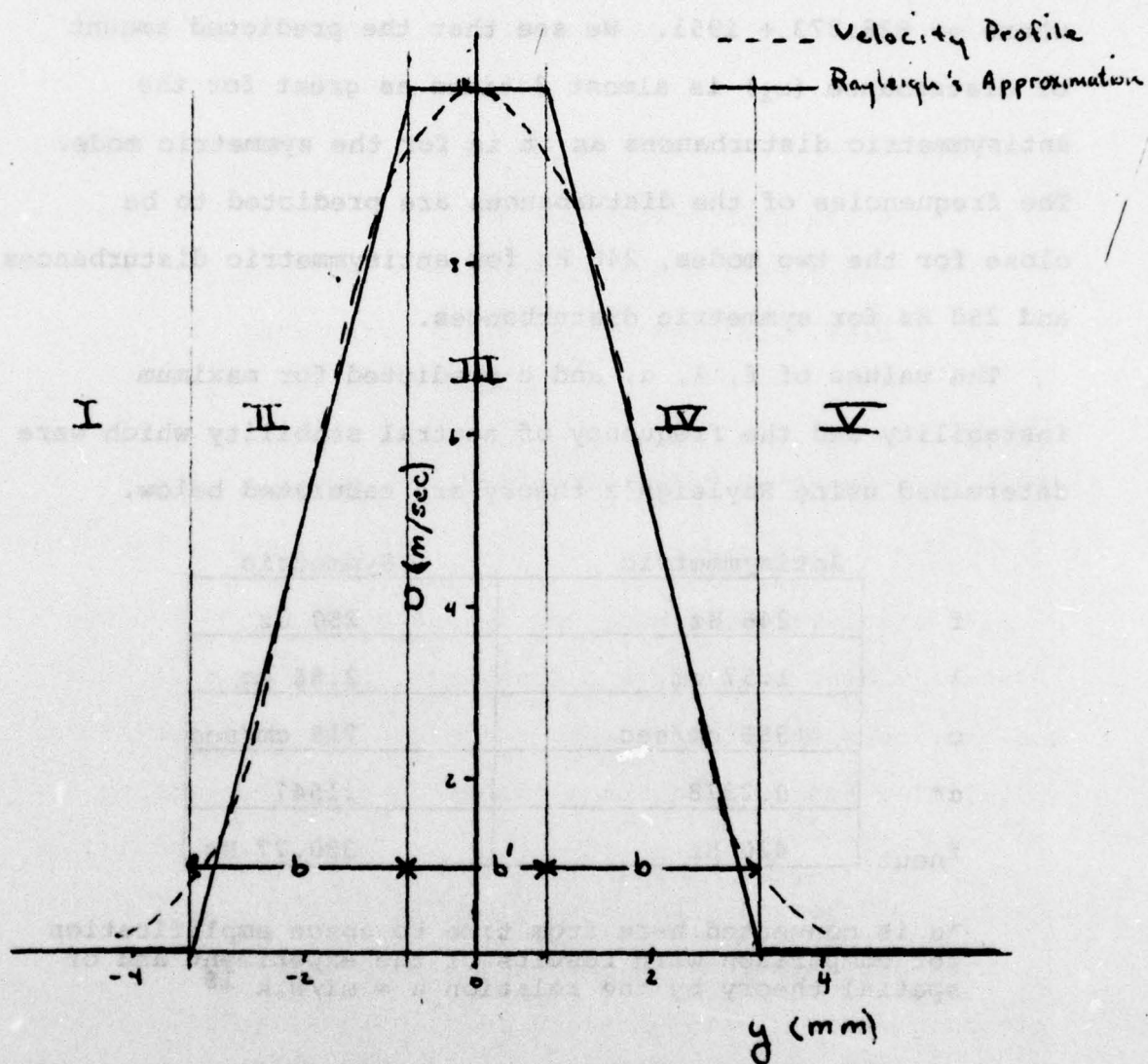
Rayleigh's Velocity Profile

Figure 9

for symmetrical disturbances, the maximum disturbance occurs at $k=2.2$ cm^{-1}. The corresponding value of $\omega = 1569 + i340.3$. For antisymmetrical disturbances, the maximum is at $k=4$ cm^{-1}, where $\omega= 828.873 + i951$. We see that the predicted amount of disturbance (ω_i) is almost 3 times as great for the antisymmetric disturbances as it is for the symmetric mode. The frequencies of the disturbances are predicted to be close for the two modes, 246 Hz for antisymmetric disturbances and 250 Hz for symmetric disturbances.

The values of f, λ, α, and c predicted for maximum instability and the frequency of neutral stability which were determined using Rayleigh's theory are tabulated below.

	Antisymmetric	Symmetric
f	246 Hz	250 Hz
λ	1.57 cm	2.86 cm
c	386 cm/sec	715 cm/sec
α*	0.2378	.1547
f_{neut}	420 Hz	330.77 Hz

*α is converted here from time to space amplification for comparison with results of the experiment and of spatial theory by the relation $\alpha = \omega i / U_o k$ [18]

Rayleigh's theory of temporally amplified disturbances has been questioned by Gaster[19] and Freymuth.[20] Our intuition tells us that the jet grows in space, not in time. Gaster came to the conclusion that growth rates obtained by temporal calculations can not be linearly transformed into spatial growth rates as we did with Rayleigh's theory. A theory of spatially growing disturbance is needed.

35
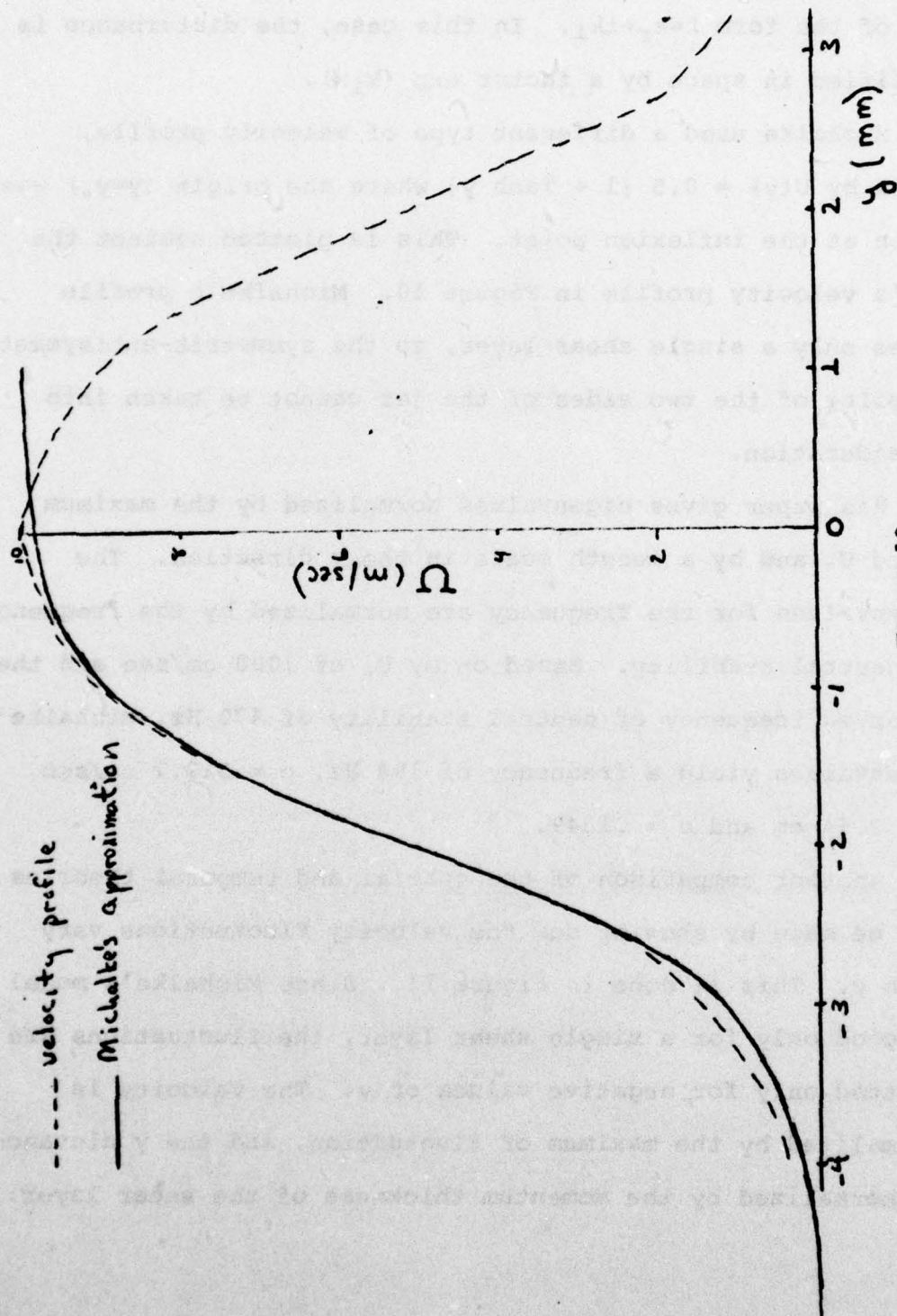
Figure 10

Michalke's Velocity Profile

Michalke's paper gives solutions using a spatial theory.[21] He assumes that ω is real and that the wave number is complex and of the form $k=k_r+ik_i$. In this case, the disturbance is amplified in space by a factor exp $(k_i x)$.

Michalke used a different type of velocity profile, given by $U(y) = 0.5 [1 + \text{Tanh } y]$ where the origin $(y=y_0)$ was taken at the inflexion point. This is plotted against the jet's velocity profile in Figure 10. Michalke's profile gives only a single shear layer, so the symmetric-antisymmetric coupling of the two sides of the jet cannot be taken into consideration.

His paper gives eigenvalues normalized by the maximum speed U_0 and by a length scale in the y direction. The eigenvalues for the frequency are normalized by the frequency of neutral stability. Based on my U_0 of 1000 cm/sec and the observed frequency of neutral stability of 470 Hz, Michalke's eigenvalues yield a frequency of 194 Hz, $c = 512.7$ cm/sec, $\lambda = 2.64$ cm and $\alpha = .1349$.

Another comparison of the spatial and temporal theories can be made by showing how the velocity fluctuations vary with y. This is done in Figure 11. Since Michalke's model is good only for a single shear layer, the fluctuations are plotted only for negative values of y. The velocity is normalized by the maximum of fluctuation, and the y distance is normalized by the momentum thickness of the shear layer.

u
normalized

1.0

.8

.6

.4

.2

0

-.2

-.4

1 2 3 4 5 6 7 8 9

y (normalized)

spatial theory
temporal theory
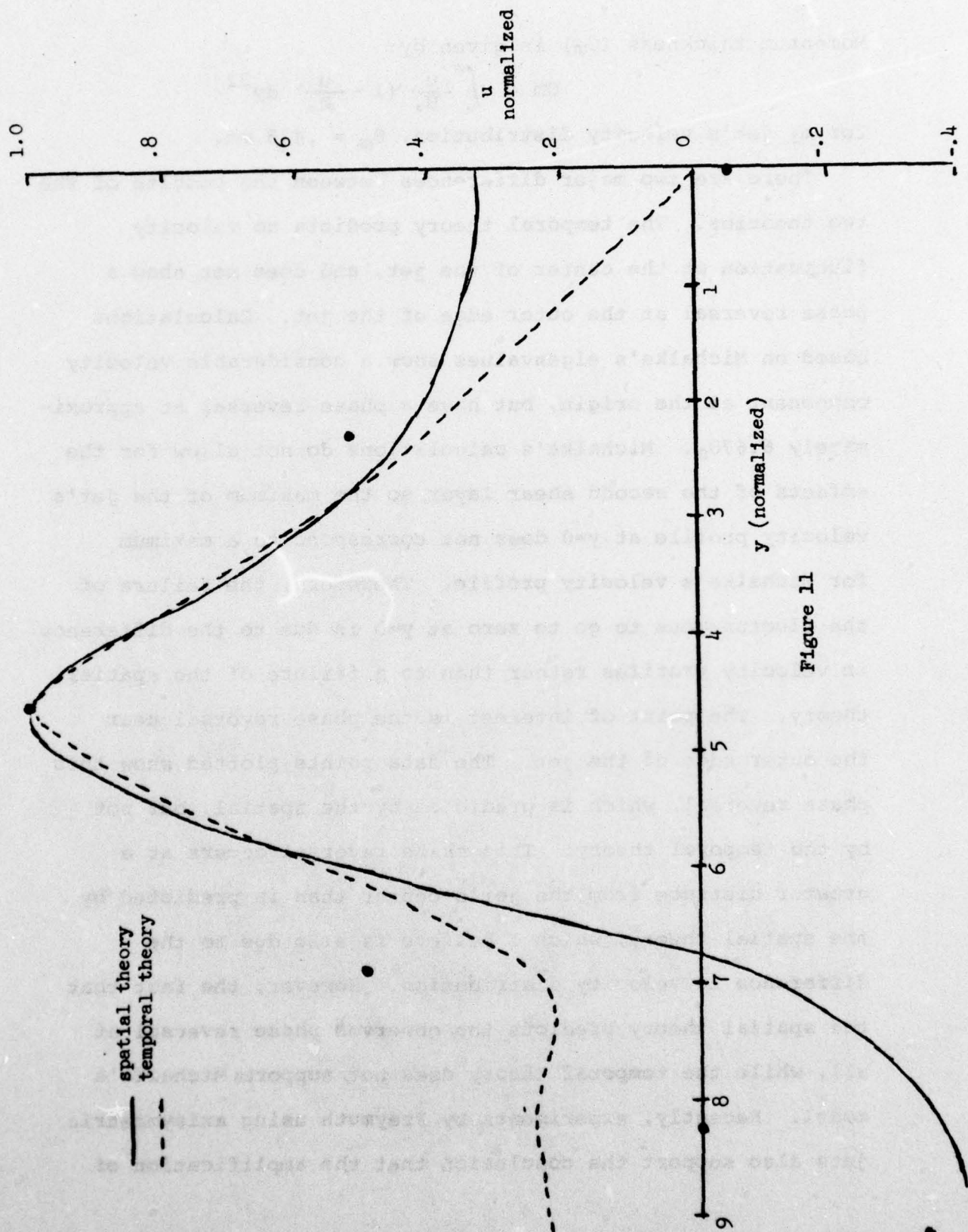
Figure 11

Momentum thickness (Θ_m) is given by:

$$\Theta_m = \int_0^\infty \frac{u}{U_0}\left(1 - \frac{u}{U_0}\right) dy^{22}$$

for my jet's velocity distribution, $\Theta_m = .435$ mm.

There are two major differences between the results of the two theories. The temporal theory predicts no velocity fluctuation at the center of the jet, and does not show a phase reversal at the outer edge of the jet. Calculations based on Michalke's eigenvalues show a considerable velocity component at the origin, but have a phase reversal at approximately $6.67\Theta_m$. Michalke's calculations do not allow for the effects of the second shear layer, so the maximum of the jet's velocity profile at y=0 does not correspond to a maximum for Michalke's velocity profile. Therefore, the failure of the fluctuations to go to zero at y=0 is due to the difference in velocity profiles rather than to a failure of the spatial theory. The point of interest is the phase reversal near the outer edge of the jet. The data points plotted show this phase reversal, which is predicted by the spatial, but not by the temporal theory. This phase reversal occurs at a greater distance from the jet's center than is predicted by the spatial theory, which I believe is also due to the difference in velocity distribution. However, the fact that the spatial theory predicts the observed phase reversal at all, while the temporal theory does not, supports Michalke's model. Recently, experiments by Freymuth using axisymmetric jets also support the conclusion that the amplification of

disturbances in free boundary layers can only be described by a theory of spatially growing disturbances.[13]

The following table summarizes the predictions of the two theories and compares them to the values measured experimentally.

	Experimental Result	Temporal Prediction	Spatial Prediction
Freq. of max disturbance	200 Hz	246 Hz	194 Hz
Wavelength	2.42 cm	1.57 cm	2.64 cm
Phase velocity	483 cm/sec	386 cm/sec	513 cm/sec
Amplification factor	.1568	.2378	.1349
Freq. of neutral disturbance	470 Hz	420 Hz	470 Hz*
Phase reversal	Yes	No	Yes

*The value of 470 Hz used for neutral stability in the spatial model was not predicted but was taken from the observed data.

Rayleigh assumes that his two inflexion points remain a constant distance apart. Common sense tells us that the jet widens as it goes downstream and that therefore, the distance between the inflexion points should spread. Crighton and Gaster[24] treat the stability of a slowly diverging jet, and show that this divergence has a considerable effect on such quantities as the phase velocity and amplification factor.

However, in the laminar region of my jet the distance between the shear layers does not change appreciably. (See Figure 7) It is instead the amount of displacement of the

entire profile in y direction which makes the jet seem to widen. Therefore, the effects of divergence described by Crighton and Gaster need not be taken into consideration.

V. Conclusion

The results obtained from experimental and theoretical analysis of the two dimensional jet are summarized below.

1. Comparison of the experimental results to linearized theories shows that fluctuations in the jet's speed grow as a function of distance downstream rather than of time, in agreement with Michalke's theory.

2. The fluctuation grows exponentially as predicted by the linearized theory up to a distance of 5 slit widths downstream $(\frac{x}{b} = \frac{30mm}{6mm})$, after which the amplification is less than exponential. This is in good agreement with the results of Sato. The region of less than exponential growth is where the flow changes from laminar to turbulent flow.

3. The sound wave's particle velocity was calculated to be .33% of the jet's velocity. Moore[25] predicts that mild non-linear effects are obtained when the amplitude of a disturbance is as little as .02% of the jet's speed. These non-linear effects almost surely cause the jet's deviation from exponential growth.

4. In the transition region, the non-linear effects split the jet into two peaks which oscillate 180° out of phase with each other.

5. The feasibility of the CASH method for studying the stability of shear layers has been demonstrated. This method is superior to former methods in that it takes phase into account, and this permits the measurement of the wave's

phase velocity and wavelength. The CASH technique permits reconstruction of the actual oscillating displacement profile of the periodic disturbances of the jet. This method can be used also for turbulent flow, where a larger number of cycles would be averaged in order to pick out the oscillating disturbance from a greater amount of noise. Direct quantitative velocity is obtained, (as apposed to optical methods) and stored in a convenient form for further data reduction.

6. The spatial theory developed by Michalke is for a single shear layer. Spatial predictions for a velocity profile with two interacting shear layers would be more directly applicable to the results of my experiment.

7. The next step in analyzing the causes and effects of flow-induced cavity resonance is to build a cavity in the linear region of the jet's flow. Velocity fluctuations of the system would be compared to those observed in the free jet. This is another project in itself and is recommended for further research. Flow induced cavity resonance has been recognized for years as an important cause of noise and vibrations in Naval ships and aircraft.

8. Further investigation could also be carried out by studying effects of changing the width of the slit. This would change the shape of the velocity profile, which is the determining factor in stability considerations.

FOOTNOTES

[1]A. Michalke, "On Spatially Growing Disturbances in an Inviscid Shear Layer," Journal of Fluid Mechanics, 23 (1965), p. 521.

[2]Lord Rayleigh, The Theory of Sound. (New York: Dover Publications, 1945) pp. 376-401.

[3]C. E. Lin, The Theory of Hydrodynamic Instability. (Cambridge: Cambridge University Press, 1955) pp. 27-43

[4]Hiroshi Sato, "The Stability and Transition of a Two-Dimensional Jet," Journal of Fluid Mechanics, 7 (1960) pp. 53-80.

[5]Samuel Elder, "A Computer-Assisted Hot Wire Technique for Measuring Oscillating Velocity Profiles," (Annapolis, MD: Michelson Laboratory Preprint E7304, Oct., 1973) pp 1-7.

[6]Rayleigh, pp. 392-98.

[7]Michalke, pp. 521-44.

[8]Alan Pope and J. J. Harper, Low Speed Wind Tunnel Testing (New York: John Wiley and Sons, Inc., 1966) pp. 271-272.

[9]Stanley Mack, "Similarity Law Investigation of Flow Induced Cavity Resonance," (Annapolis, MD: Trident Scholar Project Report, no. 31, 1972) p. 5.

[10]Samuel Elder, "Mechanics of Flow-Excited Cavity Resonance," an unpublished paper. p. 1.

[11]Elder, "AVRG: A PDP 8/I Data Acquisition and Averaging Program for Synchronous Hot Wire Measurements," (Annapolis, MD: Michelson Laboratory Report E7303, May 1973) p. ii.

[12]Mack, p. 1.

[13]Sato, p. 56.

[14]Ibid., p. 64-66.

[15]Ibid., p. 63.

[16]Rayleigh, p. 383.

[17]Ibid., p. 397.

[18]Sato, pp. 70-71.

[19]M. Gaster, "The Role of Spatially Growing Waves in the Theory of Hydrodynamic Stability." Progress in Aeronautical Sciences, 6 (1965), pp. 257-62.

[20]Peter Freymuth, "On Transition in a Separated Laminar Boundary Layer," Journal of Fluid Mechanics, 25 (1966), 699-703.

[21]Michalke, pp. 521-44.

[22]Hermann Schlichting, Boundary Layer Theory (New York: McGraw Hill Book Company, Inc., 1960) p. 123.

[23]Freymuth, p. 698.

[24]D. G. Crighton and M. Gaster, "Stability of Slowly Diverging Jet Flow," Journal of Fluid Mechanics 77 (1966), pp. 397-400.

[25]C. J. Moore, "The Role of Shear-Layer Instability Waves in Jet Exhaust Noise," Journal of Fluid Mechanics (1977) in Press.

BIBLIOGRAPHY

Crighton, D. G., and M. Gaster. "Stability of Slowly Diverging Jet Flow." Journal of Fluid Mechanics, 77 (1976), pp. 397-413.

Elder, Samuel A. "AVRG: A PDP8/I Data acquisition and Averaging Program for Synchronous Hot Wire Measurements." Annapolis, MD: USNA Michelson Laboratory Report E7303, May, 1973.

Elder, Samuel A. "Computer Assisted Hot Wire Technique for Measuring Oscillating Velocity Profiles." Annapolis, MD: USNA Michelson Laboratory Preprint E7304, October 1973.

Elder, Samuel A. "Mechanics of Flow-Excited Cavity Resonance." (Unpublished Paper)

Freymuth, Peter "On Transition in a Separated Laminar Boundary Layer." Journal of Fluid Mechanics, 25 (1966), 683-704.

Gaster, M. "The Role of Spatially Growing Waves in the theory of Hydrodynamic Stability." Progress in Aeronautical Sciences, 6 (1965), pp. 251-270.

Kinsler, L. and A. Frey, Fundamentals of Acoustics. New York: John Wiley and Sons, Inc., 1962.

Lin, C. C. The Theory of Hydrodynamic Instability. Cambridge: Cambridge University Press, 1955.

Mack, Stanley "Similarity-Law Investigation of Flow-Induced Cavity Resonance." Annapolis, MD: Trident Scholar Project Report no. 31, 1972.

Michalke, A., "On Spatially Growing Disturbances in an Inviscid Shear Layer." Journal of Fluid Mechanics, 23 (1965), pp. 521-544.

Moore, C. J., "The Role of Shear Layer Instability Waves in Jet Exhaust Noise." Journal of Fluid Mechanics, (1977), in print.

Pope, A., and J. Harper, Low Speed Wind Tunnel Testing. New York: John Wiley and Sons, Inc., 1966.

Rayleigh, J. W. S., The Theory of Sound, Vol. II. New York: Dover Publications, 1945.

Sato, Hiroshi "The Stability and Transition of a Two-Dimensional
Jet." Journal of Fluid Mechanics, 7 (1960), pp. 53-80.

Schlichting, Hermann Boundary Layer Theory, New York: McGraw-
Hill Book Company, Inc., 1960.

Instantaneous Velocity Profiles (x=16)

$\phi = 108°$ 126° 144°

162° 180° 198°

$x = 16$

$\phi = 324°$

$342°$

υ (m/sec)

y (mm.)

-3 -2 -1   1   2   3

x=16

$\phi = 324°$

$342°$

$\upsilon\,(m/sec)$

$y\,(mm)$

$x = 24$

55

180°

540

$\phi = 0°$

36 0

y (mm)

U (m/sec)

5

x=72

56

1620°

1980°

1440°

1800°

U (m/sec)

y (mm)

10

5

5

4

3

2

1

-2

-4

59

$\phi = 0°$

$18°$

$y(mm)$

$U\ (m/sec)$

$x = 40$

65

66

67

68

324°

342°

y (mm)

U (m/sec)
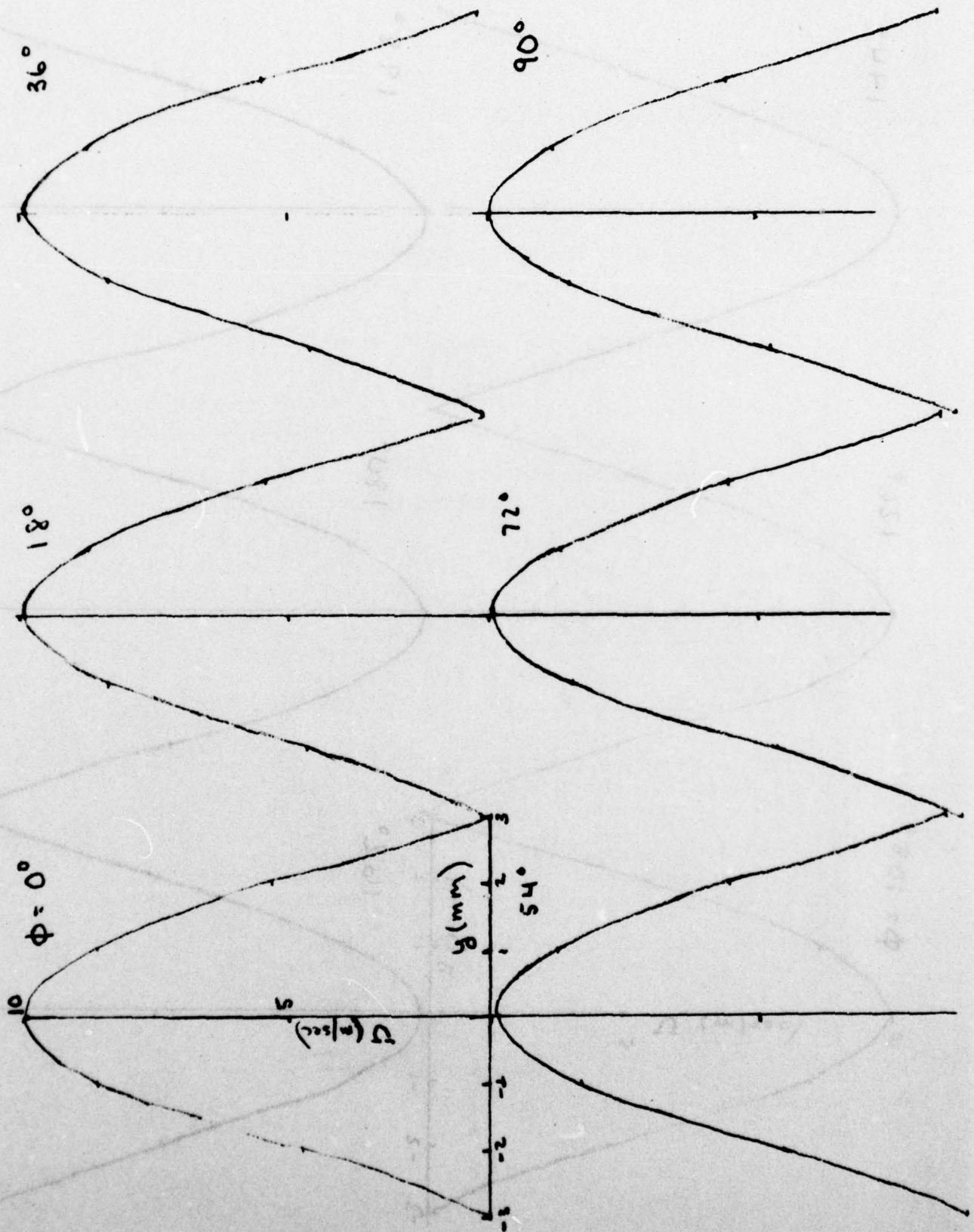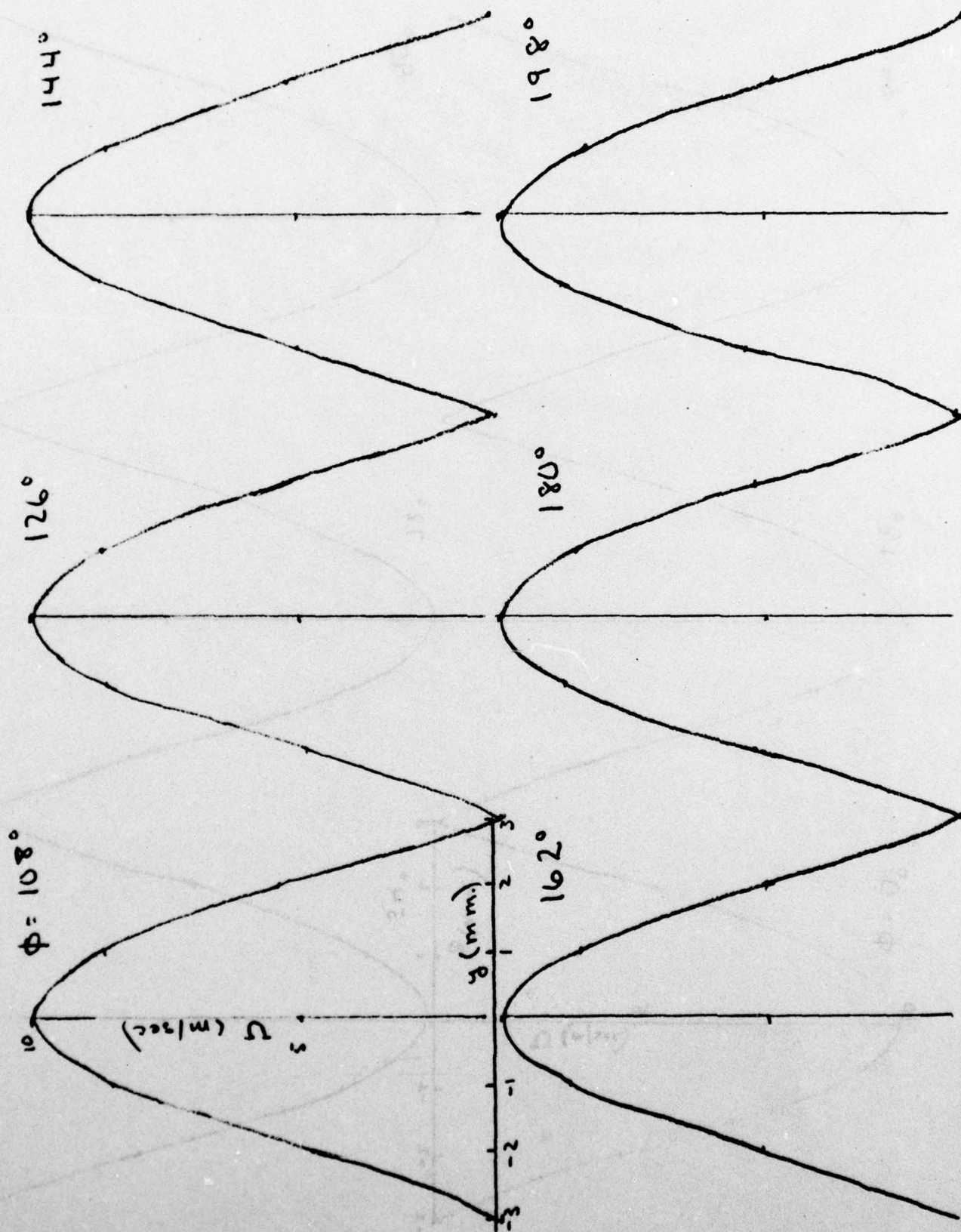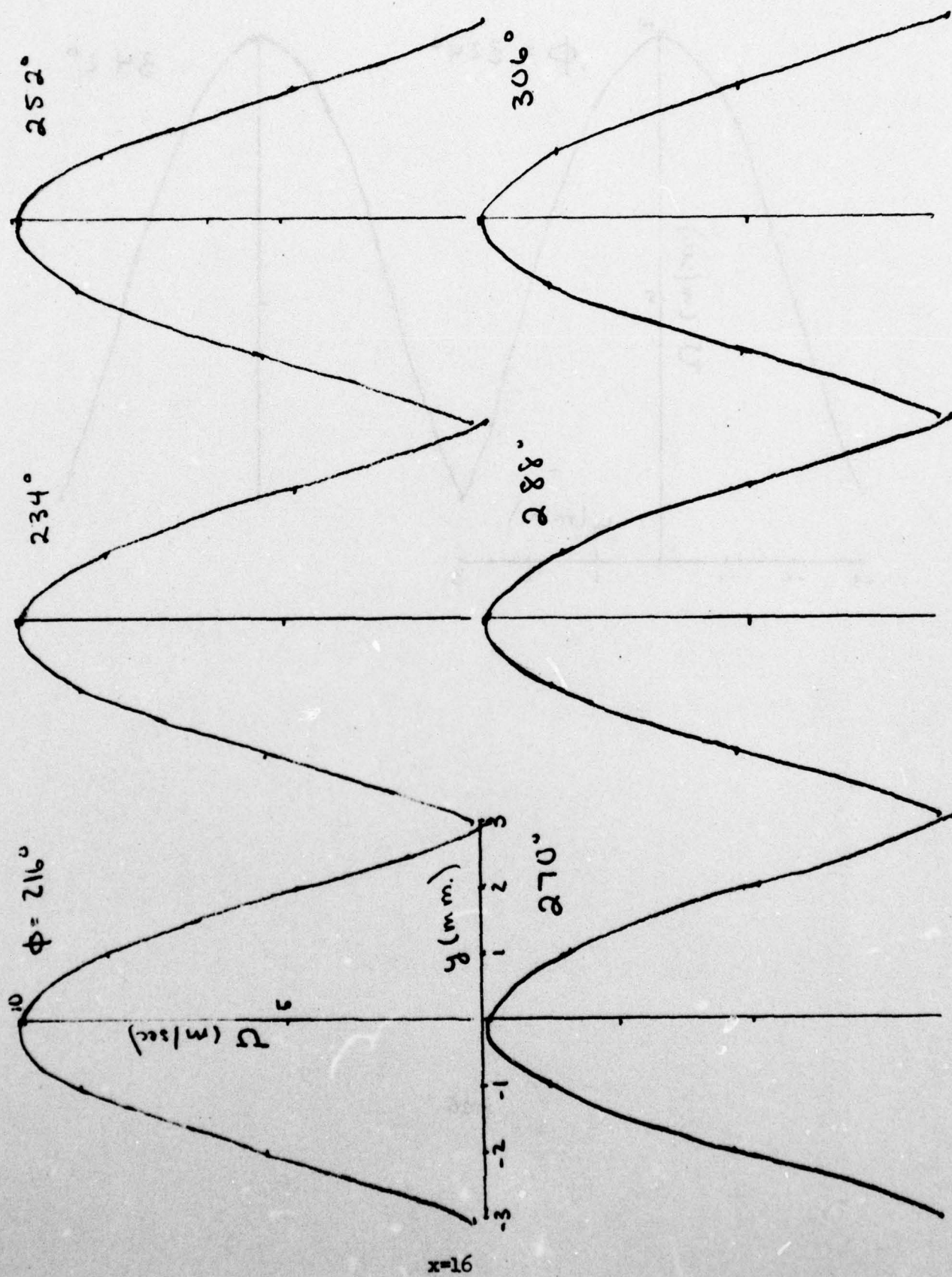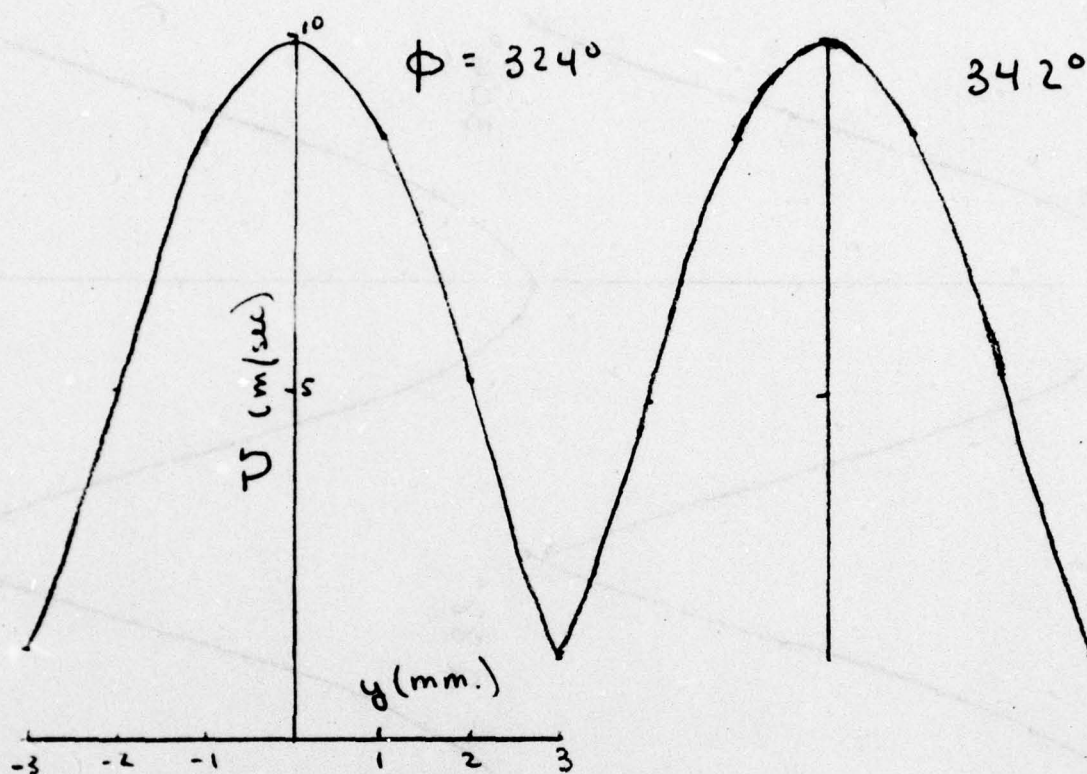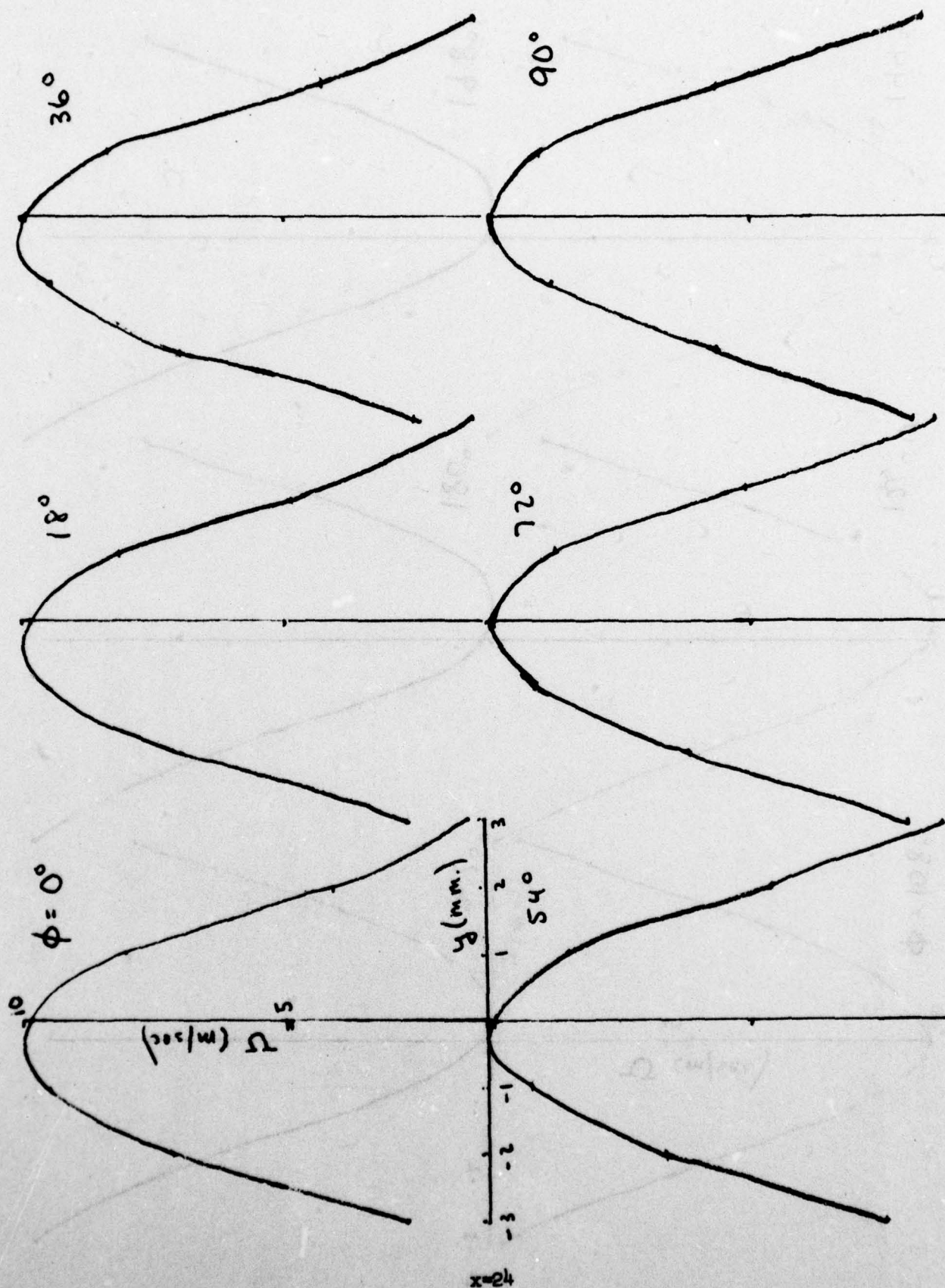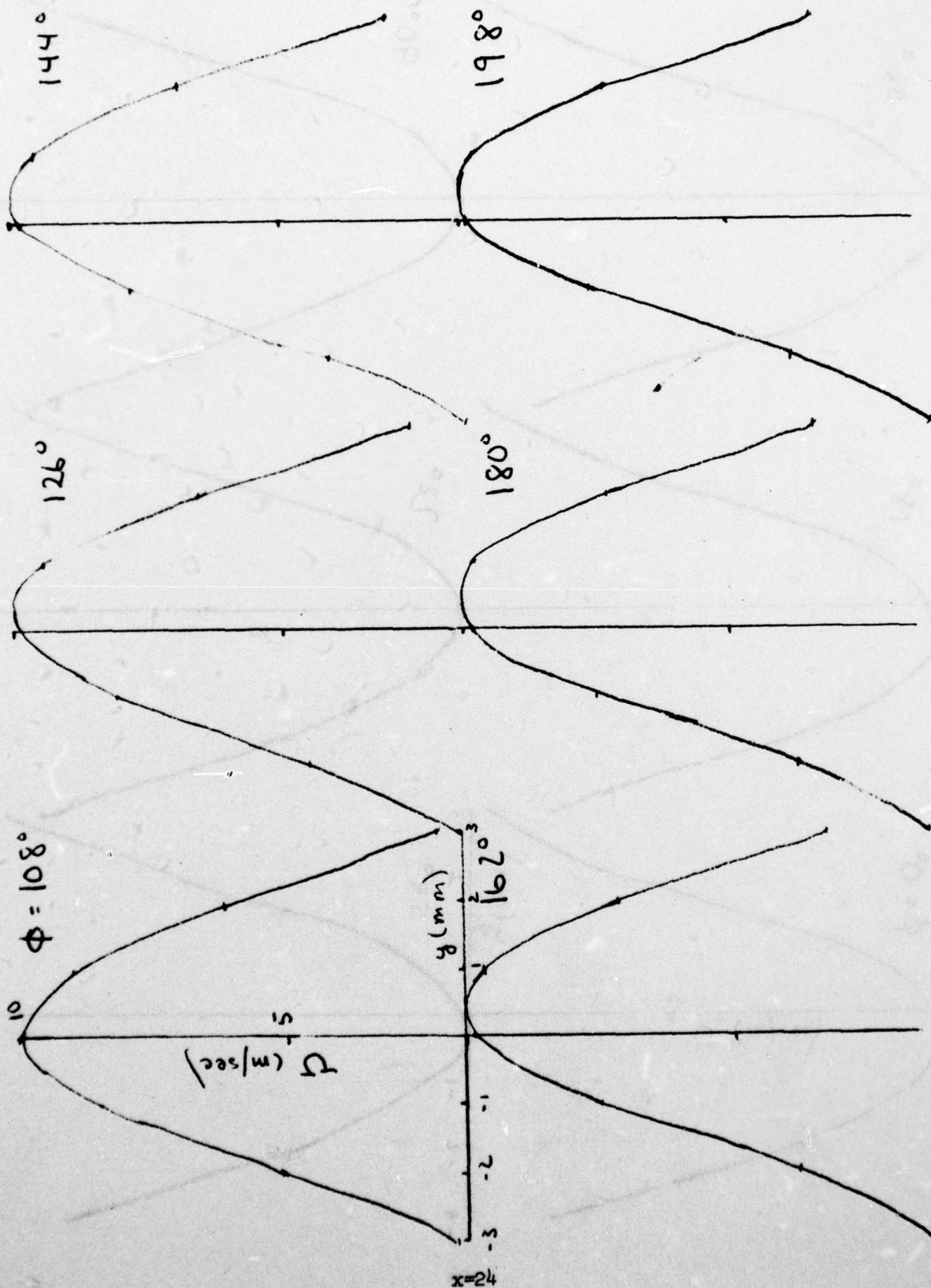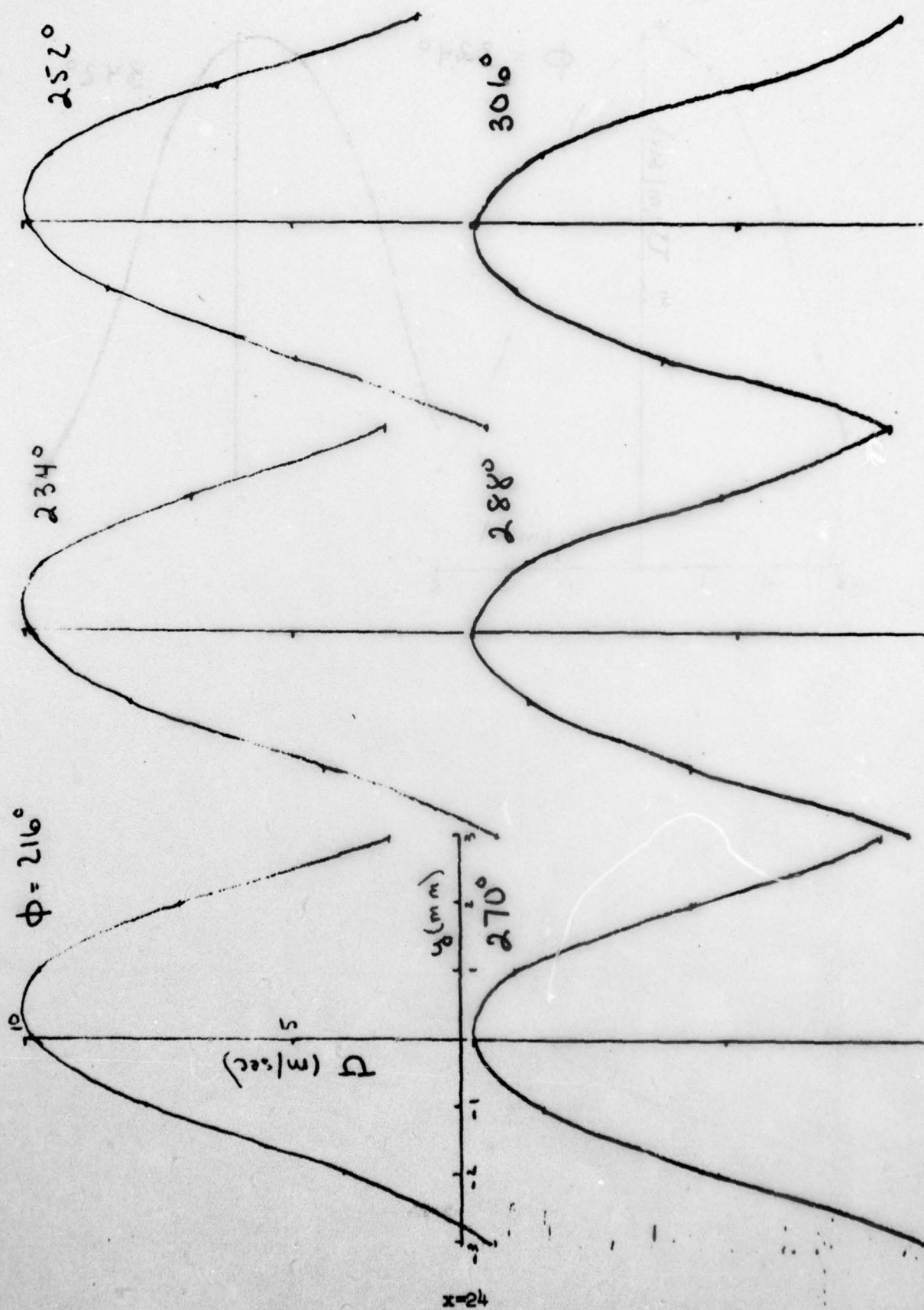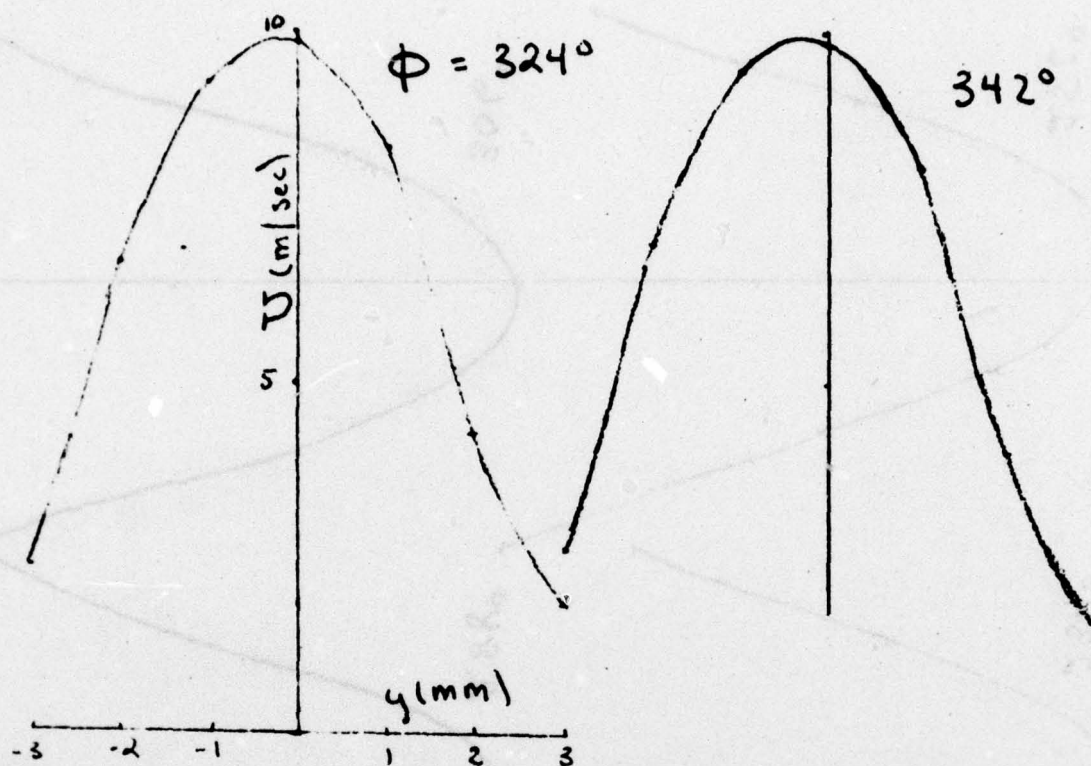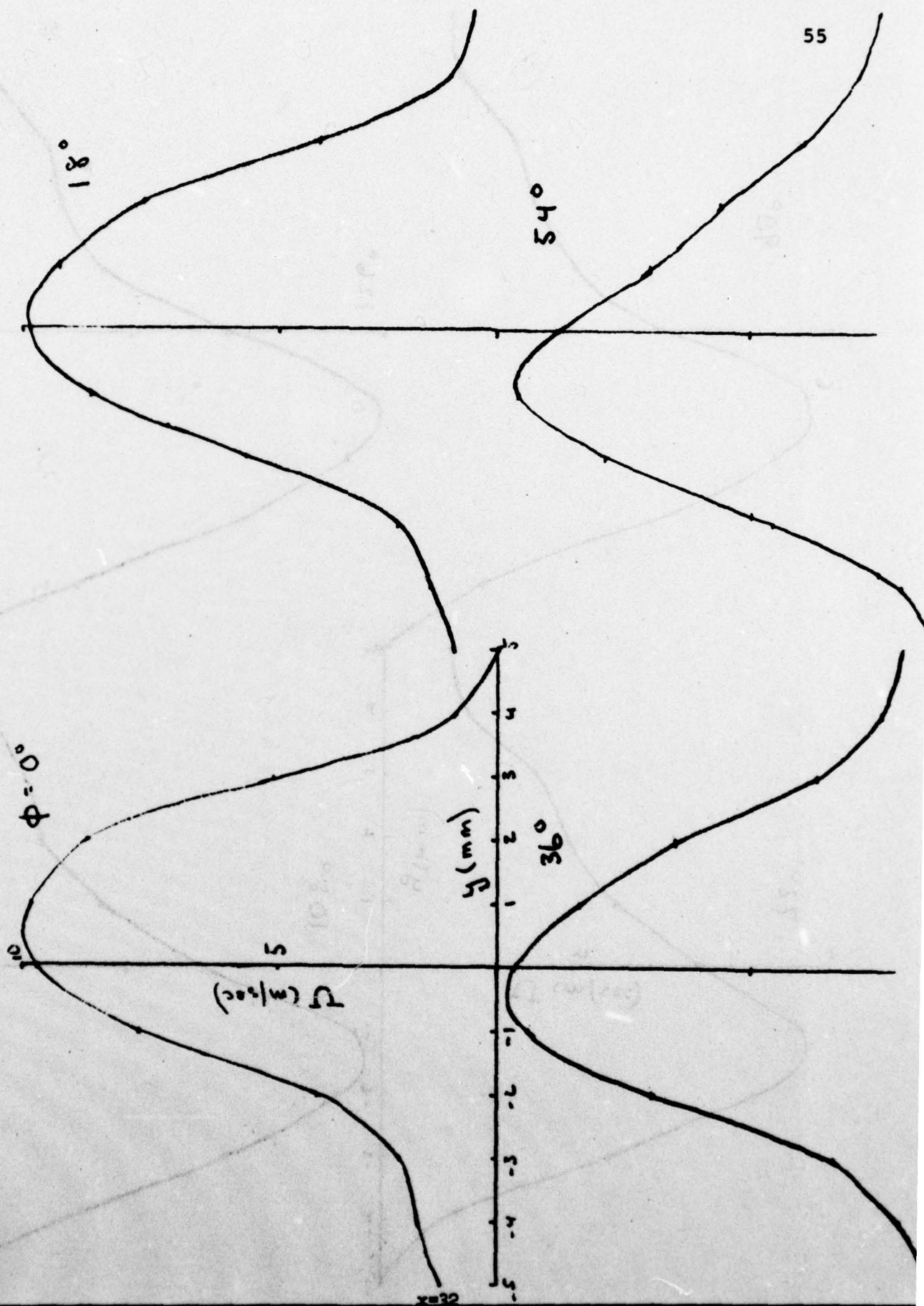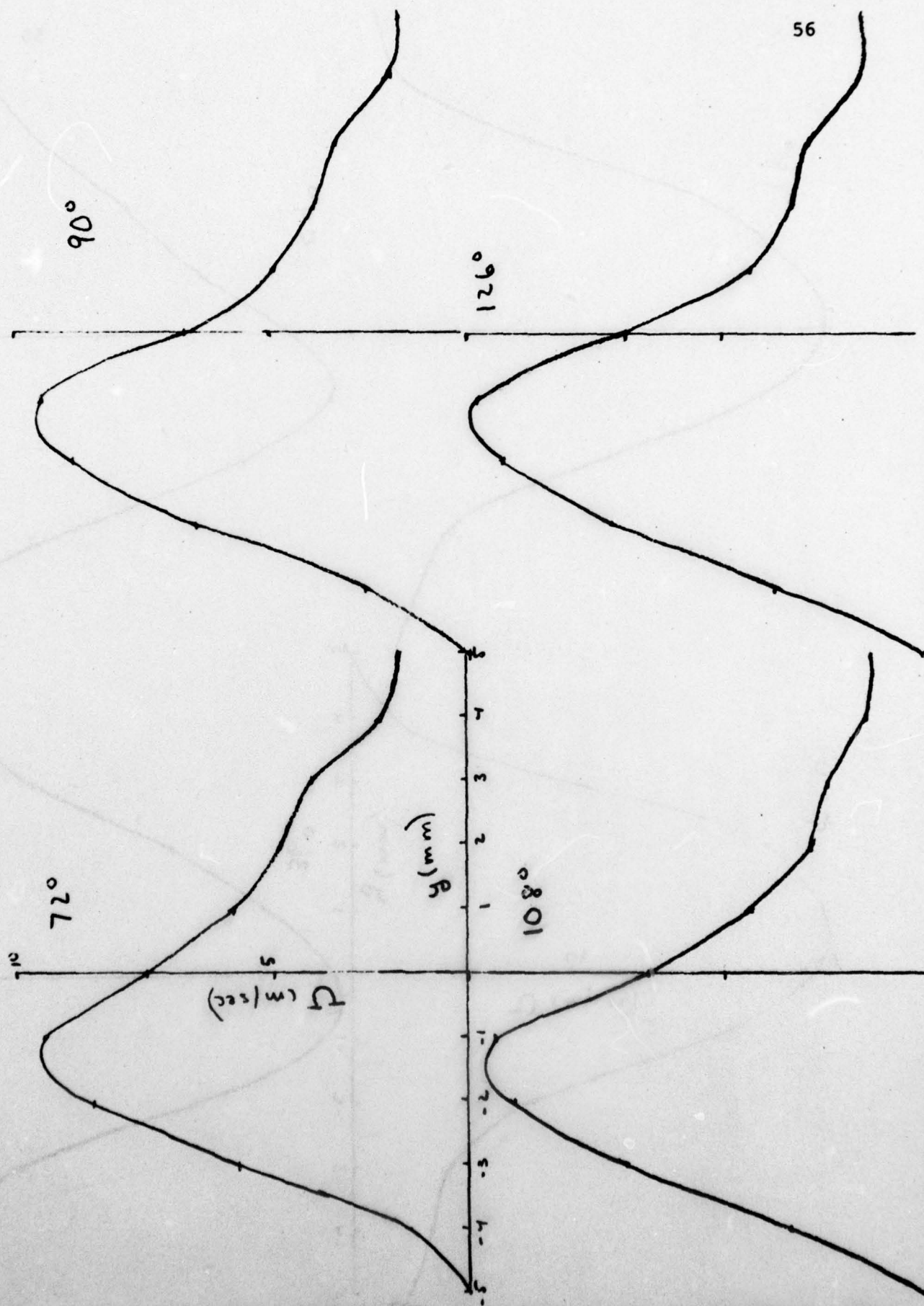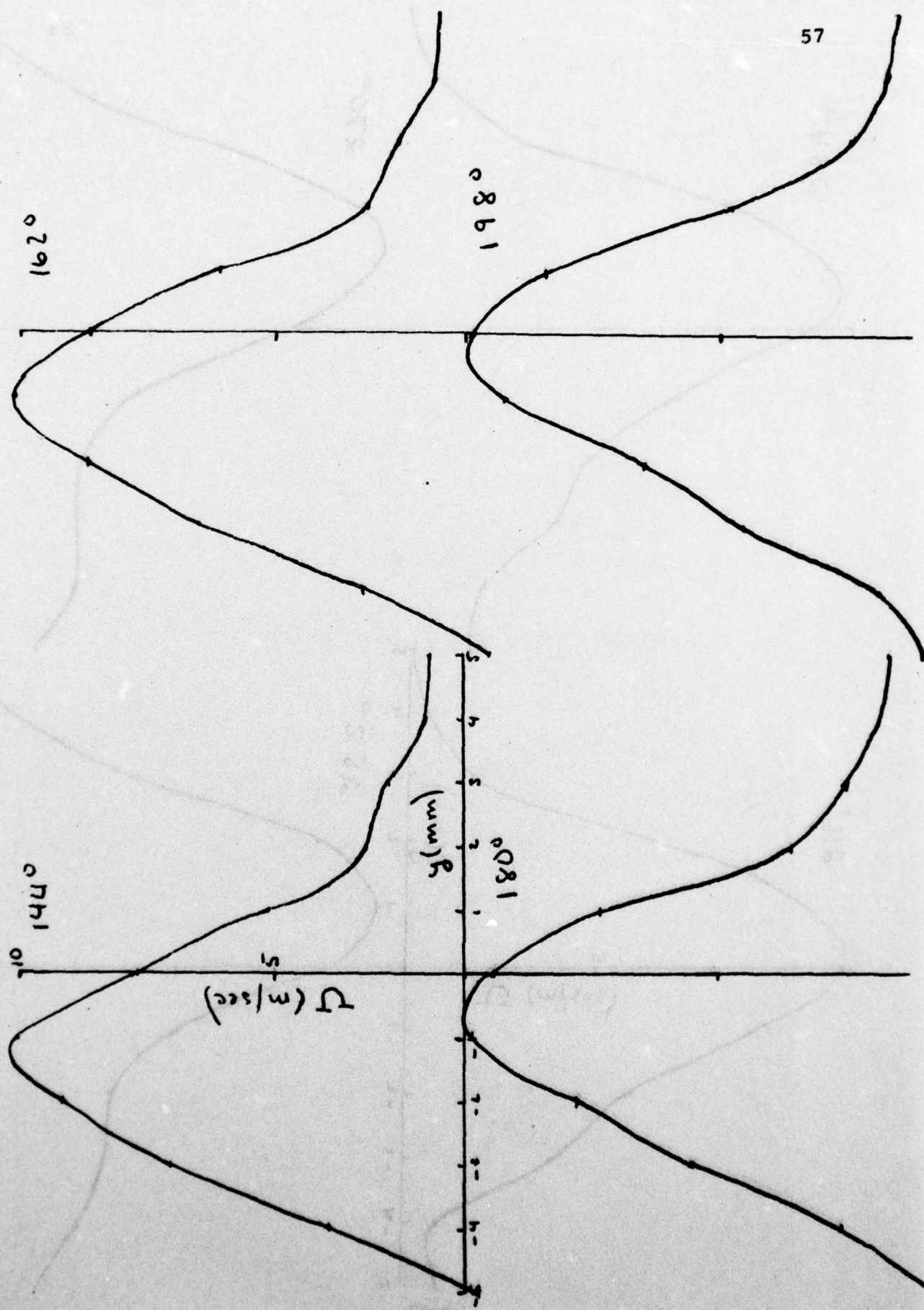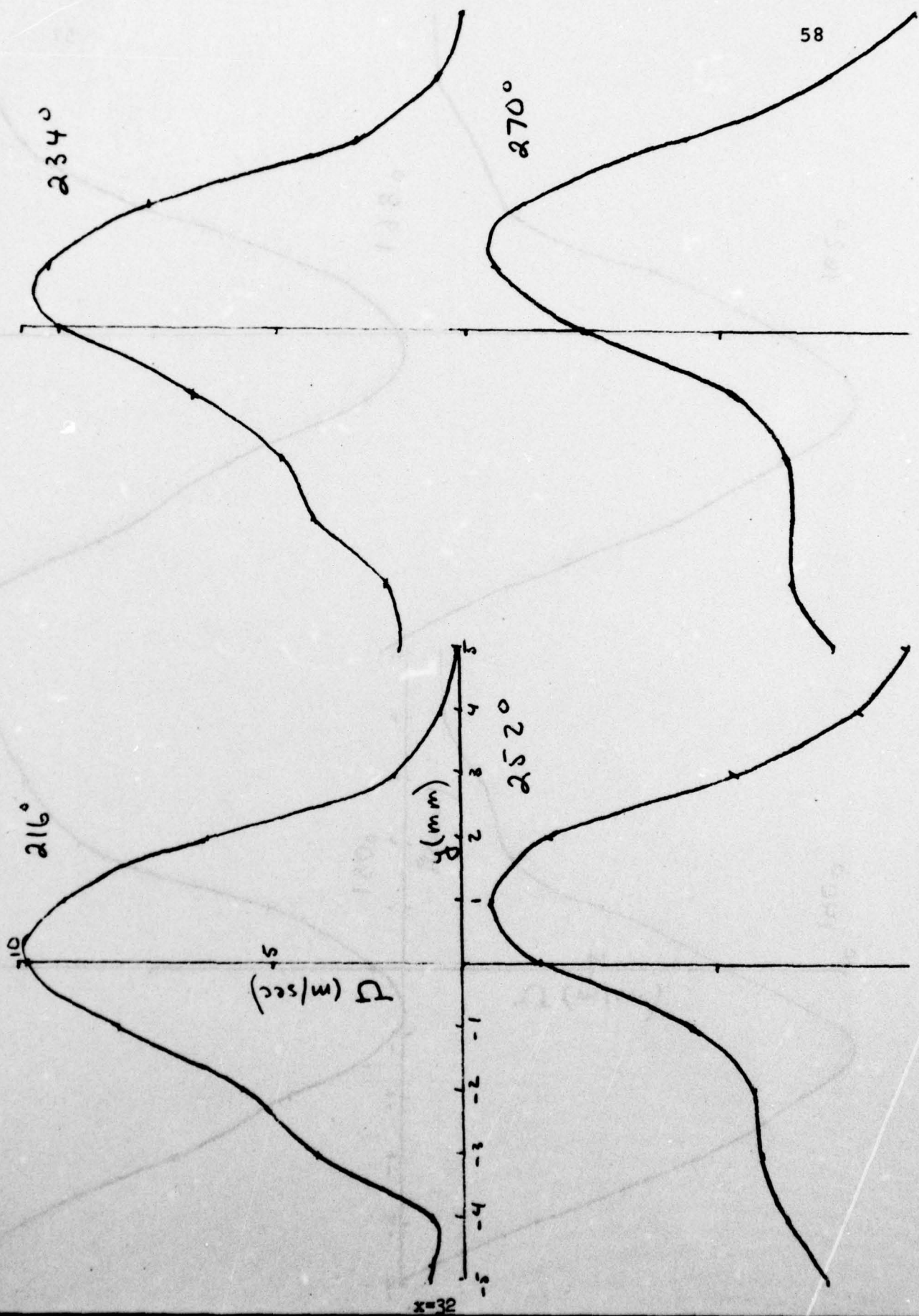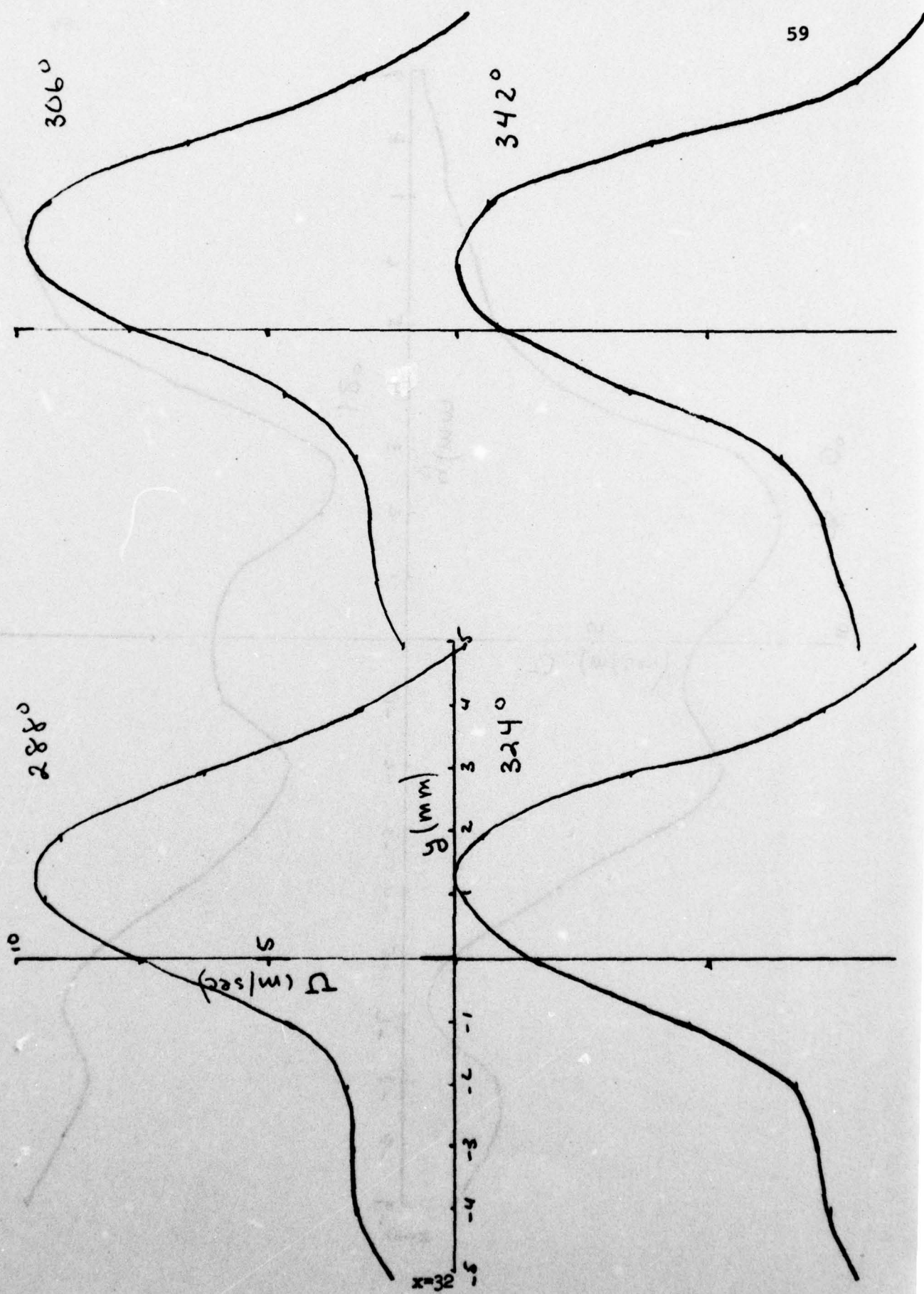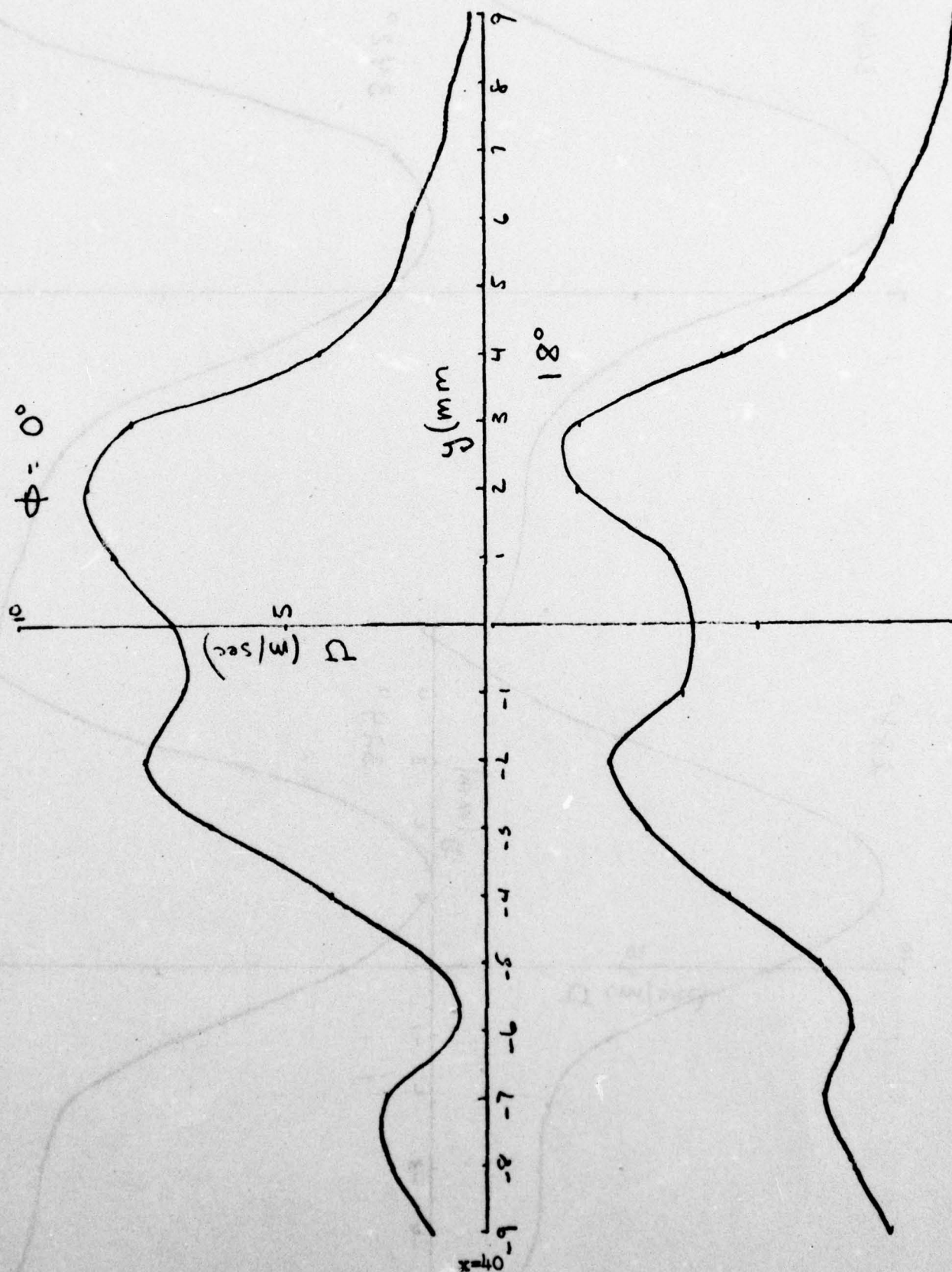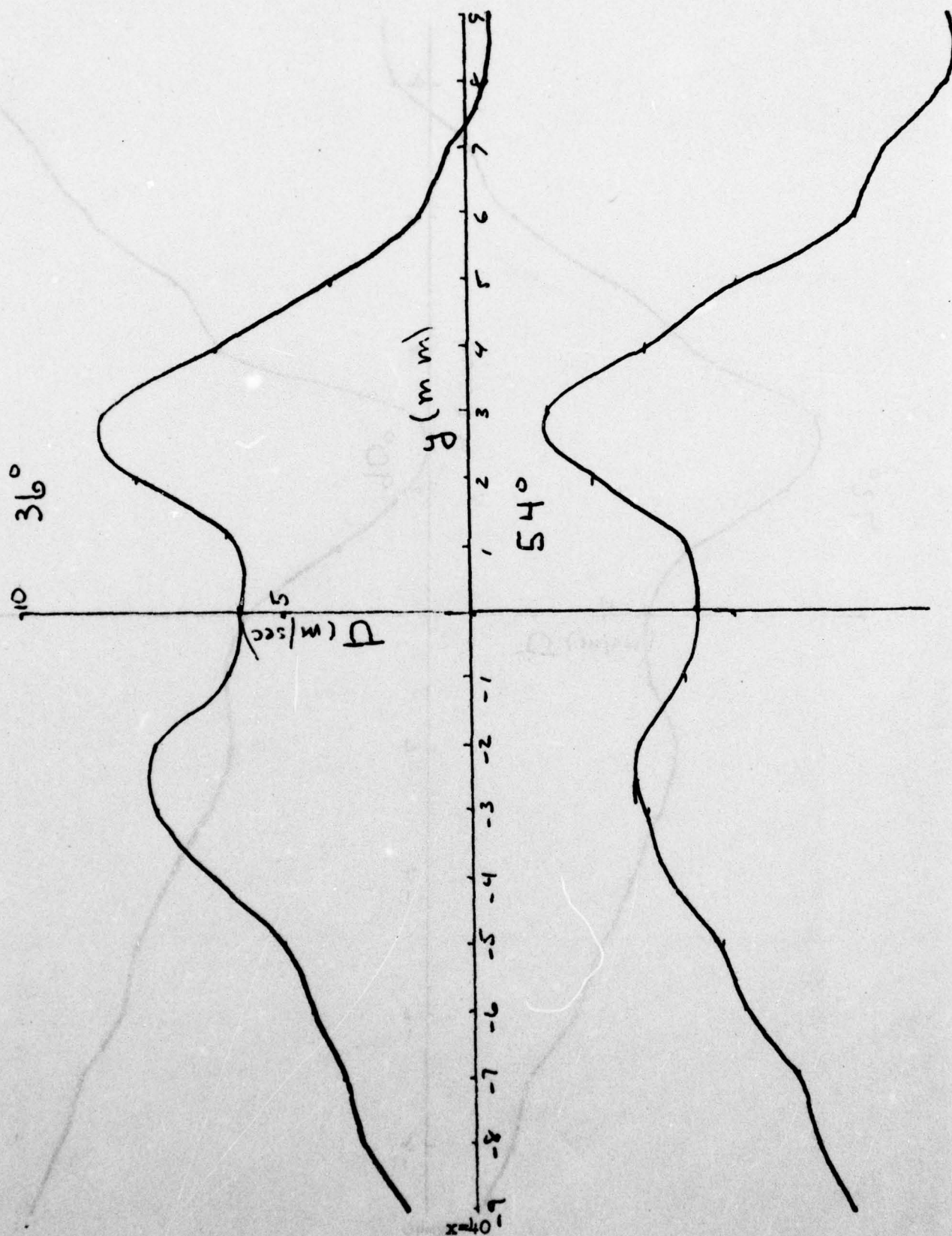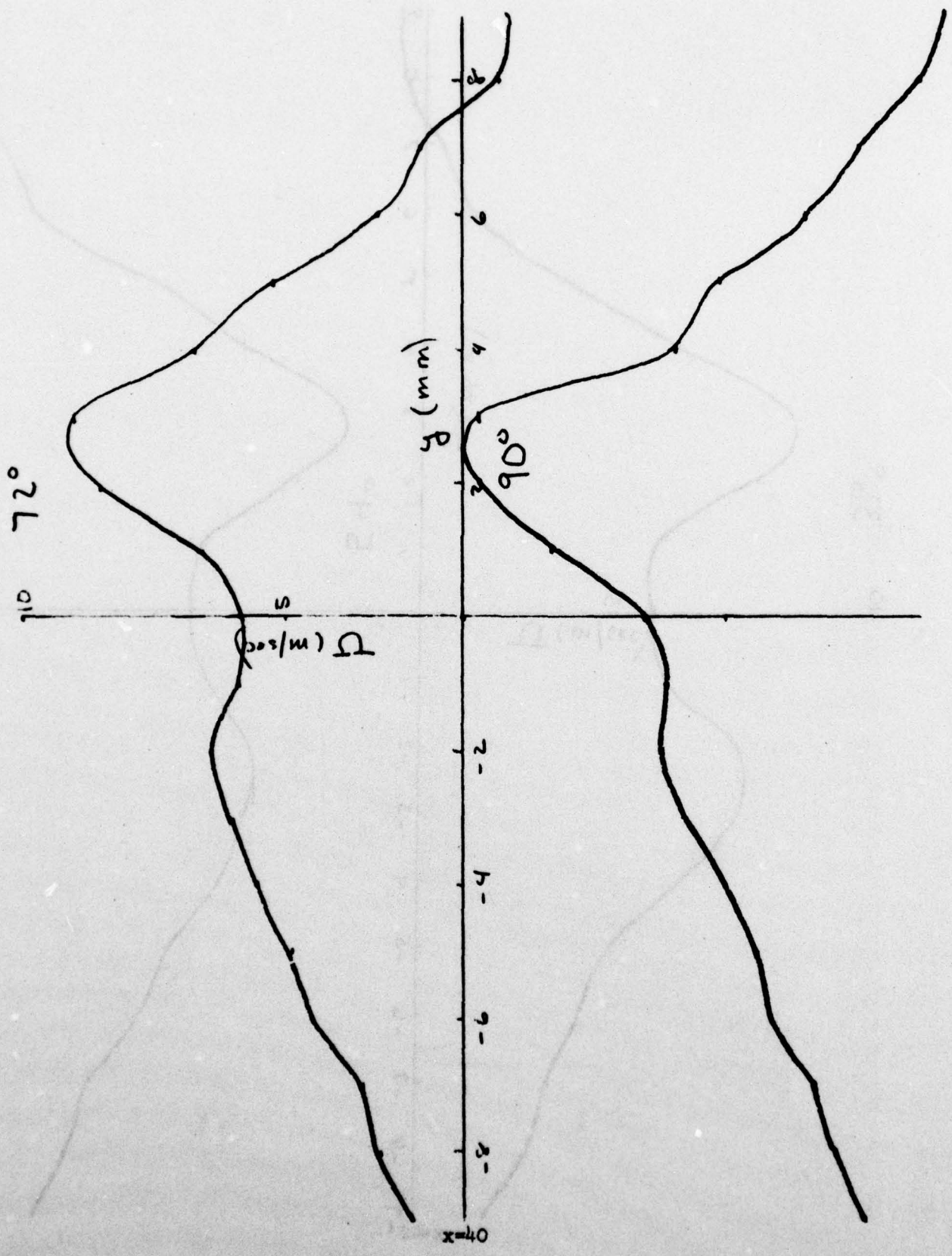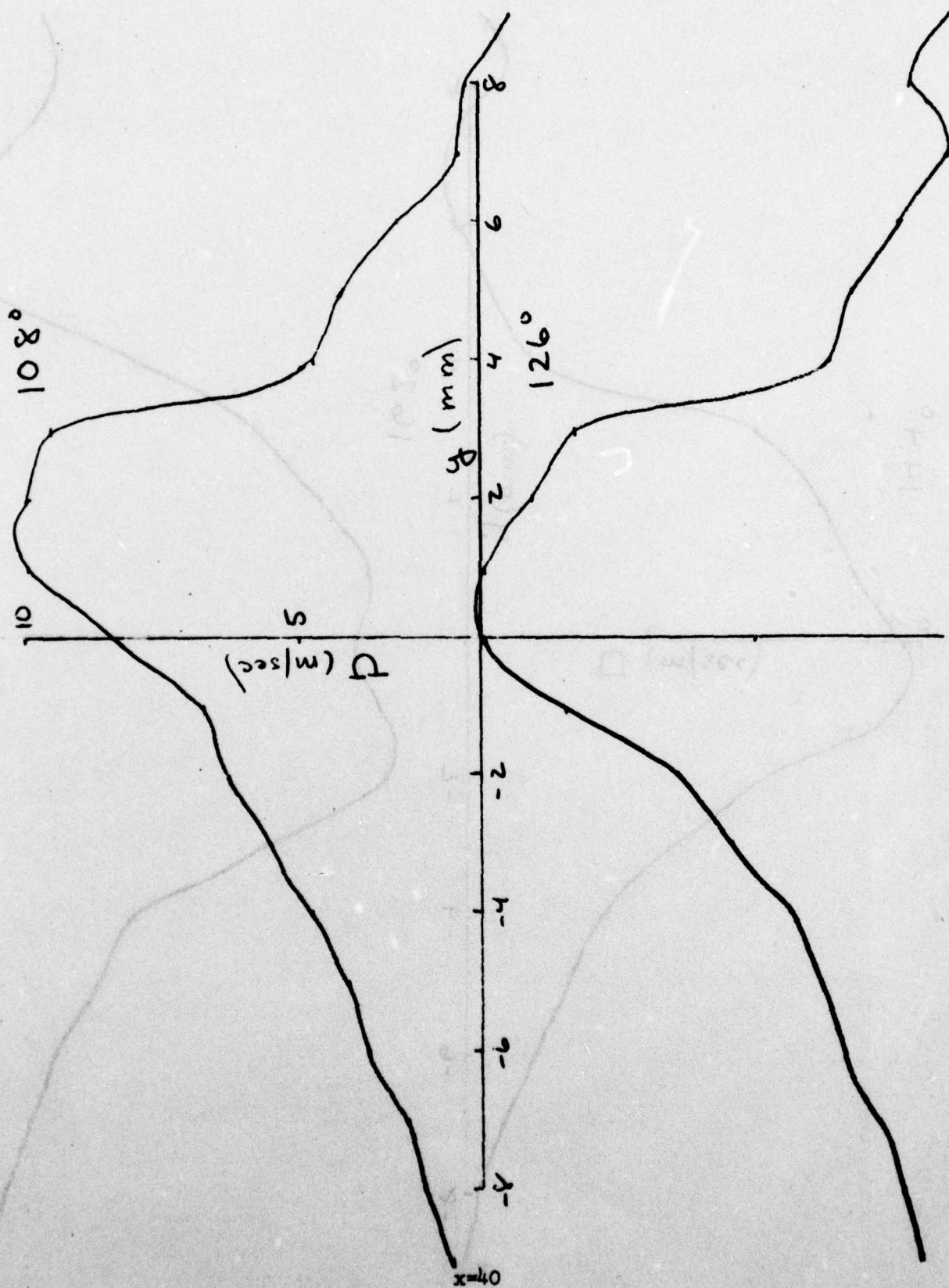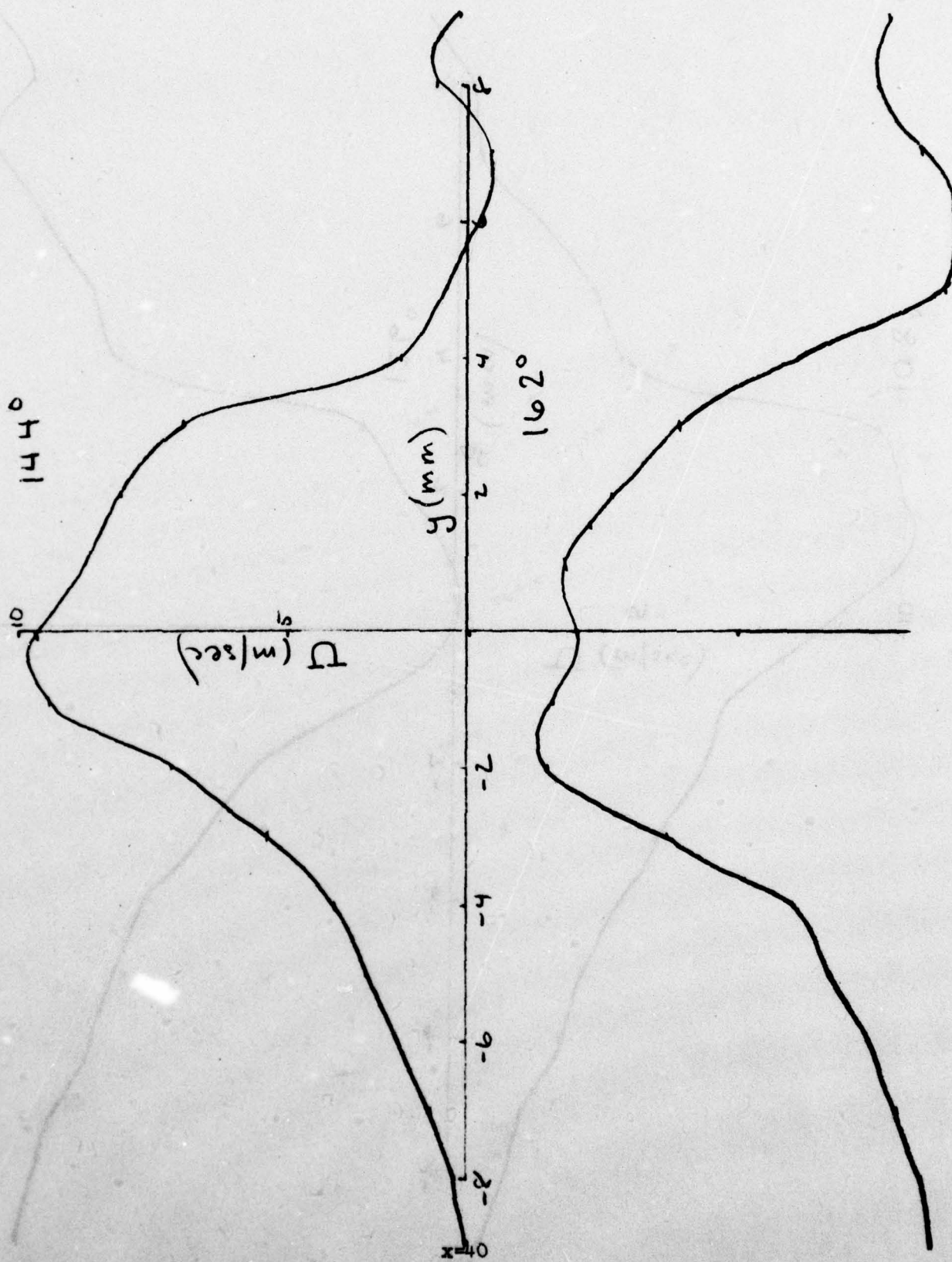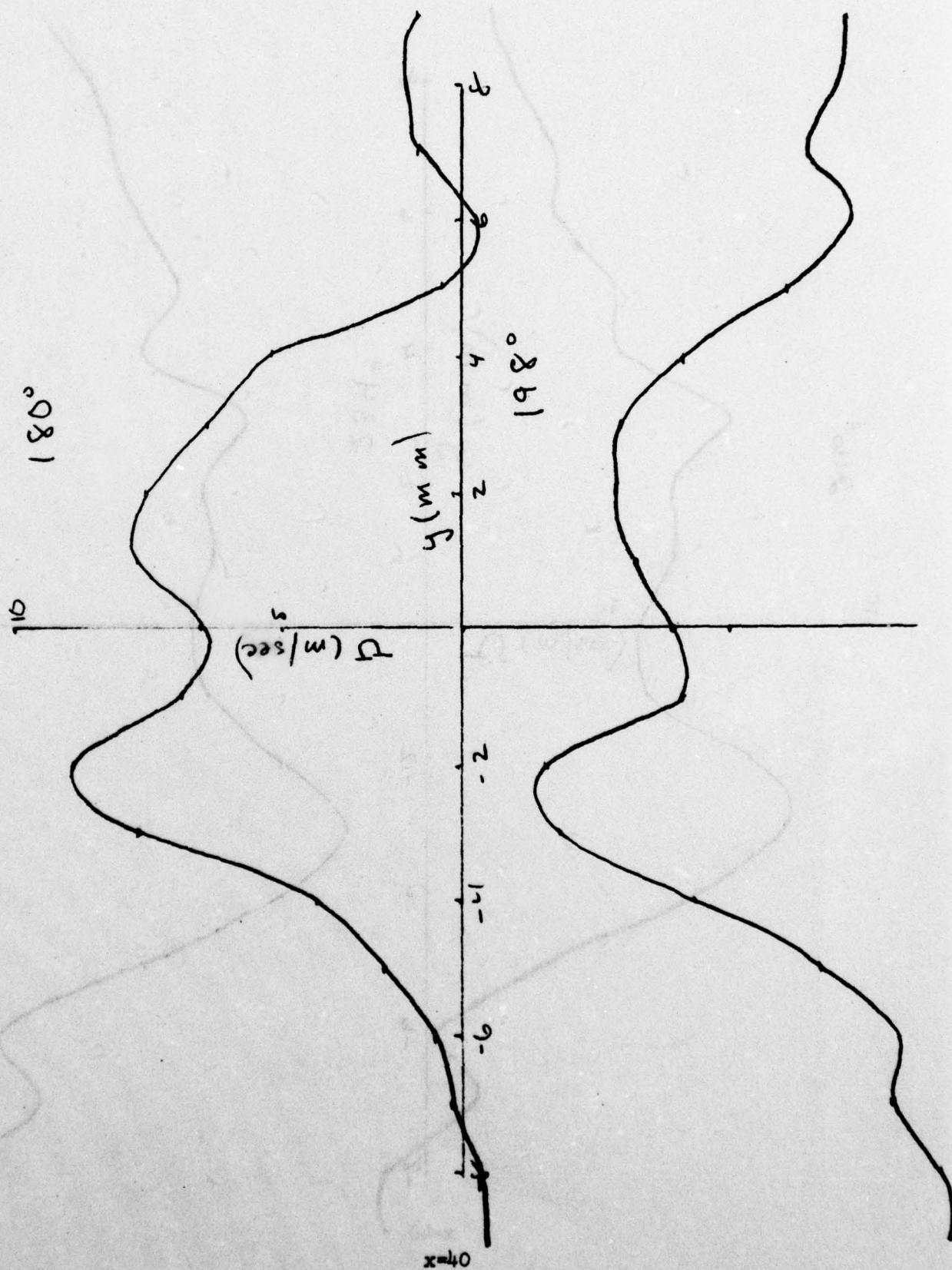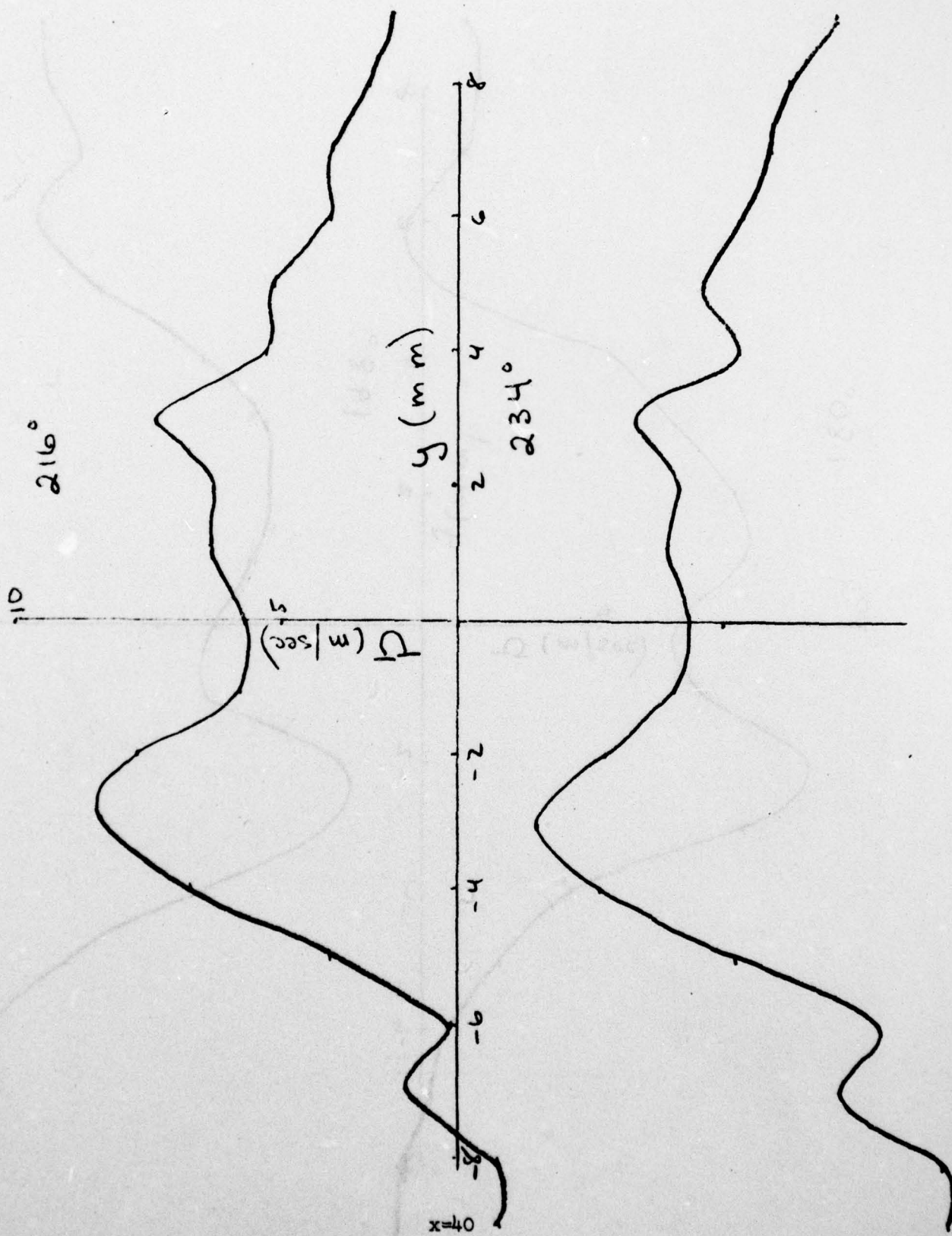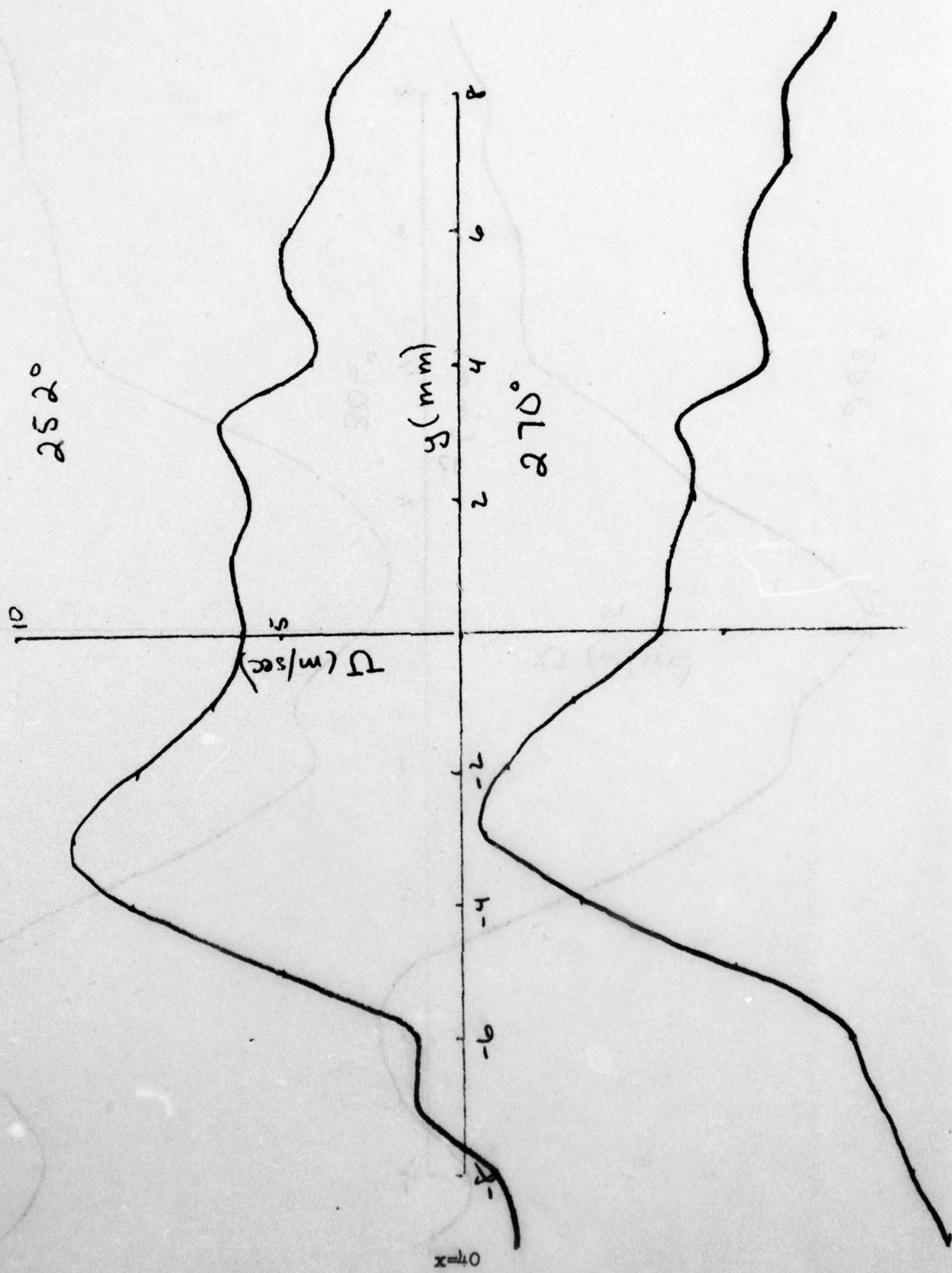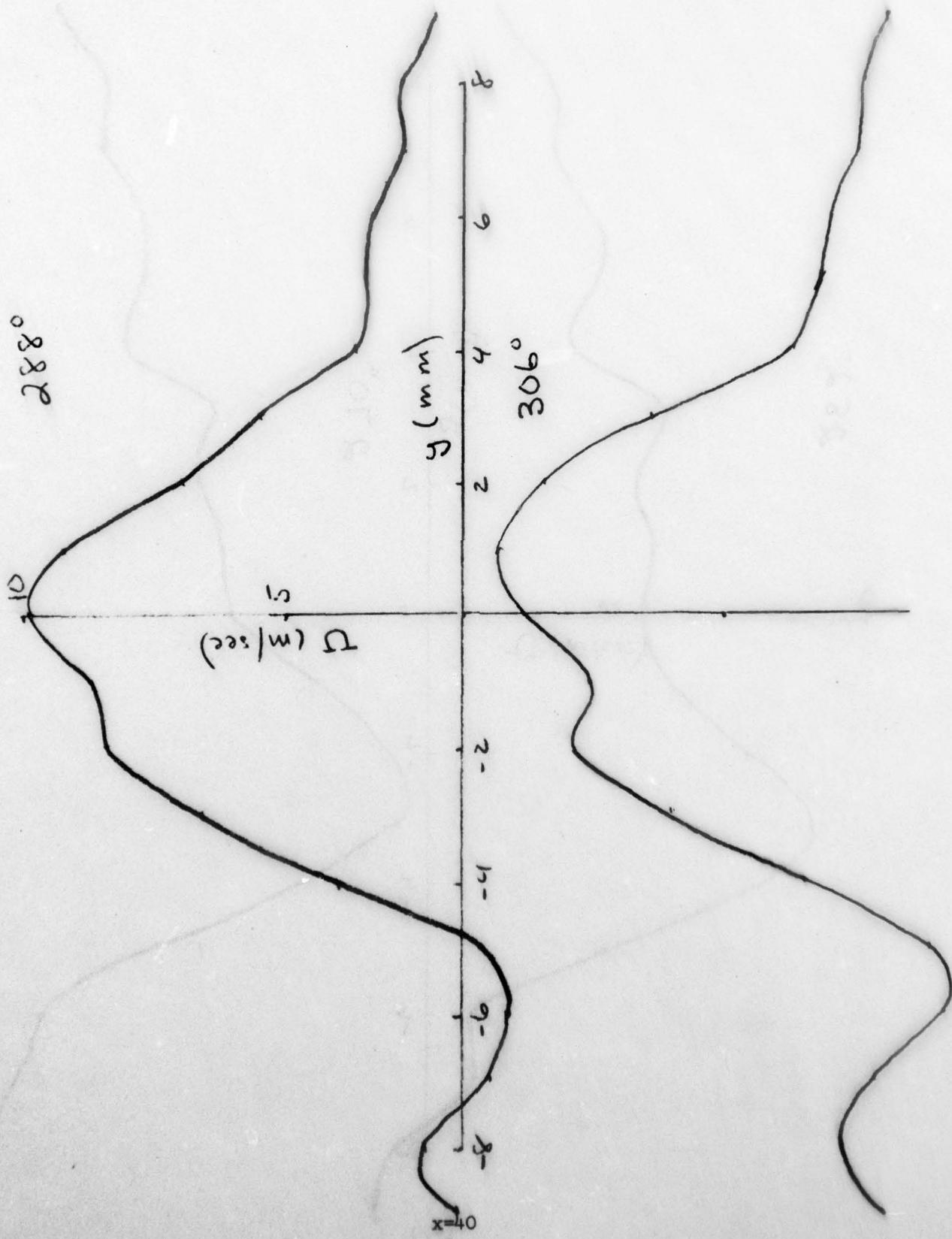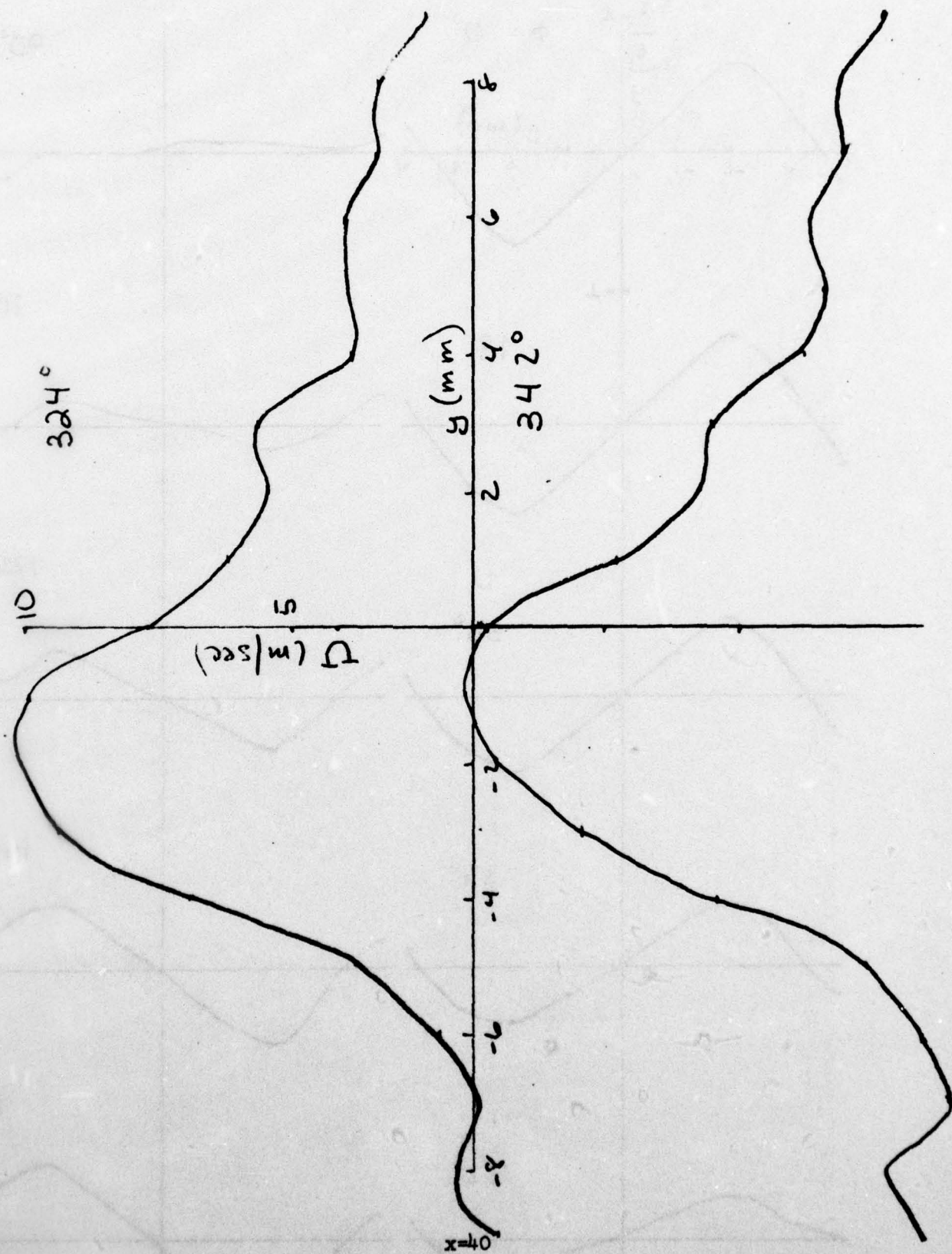
x=40

Fluctuating Velocity Component (u) Profiles
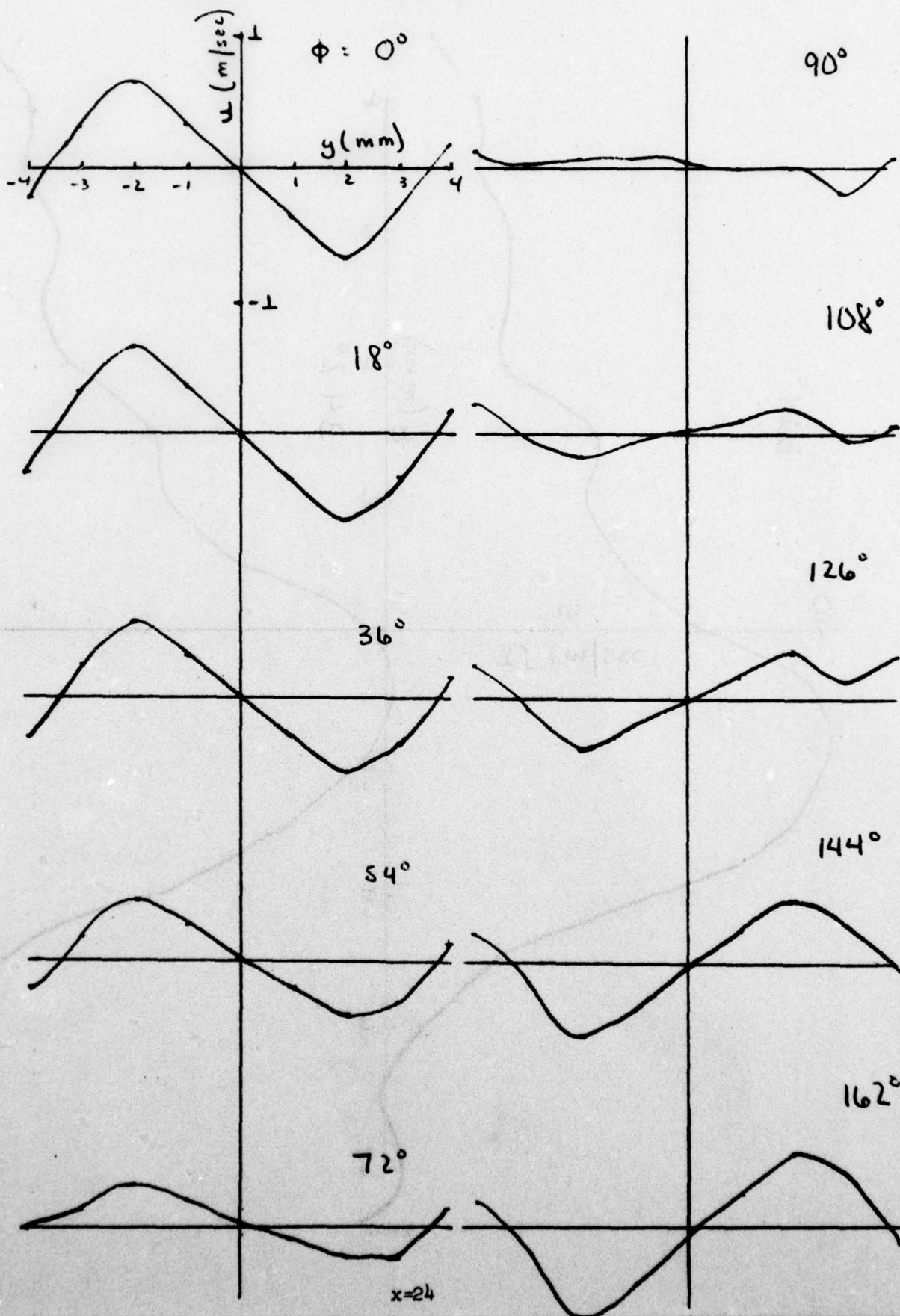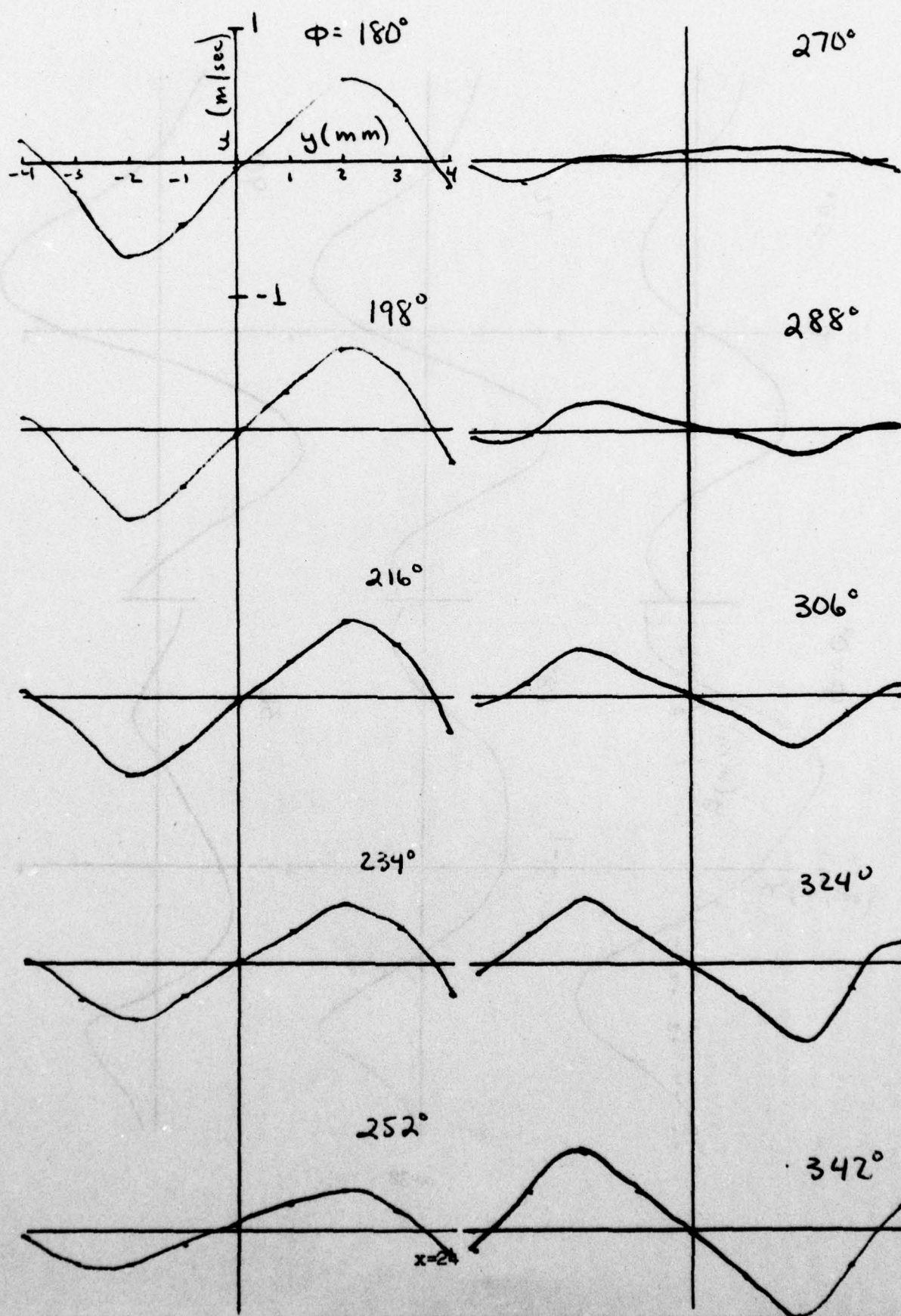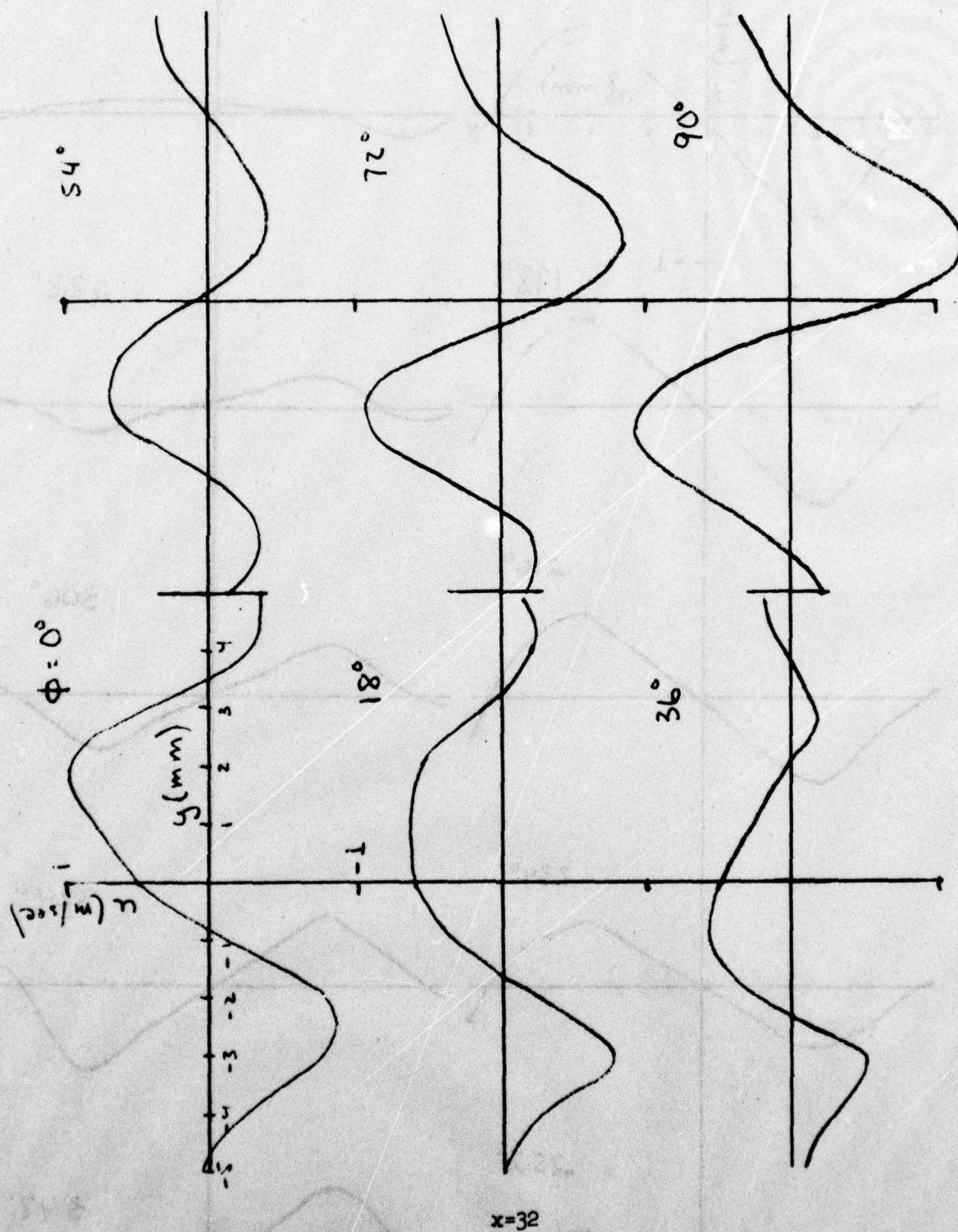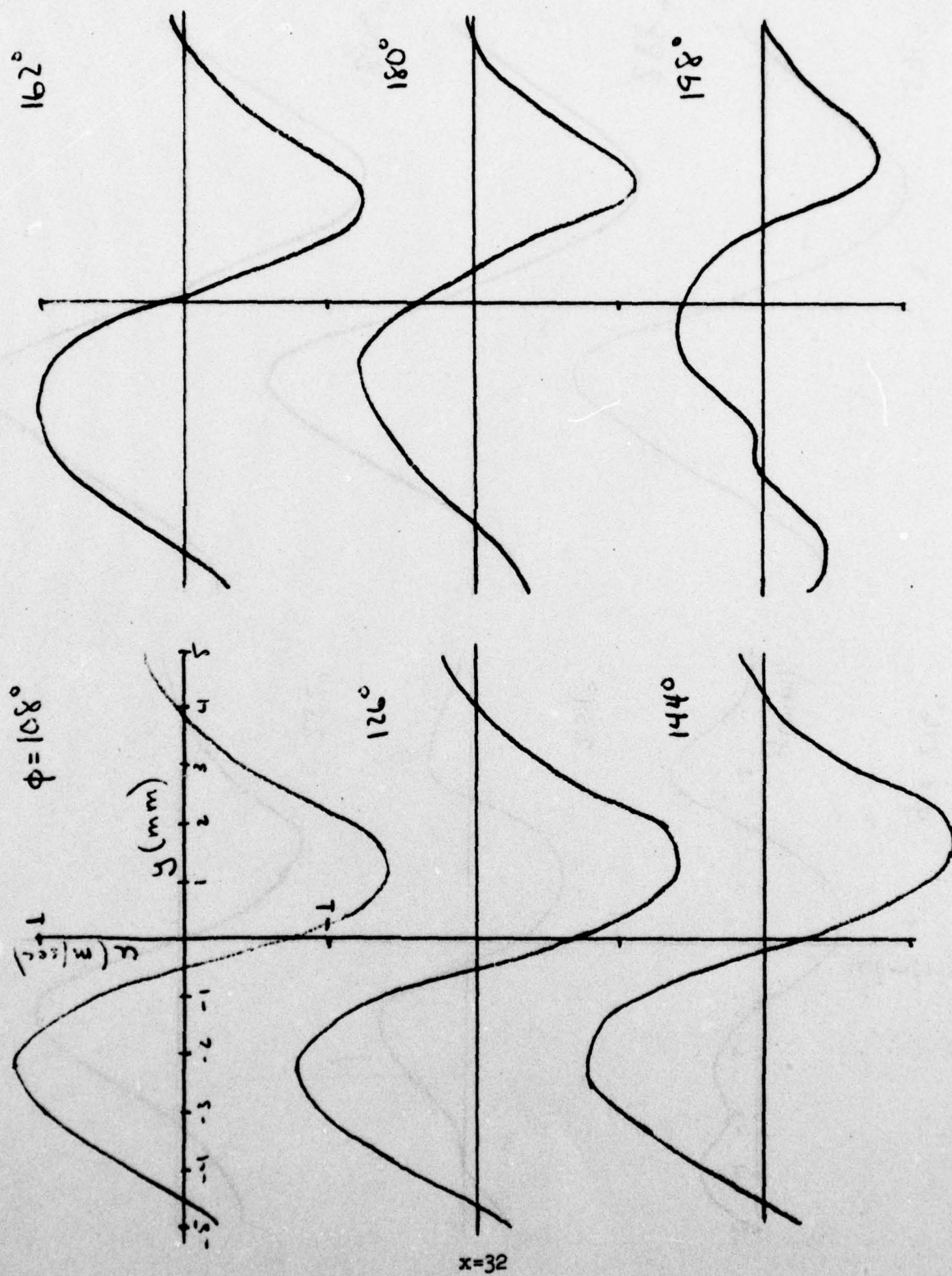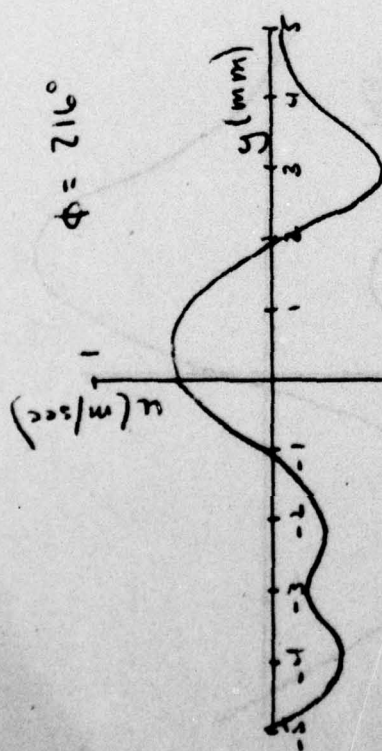
$\Phi = 216°$
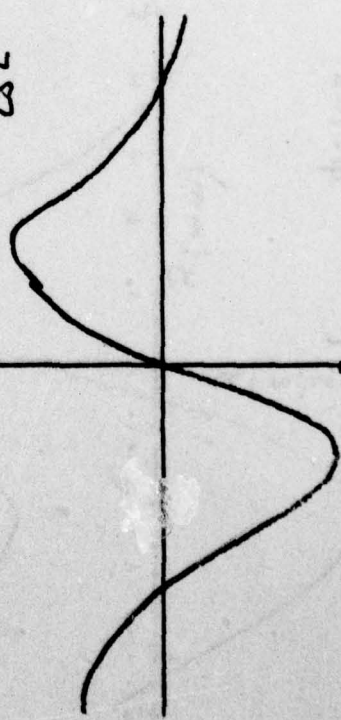
234°

252°

270°

288°

306°

$y(mm)$

$u(m/sec)$

x=32

$\phi = 180°$

78

$u\,(m/sec)$

$y\,(mm)$

$198°$

$216°$

$234°$

$252°$

$x=40$

$\phi = 270°$

$u\ (m/sec)$

$y\ (mm)$
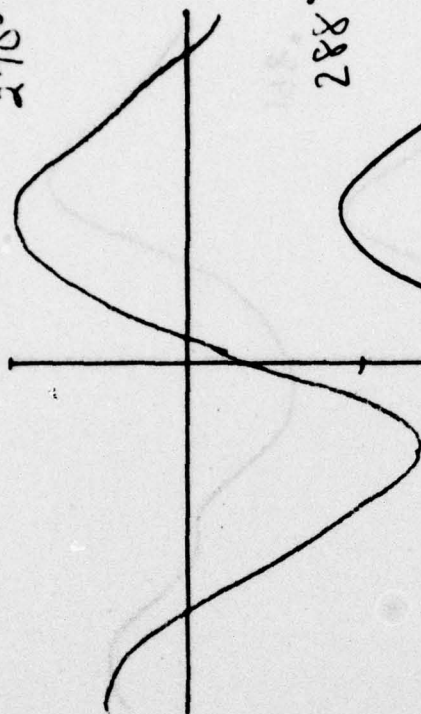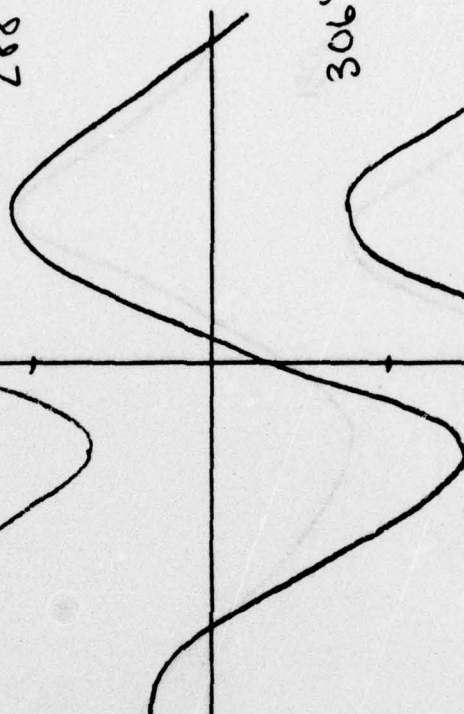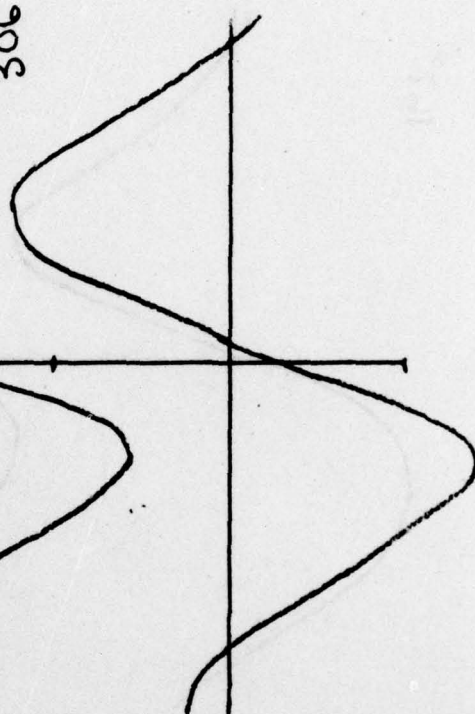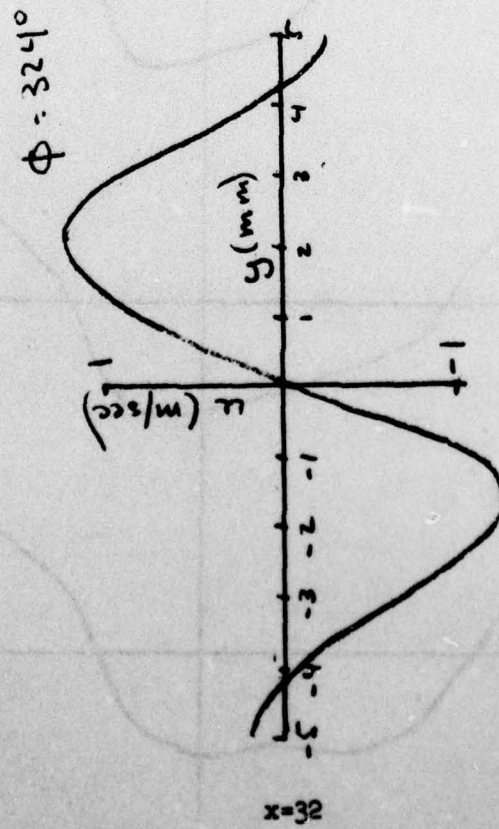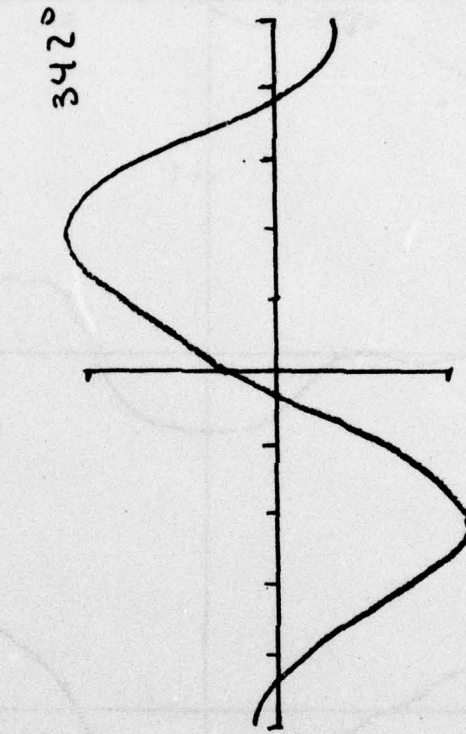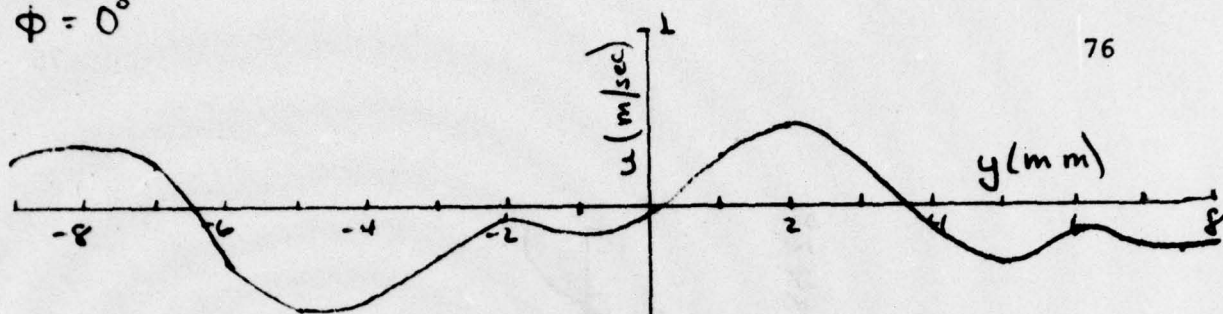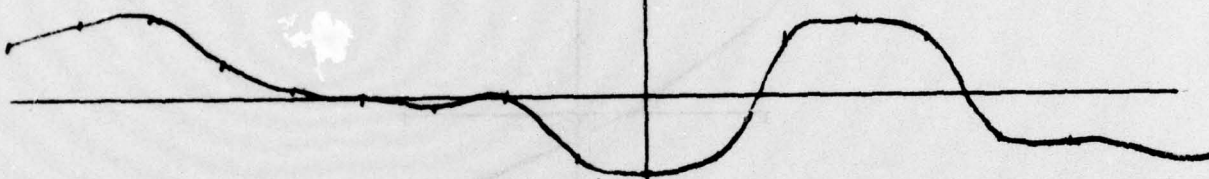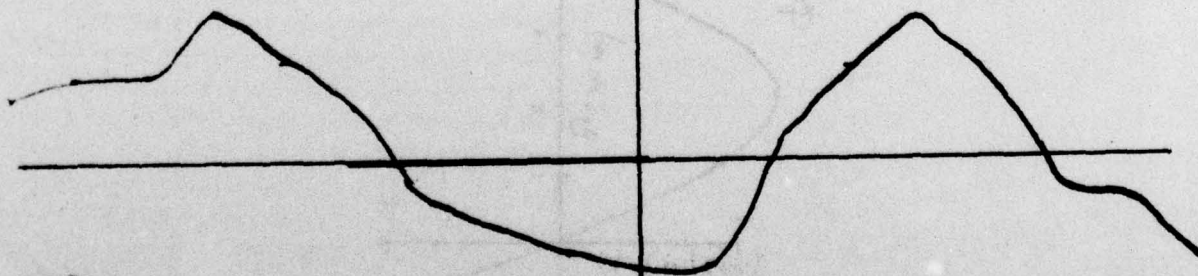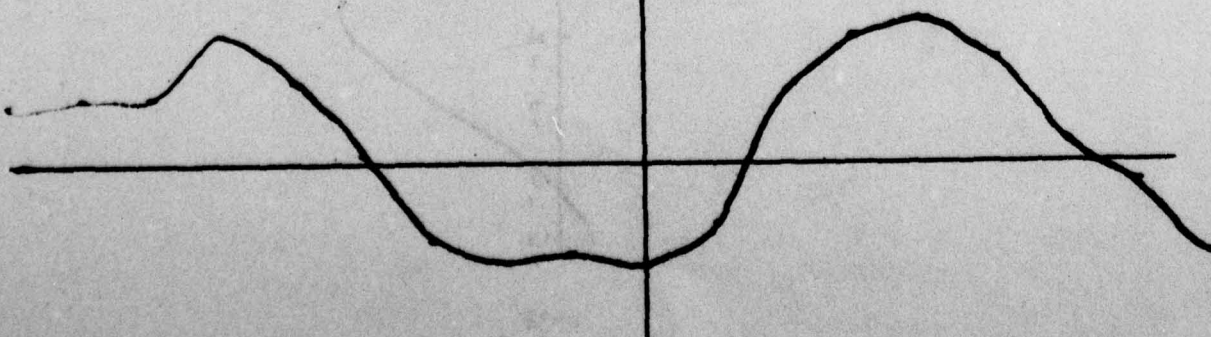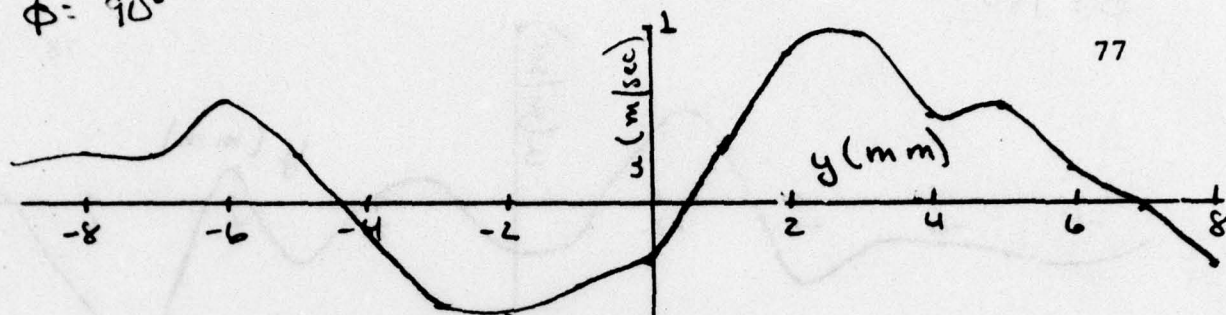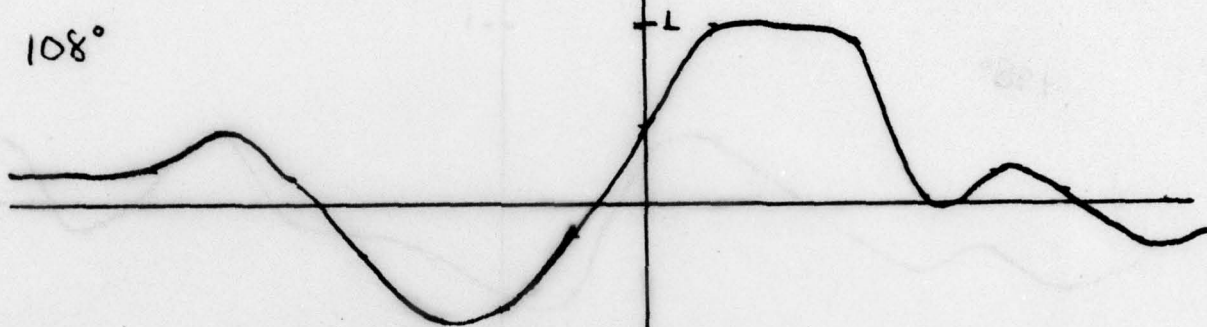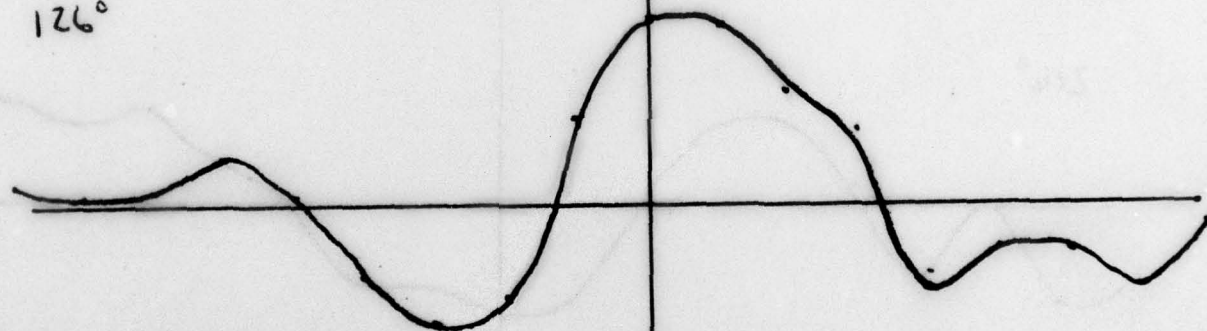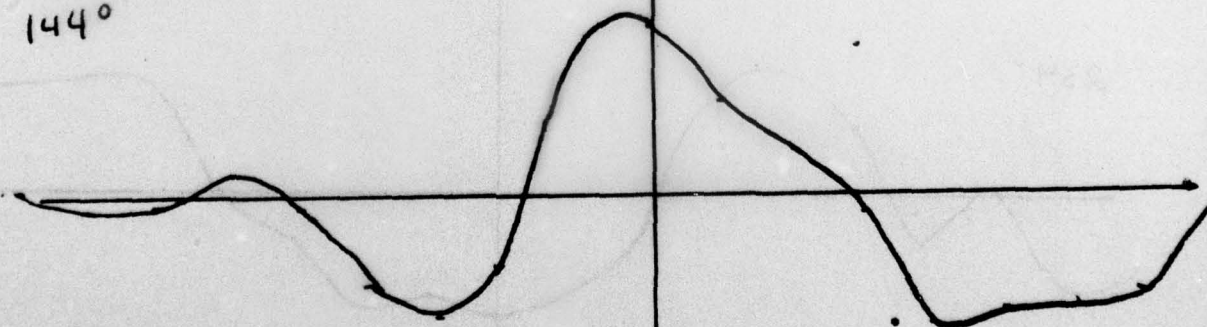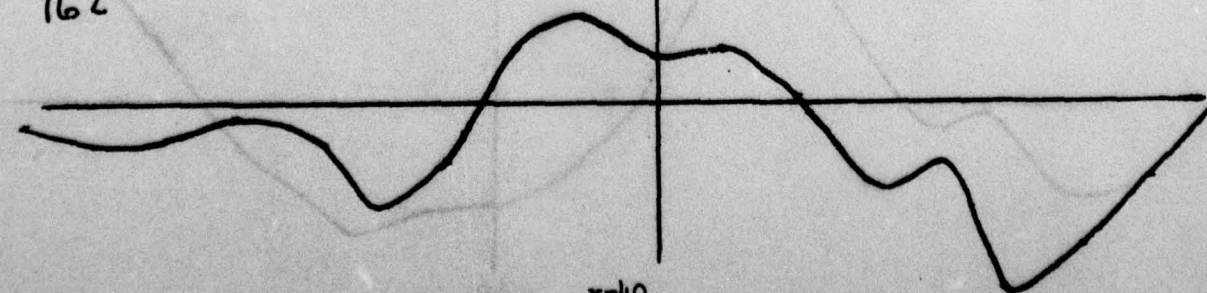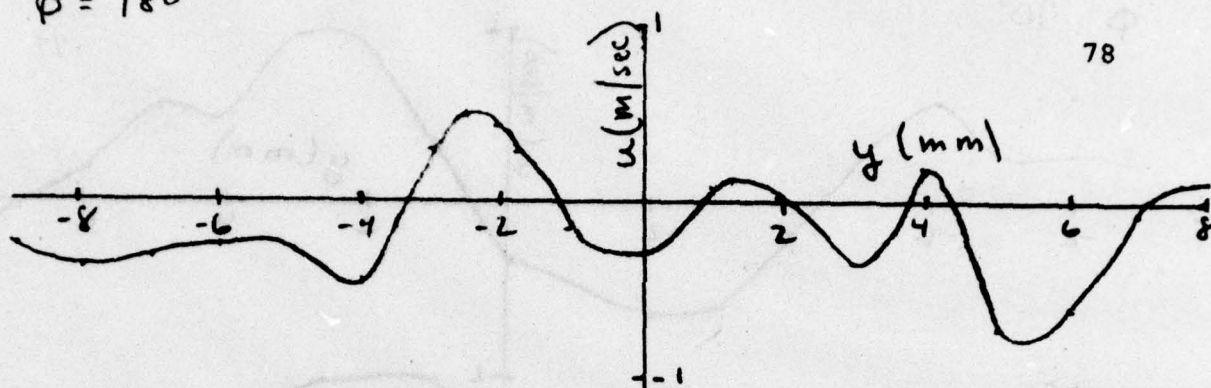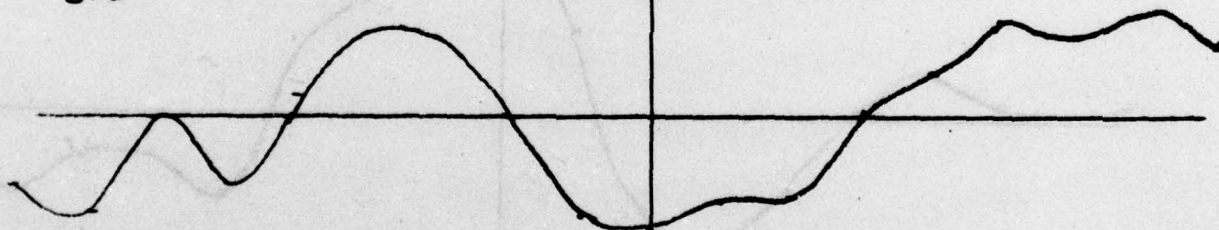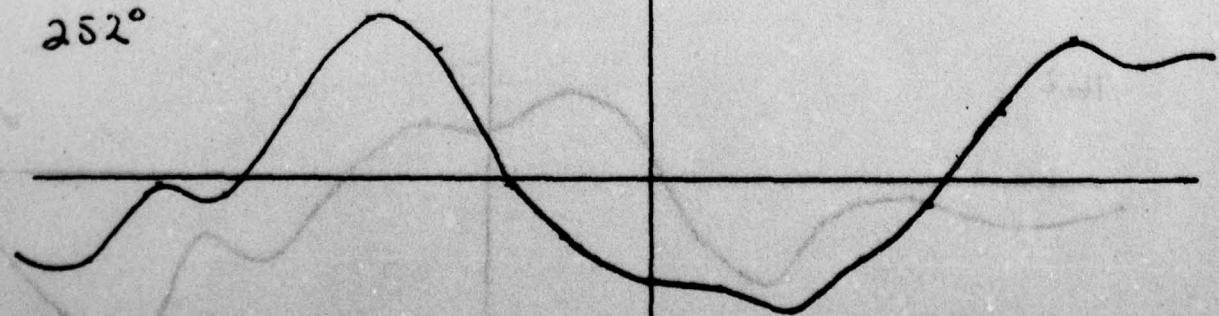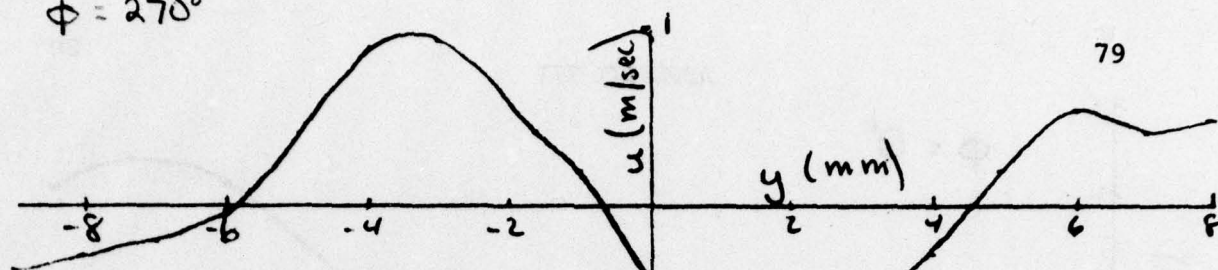
79

$288°$

$306°$

$324°$

$342°$
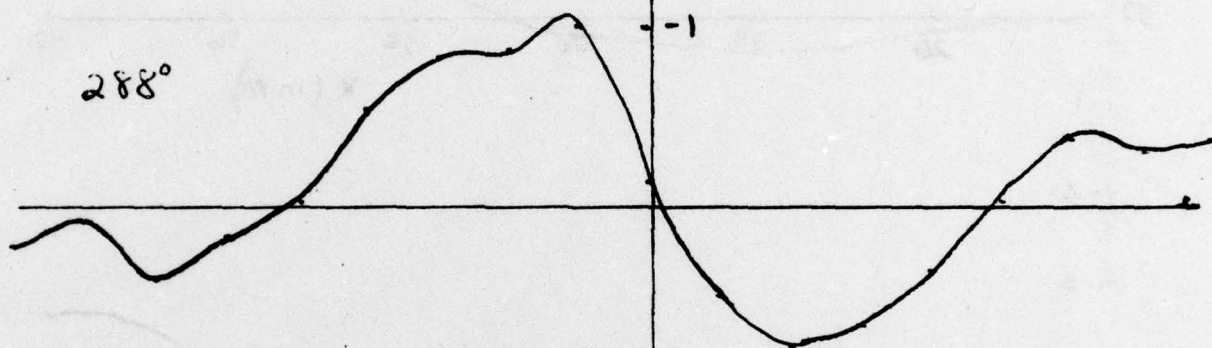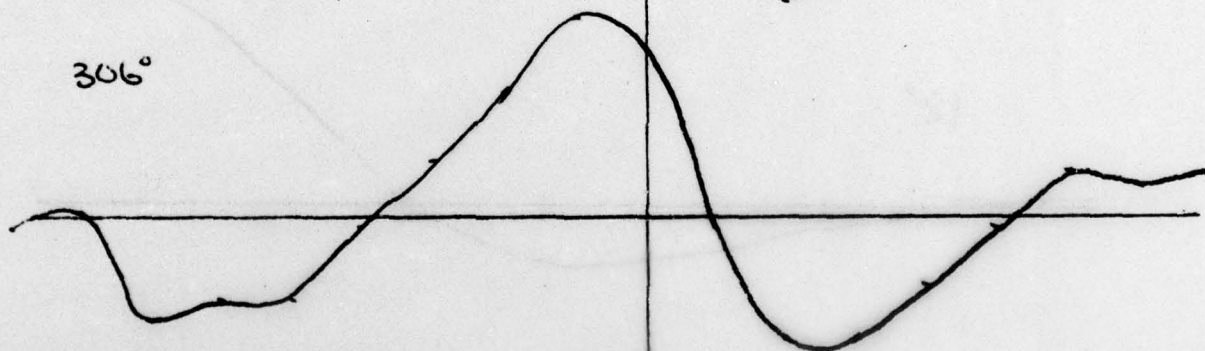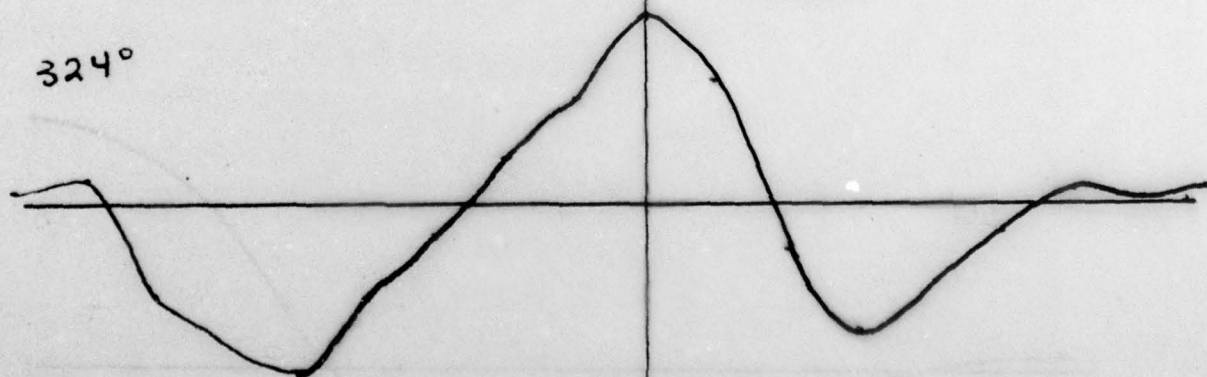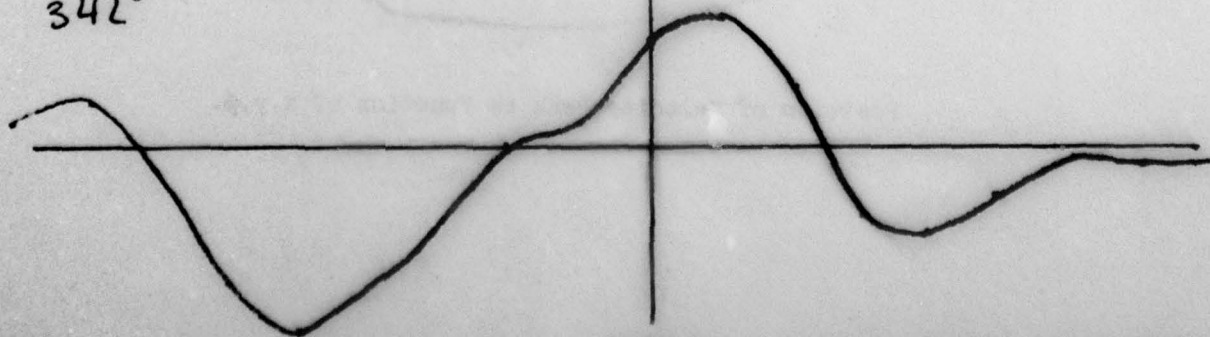
$x = 40$
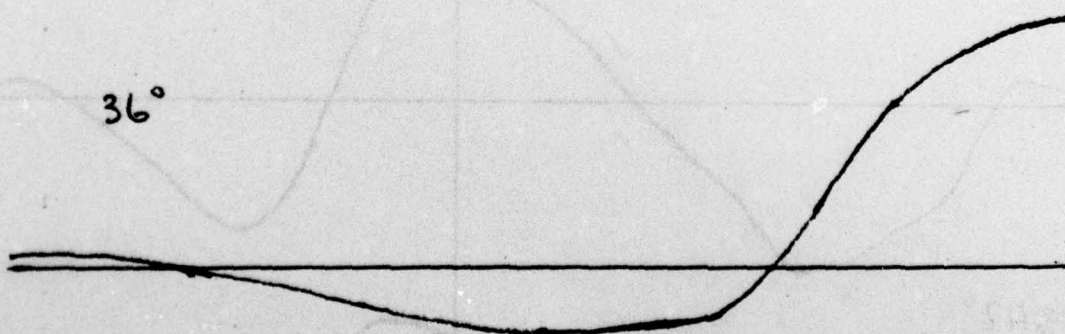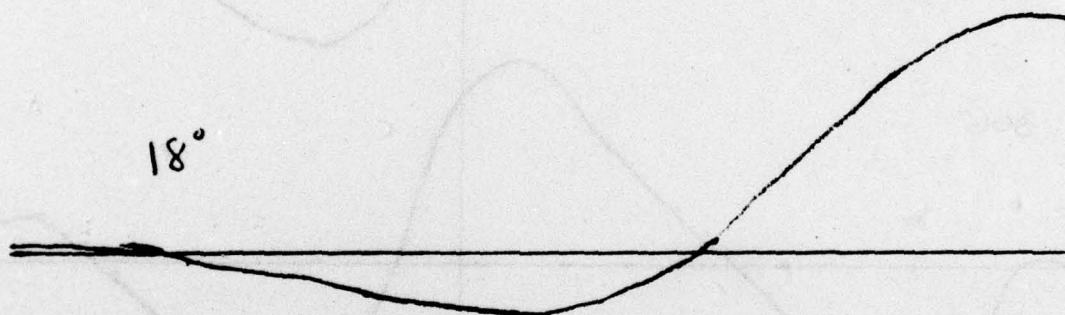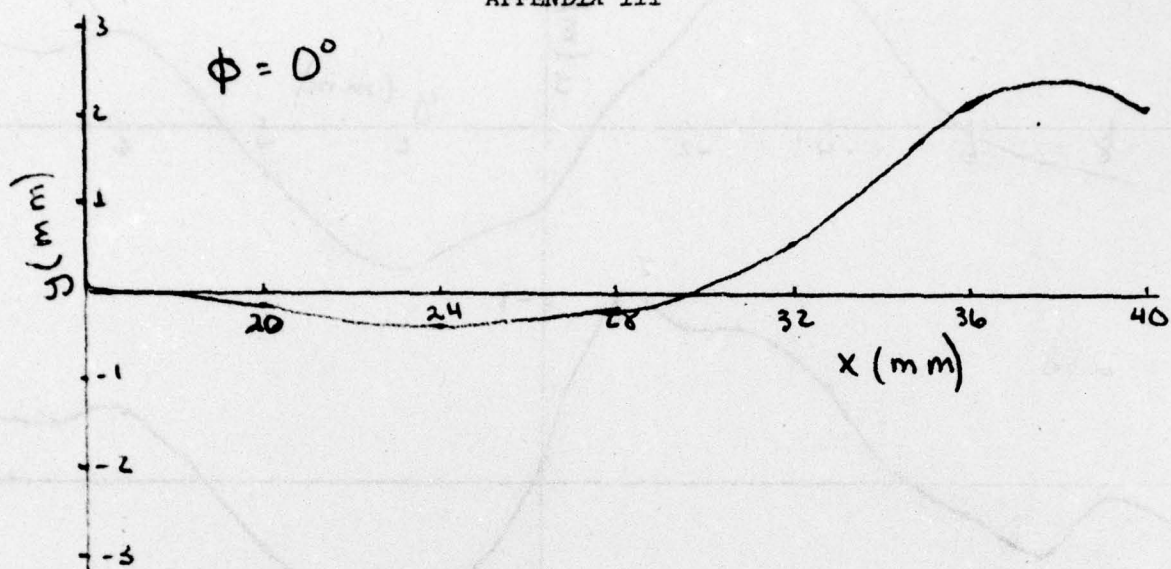
Position of Velocity Peak as Function of x, y, φ.
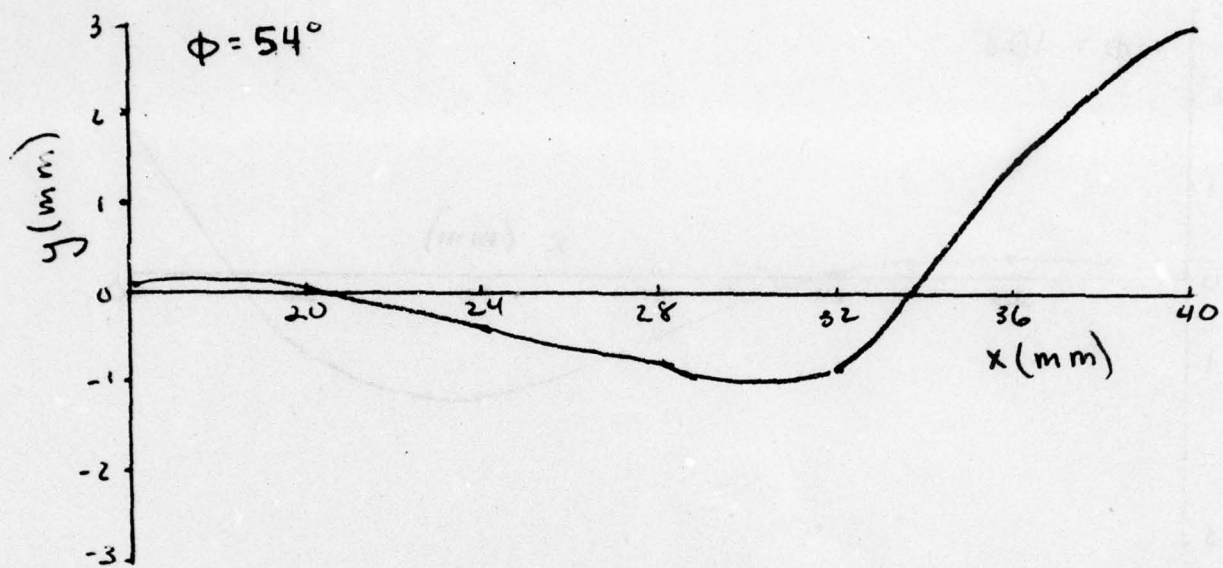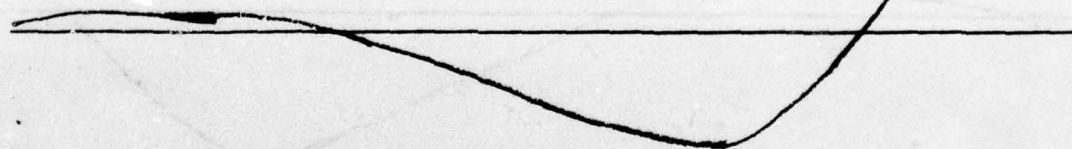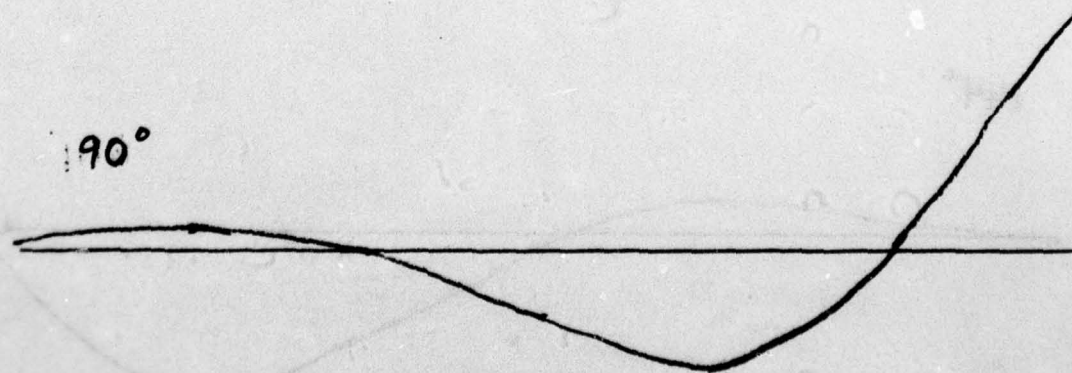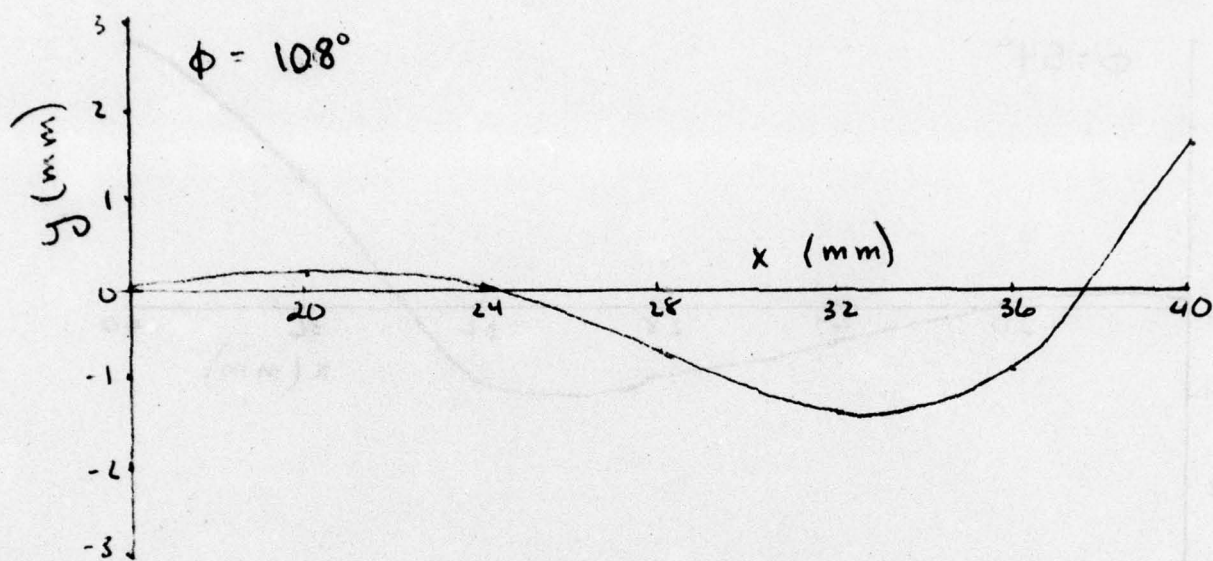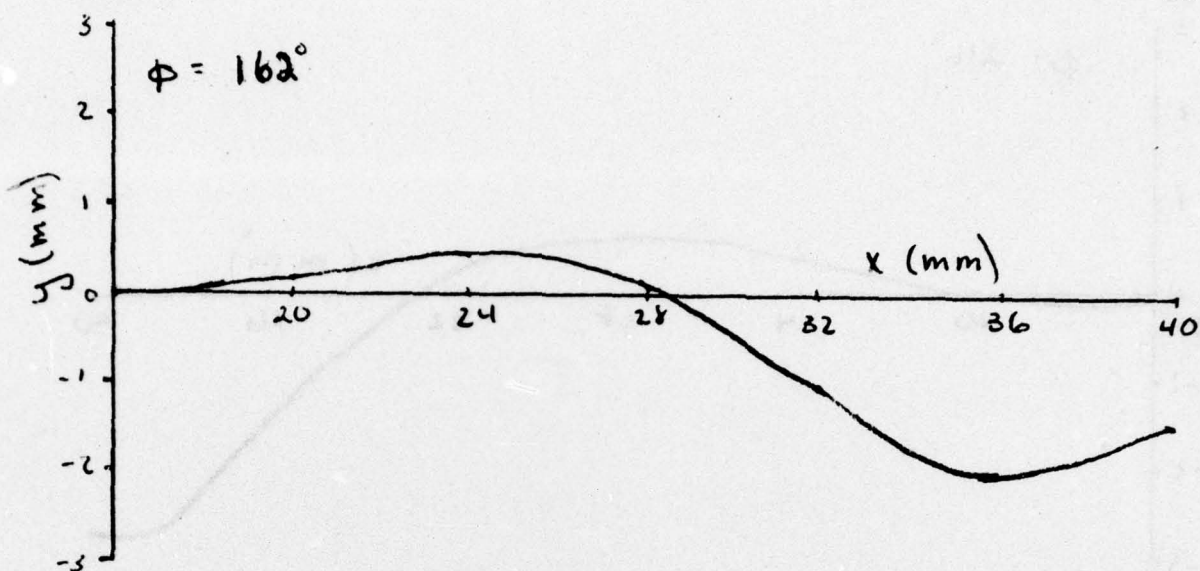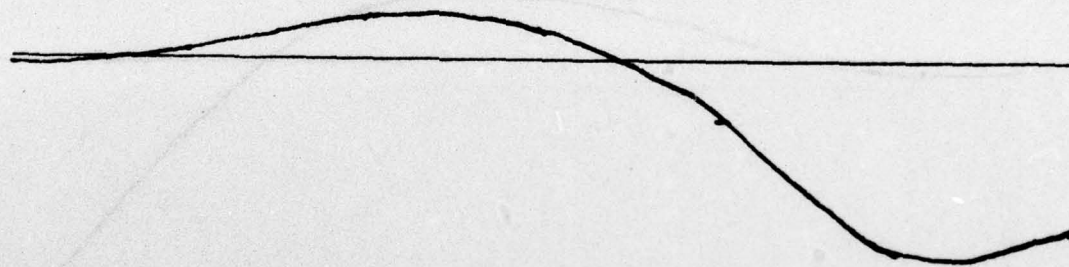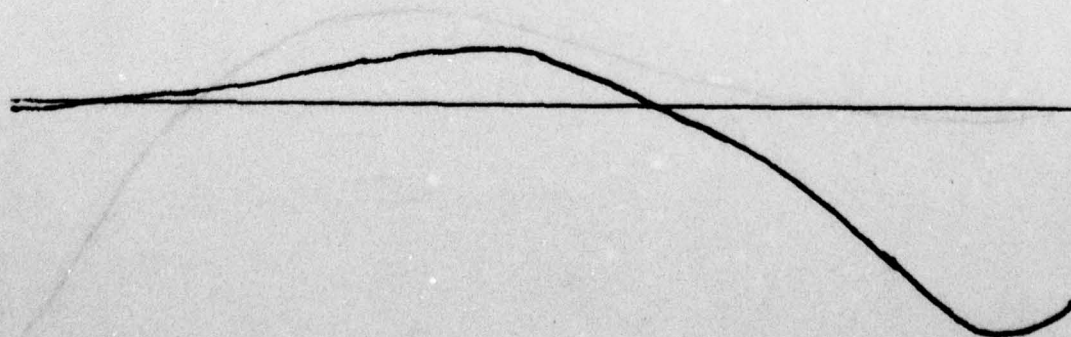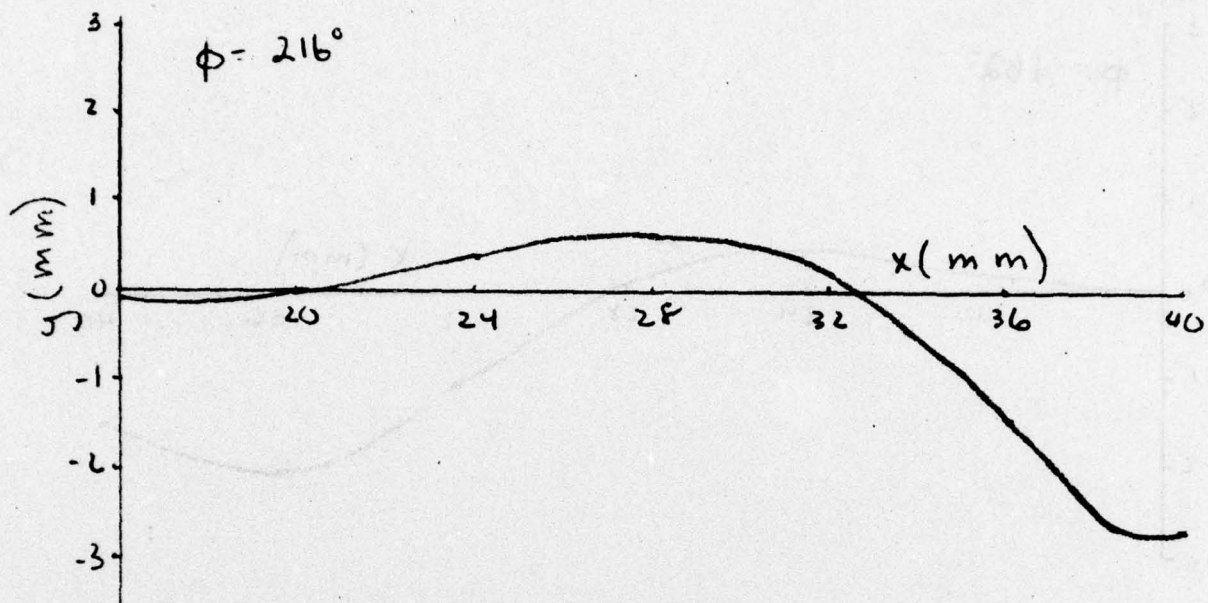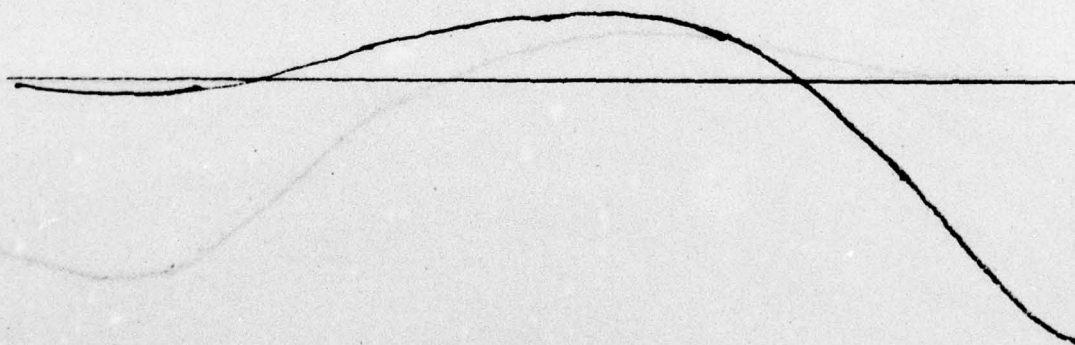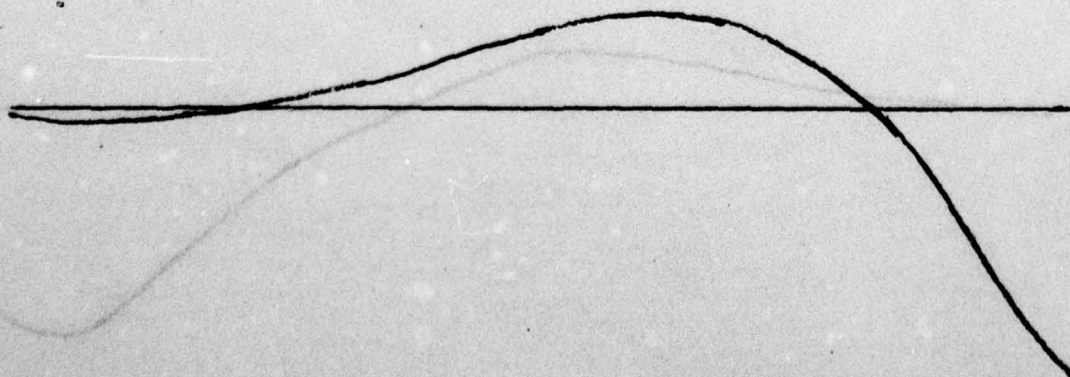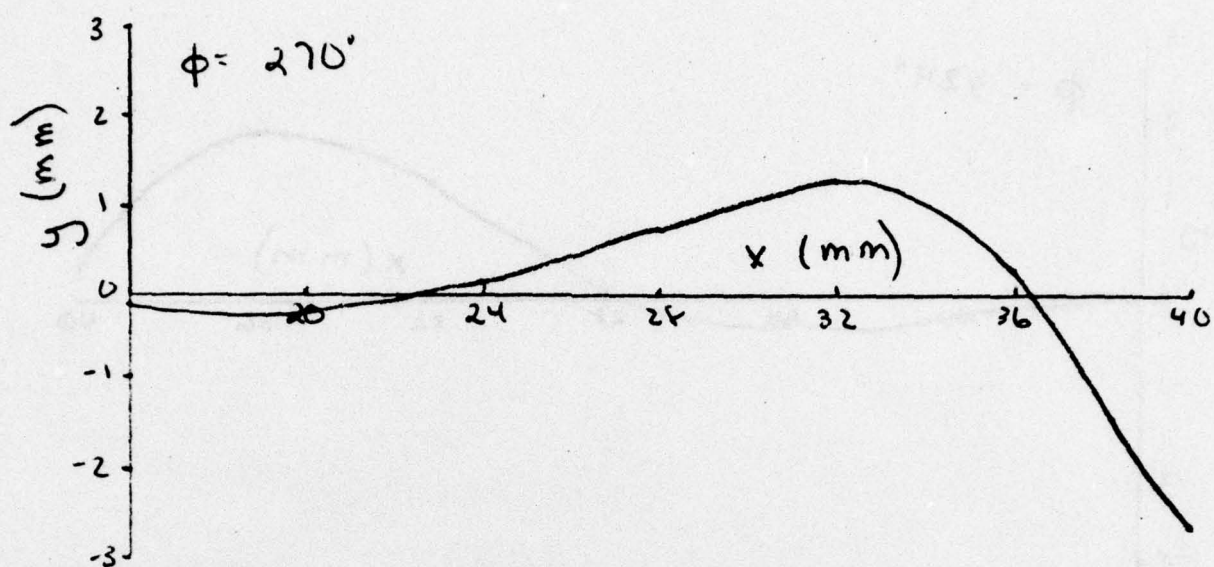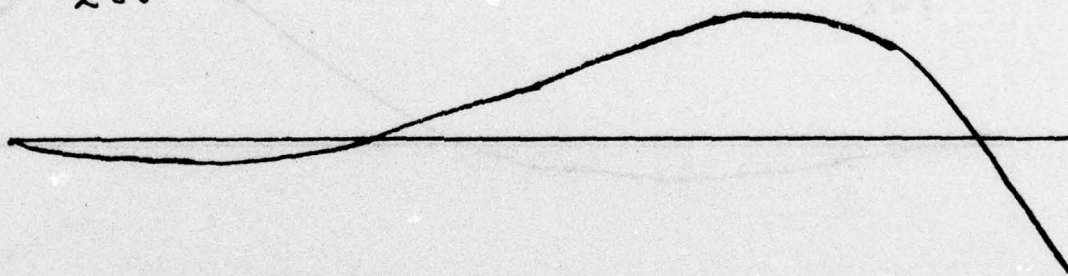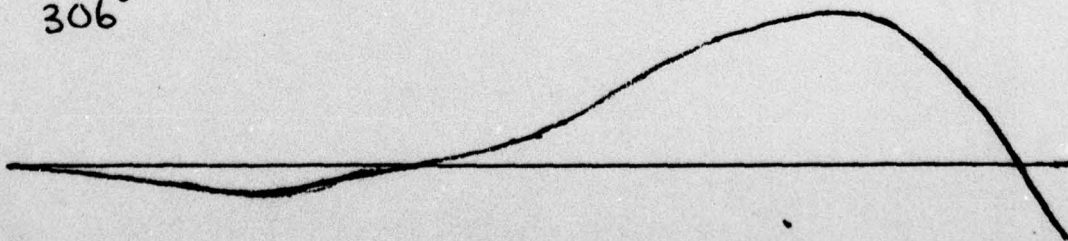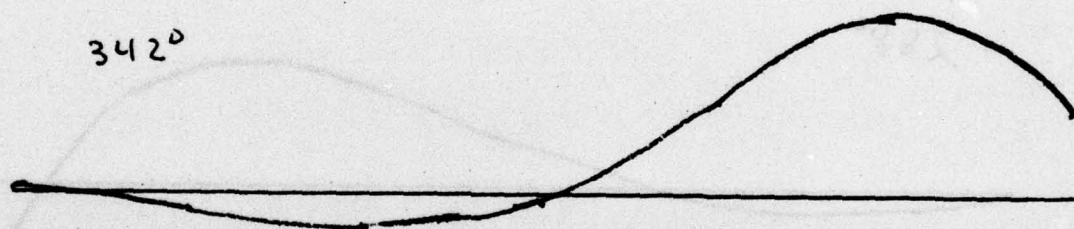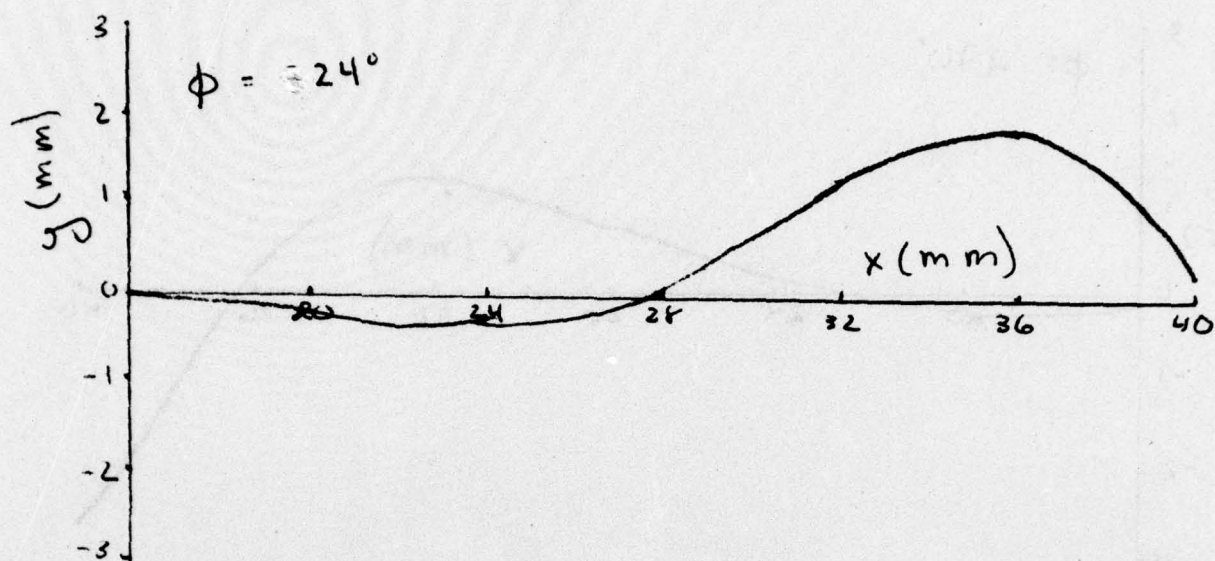
$\phi = 270°$

$288°$

$306°$

$\phi = \pm 24°$

$342°$

REPORT DOCUMENTATION PAGE	READ INSTRUCTIONS BEFORE COMPLETING FORM

1. REPORT NUMBER U.S.N.A. - TSPR; no. 89 (1977)	2. GOVT ACCESSION NO.	3. RECIPIENT'S CATALOG NUMBER

4. TITLE (and Subtitle)

A COMPUTERIZED HOT-WIRE INVESTIGATION OF THE STABILITY OF SEPARATED SHEAR LAYERS WITH APPLICATION TO SHIP SILENCING.

5. TYPE OF REPORT & PERIOD COVERED

Final, 1976-1977.

6. PERFORMING ORG. REPORT NUMBER

7. AUTHOR(s)

David Michael Schubert

8. CONTRACT OR GRANT NUMBER(s)

9. PERFORMING ORGANIZATION NAME AND ADDRESS

United States. Naval Academy
Annapolis, Md. 21402.

10. PROGRAM ELEMENT, PROJECT, TASK AREA & WORK UNIT NUMBERS

11. CONTROLLING OFFICE NAME AND ADDRESS

United States. Naval Academy
Annapolis, Md. 21402.

12. REPORT DATE

23 May 1977

13. NUMBER OF PAGES

86.

14. MONITORING AGENCY NAME & ADDRESS(if different from Controlling Office)

15. SECURITY CLASS. (of this report)

UNCLASSIFIED.

15a. DECLASSIFICATION/DOWNGRADING SCHEDULE

16. DISTRIBUTION STATEMENT (of this Report)

This document has been approved for public release;
its distribution is UNLIMITED.

17. DISTRIBUTION STATEMENT (of the abstract entered in Block 20, if different from Report)

This document has been approved for public release;
its distribution is UNLIMITED.

18. SUPPLEMENTARY NOTES

Presented to the Chairman of the Trident Scholars of the U.S. Naval Academy.

19. KEY WORDS (Continue on reverse side if necessary and identify by block number)

Ships.
Noise.
Laminar flow
Boundary layer noise.
Air jet.

20. ABSTRACT (Continue on reverse side if necessary and identify by block number)

This study was made of the stability of a two-dimensional air jet applicable to ships' noise silencing.

The initially laminar flow was excited using sound from a loudspeaker. Due to the instability of the free boundary layers, the initial disturbance caused by sound pressure was found to be amplified exponentially. The laminar flow was found to turn turbulent at a downstream distance of approximately five jet widths. At this distance the amplification rate of the disturbance

OVER 11

DD FORM 1473 EDITION OF 1 NOV 65 IS OBSOLETE

S/N 0102-LF-014-6601

245600

became less than exponential. Use was made of a new computer-assisted hot
wire technique. The procedures and results are included in the paper.

The results of this study are applicable to studies of flow induced
cavity resonance, which is a major cause of sonar self-noise and of vibration
in ships and aircraft.

0 - 0